UiT
THE ARCTIC UNIVERSITY OF NORWAY

The Faculty of Science and Technology

Department of Geosciences

Subglacial hydrology of the Fennoscandian and Barents Sea ice sheets

Empirical and modelling investigations of palaeo-ice sheet drainage

—

Calvin Shackleton

A dissertation for the degree of Philosophiae Doctor – March 2019

Subglacial hydrology of the Fennoscandian and Barents Sea ice sheets

Empirical and modelling investigations of palaeo-ice sheet drainage

Calvin S. Shackleton

A dissertation for the degree of Philosophiae Doctor

Tromsø, March 2019

Department of Geosciences

Faculty of Science and Technology

UiT – The Arctic University of Norway

Photos:
Cover page – Looking down into a moulin on Steindalsbreen, Lyngen (Photo: Mariana Esteves)

Page 1 – Climbing the couloir on Holmbukttinden, Lyngen Alps (Photo: Pavel Serov)

I. Preface

The work presented in this doctoral thesis was undertaken at the Centre for Arctic Gas Hydrate, Environment and Climate (CAGE), Department of Geosciences, University of Tromsø (UiT) - The Arctic University of Norway, between October 2014 and February 2019. The project was funded through a four-year stipend from CAGE, which is supported by the Research Council of Norway Centres of Excellence funding scheme, grant No. 223259. The main supervisor was Dr. Monica Winsborrow (CAGE, UiT), with co-supervisors Prof. Karin Andreassen (CAGE, UiT), Dr. Lilja Bjarnadóttir (Geological Survey of Norway), and Dr. Henry Patton (CAGE, UiT).

The PhD program at UiT requires that 25% of the four-year period be dedicated to undertaking duty work, which is assigned in collaboration with the supervisors and the requirements of the Department of Geosciences. This was fulfilled through preparing and teaching exercises in Quaternary Geology, assisting teaching on two ArcGIS software courses at UiT, and taking part in outreach events including the Arctic Frontiers 'Science for Schools' day and UiT Forskningsdagene (Research Day). Eleven months were spent working and collaborating with researchers at the Lamont Doherty Earth Institute, University of Columbia, New York, USA and was funded by the UiT 'Research stays abroad' scheme.

The following ECTS-accredited courses were completed as part of the PhD programme: Glaciology (University Centre in Svalbard (UNIS)); Reconstruction of glacial marine sedimentary processes and environments (UNIS); Philosophy of science and ethics (UiT); Arctic Marine Geology and Geophysics (AMGG) cruise and workshop (UiT). Additionally, a course on Arctic field skills was attended on Disko Island, west Greenland (University of Bergen) and on Fluid emission fossil analogues and climatic changes in Sicily, Italy (AMGG, UiT). Courses and training in ArcGIS and IVS Fledermaus software, research cruise safety, and first aid were also undertaken at the Department of Geosciences. During the PhD 7 research cruises were attended in the Barents Sea and around Svalbard, totalling 9 weeks living and working on board the R/V Helmer Hanssen collecting geophysical and sedimentological data.

Results from this thesis were presented at 5 conferences: International Glaciological Society (IGS) Hydrology Symposium in Höfn, Iceland (June, 2015); European Geosciences Union (EGU) General Assembly in Vienna, Austria (April, 2016); IGS Nordic branch meeting in Tromsø, Norway (October, 2016); American Geosciences Union (AGU) General Assembly in New Orleans, USA (December, 2017); EGU General Assembly in Vienna, Austria (April, 2018).

II. Acknowledgements

I have learned a lot over the last four years thanks to successes, failures, repetition, hard-work, patience, experiences, and set-backs, but most of all I have learned from the people I have met and collaborated with along the way. I'm grateful to my supervisors, Monica, Karin, Lilja and Henry for their collaboration and guidance while undertaking the PhD. We have overcome many challenges throughout these years, and I have learned a lot from you. I am grateful for your continued support and encouragement throughout the journey.

I am fortunate enough to have had the opportunity to visit and work in Greenland, Iceland, New York, and Svalbard during my time as a PhD, and I've met a great number of inspiring people while travelling and working in these places to whom I owe thanks. To new and old friends from Tromsø and beyond, thank you for an endless amount of fun over the years. Between hiking, running, skiing, snowboarding, camping, climbing and partying, extra-curricular activities have been an important part of life here in the Arctic. Thank you to Alexey, Dasha, Pasha, Carly, Henry, Malin, Giacomo, Anna, Alexey, Sunil, Yulia, Hanne, Emmelie, David, Martin, Mark, Anna, Andrea, Kate, Frieda, Sarah, Karina, Diane, Lis, Ole, Astrid, Per-Inge, Eythor, Warren, Louise, Ellery, Jack, Naima, Arunima, Chris, Ric, Sam, and others who have all contributed to such a positive experience living in Tromsø. To Jonny and Jen, you made our time in New York endlessly entertaining, and I'm thankful to have had the opportunity to spend time in that exciting city with you.

My family have always been an important part of my life and I am thankful for the enthusiasm that my brothers, parents and grandparents always seem to have for my various endeavours. In particular, my parents continue to inspire me to do my best and its thanks to their encouragement and support that I was able to have the confidence to undertake this PhD and overcome its various challenges. Their relaxed and calm approach to life has always been reassuring, and they have always been happy for me to take whichever path I choose in life. Thank you, Mum and Dad.

Bradley and Robert, it's impossible to not have fun when we are together. Past and present adventures with you have provided much excitement, and dreaming up new adventures to go on a most welcome distraction. Although we have spent the last few years separated by incredible distances, and at times even inhabiting opposing poles, I have felt your support and encouragement throughout. I know the adventures will continue in the future, and probably become bigger, better, and more extreme.

Mariana, I am fortunate to have a partner who I can work with, discuss scientific ideas, collaborate on papers, and trust to stop me falling off an ice cliff while scrambling over glaciers. You have been an incredible support to me throughout the PhD, and I thank you for the many exciting adventures we have had together. Over the last four years we have spent time exploring/skiing/ mountaineering/climbing in the mountains around Tromsø, having never-ending fun discovering the depths of New York City, traversing glaciers and camping in the Lyngen Alps, climbing rock outcrops and frozen waterfalls. I am grateful that you have been by my side throughout all this, supporting and inspiring ideas for more extreme ways to spend our free time, and making everything more fun.

Thank you,
Calvin

This thesis contains three first-authored research papers:

Subglacial water storage and drainage beneath the Fennoscandian and Barents Sea ice sheets. 2018. C. Shackleton, H. Patton, A. Hubbard, M.C.M. Winsborrow, J. Kingslake, M. Esteves, K. Andreassen, S.L. Greenwood. *Quaternary Science Reviews* **201:**13-28.

Ice margin retreat and grounding-zone dynamics during initial deglaciation of the Storfjordrenna Ice Stream, western Barents Sea. C. Shackleton, M.C.M. Winsborrow, K. Andreassen, R. Lucchi, L.R. Bjarnadóttir. *In review, Boreas.*

Transitions in subglacial drainage and influences on glacial dynamics in the central Barents Sea, reconstructed from assemblages of meltwater landforms C. Shackleton, M.C.M. Winsborrow, H. Patton, M. Esteves, L.R. Bjarnadóttir, K. Andreassen. *Manuscript in preparation.*

While undertaking the PhD, contributions were also made to the following research papers, which are not included in this thesis:

Retreat patterns and dynamics of the Sentralbankrenna glacial system, central Barents Sea. 2017. M. Esteves, L.R. Bjarnadóttir, M.C.M. Winsborrow, C.S. Shackleton, K. Andreassen. *Quaternary Science Reviews* 169: 131-147.

Deglaciation of the Eurasian Ice sheet complex. 2017. H. Patton, A. Hubbard, K. Andreassen, A. Auriac, P.L. Whitehouse, A.P. Stroeven, C. Shackleton, M. Winsborrow, J. Heyman, A.M. Hall. *Quaternary Science Reviews* 169: 148-172.

An interconnected palaeo-subglacial lake system in the central Barents Sea. M. Esteves, D. Rüther, M.C.M. Winsborrow, S.J. Livingstone, C. Shackleton, K. Andreassen, W. Hong, J. Knies. *In Prep.*

The influence of ice dynamics on subglacial meltwater systems: an example from the central Barents Sea. M. Esteves, M.C.M. Winsborrow, C. Shackleton, L.R. Bjarnadóttir, K. Andreassen. *In prep.*

Table of Contents

1.0 Introduction

1.1 Scientific background

1.1.1 Ice sheets and glaciers

The cryosphere is a fundamental component of the Earth system, with 10% of the present-day Earth surface covered by glaciers, ice sheets and ice caps, collectively storing approximately 75% of the world's freshwater (www.nsidc.org). Ice masses are inherently sensitive to atmospheric and oceanic temperature fluctuations over relatively short timescales, and are important to the Earth's surface energy budget, the water cycle, and global sea level (Vaughan et al., 2013). The stability of ice sheets and glaciers, and their response to changes in climate, is therefore becoming increasingly important to determine, especially given observed and projected warming of global climate (Stocker et al., 2013). Rates of change within the cryosphere are dependent on a multitude of factors, and one of the biggest challenges for the scientific community is to determine the rate and processes by which the contemporary cryosphere is likely to respond to projections of future climate change.

Mass input to ice sheets and glaciers is primarily in the form of precipitation at ice sheet interiors or high elevations. Surface melting plays a role in ice mass loss, especially in temperate locations, but loss of ice mass is predominantly controlled by the flow of ice towards lower elevations or peripheral margins. Ice flows towards the margins mainly via basal sliding, but also via deformation of ice under its own weight and sediment deformation at the ice bed (Fig. 1). Ice streams are narrow zones of ice which flow at least an order of magnitude faster than the surrounding ice, and as such account for the majority of ice, sediment and meltwater discharged from ice sheets (Bennett, 2003). Fast ice flow is facilitated by basal water and deformable sediments at the ice bed, which lubricate the ice-bed interface (*Section 1.1.2*) and promote basal sliding (Fig. 1). Fast-flowing ice streams and outlet glaciers transport ice mass from the interior of ice sheets to the margins, where it is subject to melting, or calving of icebergs into the ocean (Bennett, 2003).

As a result of climate and ocean warming over recent decades, ice mass loss to the oceans in Greenland and Antarctica is dramatically increasing (Pritchard et al., 2009; Joughin et al., 2012) and a greater quantity of surface and basal meltwater is being produced (Hanna et al., 2013). This directly influences the ice mass budget (Hanna et al., 2013), but also has consequences for ice dynamic processes such as basal sliding and sediment deformation. This thesis investigates how water is routed through the subglacial environment, and how drainage systems develop over time, impacting on the flow of overlying and surrounding ice.

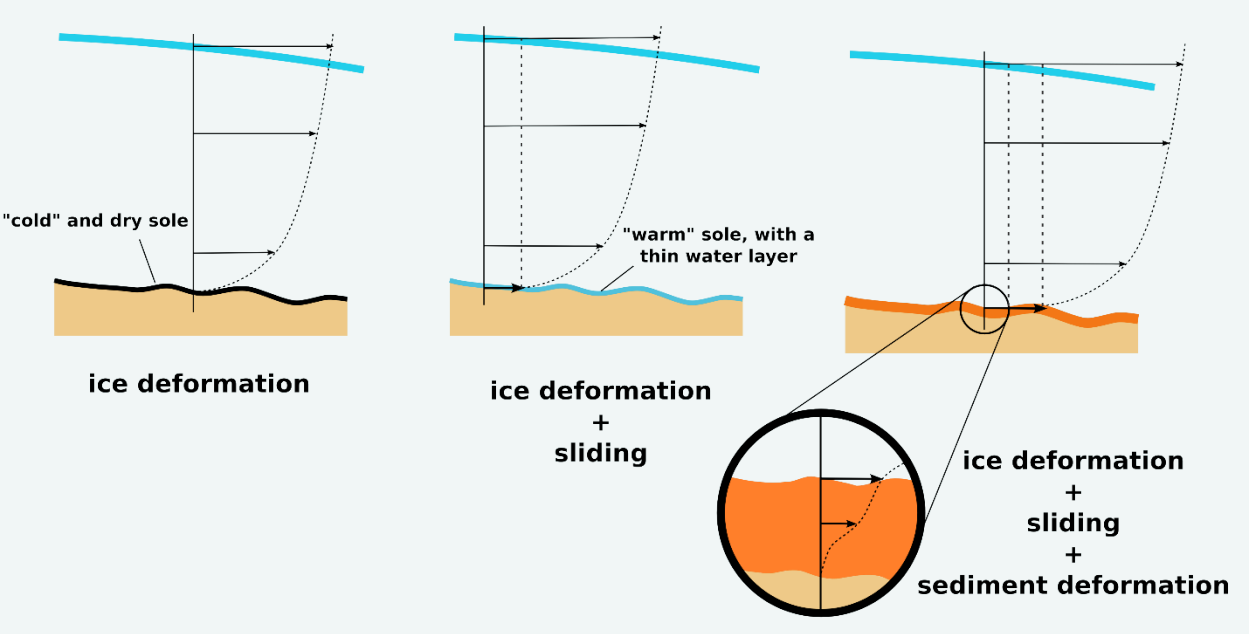

Figure 1: Glaciers flow via three main mechanisms: ice deformation (left), basal sliding (middle) and subglacial sediment deformation (right). The presence of water at the ice-bed interface, acting to reduce basal drag or by facilitating sediment deformation, can greatly increase the speed at which glaciers flow. Figure is a modified version of Glacier Flow-mechanisms.png licenced under CC BY 4.0.

1.1.2 Subglacial hydrology

Contemporary ice sheet and glacier hydrology has been widely investigated using a range of approaches, including borehole observations (Iken and Bindschadler, 1986; Iken et al., 1993; Fountain, 1994; Hubbard et al., 1995; Andrews et al., 2014; Doyle et al., 2018), geophysical studies (Oswald and Gogineni, 2008; Hart et al., 2015), remote sensing (Bell et al., 2006; Fricker et al., 2007), dye tracing and meltwater discharge/chemistry (Fountain, 1992, 1993; Sharp et al., 1993; Gulley et al., 2012a), and direct observation of dry meltwater conduits during winter months (Gulley and Benn, 2007; Gulley et al., 2009, 2012b,). Subglacial drainage of recently deglaciated or palaeo-ice sheets and glaciers has also been reconstructed through geomorphological (*Section 1.1.3*) and sedimentological investigations of deglaciated beds (Boulton et al., 2007; Shaw, 2002; Livingstone et al., 2012; Nitsche et al., 2013; Greenwood et al., 2016; Kuhn et al., 2017; Simkins et al., 2017). Additionally, conceptual and mathematical model approximations of basal effective pressure and meltwater discharge have been employed to investigate glacier hydrology and potential impacts on ice flow (Iken, 1981; Clarke et al., 1984; Kamb et al., 1985; Kamb, 1987; Fowler and Walder, 1994; Arnold and Sharp, 2002; Werder et al., 2013; Clason et al., 2014), each with advantages and limitations depending on the spatial and temporal scale of investigation (cf. De Fleurian et al., 2018).

Two modes of subglacial drainage are typically envisaged at the ice bed (Fig. 2). The first, channelized drainage through water-filled conduits incised into the ice or its substrate (Röthlisberger, 1972; Shreve, 1972; Weertman, 1972), typically operating at water pressures lower

than the ice overburden pressure, with limited influence on local effective pressure (Hewitt, 2011). The second drainage mode is distributed drainage through high-pressure water sheets, films or aquifers (Anderson et al., 1982; Fowler and Walder, 1994; Kamb, 2001; Creyts and Schoof, 2009) and groundwater flow (Boulton et al., 1995; Piotrowski, 1997). These drainage systems are susceptible to increases in water pressure up to and exceeding the ice overburden pressure, with greater potential impacts on ice flow velocities. The two end-members on the continuum of subglacial drainage modes are continually developing, in response to factors operating at temporal scales from hours to decades (Bartholomew et al., 2010; Sole et al., 2011; Cowton et al., 2013).

Subglacial drainage of meltwater beneath ice sheets directly influences ice flow speeds by regulating the lubrication of the ice-bed interface, and determining subglacial sediment shear strengths, which influence ice flow variability over diurnal and seasonal time-scales (Weertman, 1972; Alley, 1989; Boulton et al., 2001). Furthermore, increased inputs to subglacial drainage systems can build-up water pressure, potentially approaching that of the ice overburden pressure (Kamb, 2001), and leading to enhanced ice flow (Iken, 1981; Jansson, 1995). The routing of subglacial water also has impacts beyond the ice margin, as drainage outlets deliver freshwater and sediments to the ice sheet periphery. This has widespread impacts on landscape development, building large depositional landforms (e.g. Powell, 1990), contributing to continental margin development and slope instability (Laberg and Vorren, 1995; Vorren and Laberg, 1997; Lucchi et al., 2012), charging vast proglacial river systems and lakes (Mangerud et al., 2004; Toucanne et al., 2015), and influencing local and global ocean circulation (Marshall and Clarke, 1999; Slater et al., 2015).

The availability of basally derived meltwater is dependent on subglacial temperatures, which are regulated by geothermal heat flux at the bed, frictional heat generated by basal sliding, and surface energy exchange where ice is sufficiently thin. In addition to basally derived meltwater, subglacial drainage can be charged by inputs from the ice surface, such as seasonally developing supraglacial lakes and channels, which can lead to water transport down crevasses and through englacial conduits to the ice-bed interface (Fig. 2). Furthermore, storage of meltwater within subglacial lakes influences drainage system development, periodically storing and releasing large volumes of water to the ice bed (Winberry et al., 2009; Siegfried et al., 2016). Drainage events are subject to internal, ice-dynamic modulation (Wingham et al., 2006; Smith et al., 2017) and have been directly linked to accelerations in ice stream velocity (Stearns et al., 2008; Carter et al., 2013). Subglacial lakes are therefore a crucial component of the subglacial drainage system, with far-reaching impacts on the hydrology, dynamics, and mass budget of glaciers and ice sheets.

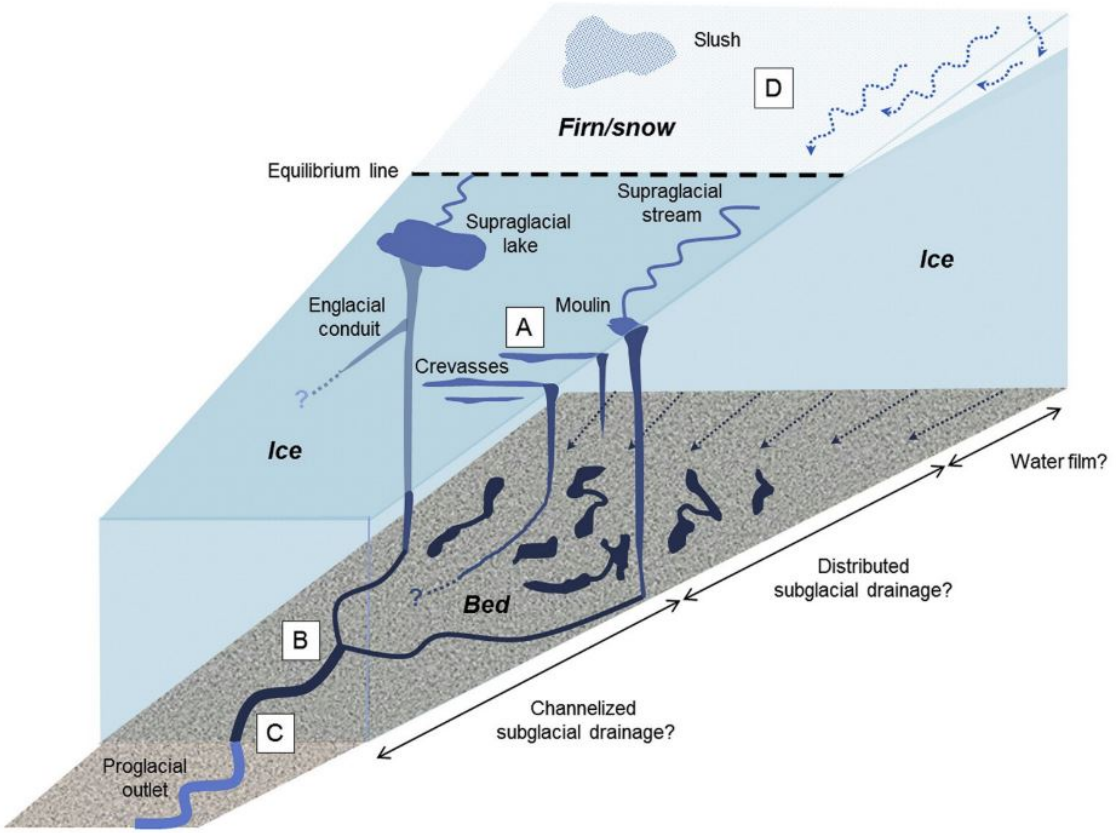

Figure 2: Conceptual diagram of supraglacial, englacial and subglacial hydrological systems. Figure from Greenwood et al. (2016a).

1.1.3 Glacial and glacifluvial geomorphology

Ice sheets are remote and often inaccessible, and the subglacial environment can be covered by thousands of metres of ice, hindering direct investigation. Observational records of contemporary subglacial hydrology are therefore spatially and temporally limited, and do not fully capture important processes that drive drainage system evolution over operational timescales. Additionally, the spatial scale of observational records calls for extensive extrapolation in order to apply findings to the entire glacial system. An alternative approach is to use the geomorphic imprint of palaeo-ice sheets, which offer the potential to inform their responses to past climatic changes, reconstruct ice extents, thicknesses and margin limits over entire glaciations, distributions of fast/slow flowing ice and the impact that a glaciation had on the landscape, oceans and atmosphere.

During the maximum ice extent phases of the last ice age, glacial ice covered an estimated 32% of the Earth's surface (www.nsidc.org). The transition from past ice-sheet configurations to those observed today had a tremendous impact on global ocean circulation, climate and landscapes. Ice sheets erode, transport and deposit large quantities of sediments as they advance and decay, with an immense capacity to mould the landscape. Erosional glacial and meltwater landforms are produced through scouring, abrading and incising of the ice bed by the more dynamic components

of the ice sheet system, such as fast-flowing ice streams, outlet glaciers, and channelized subglacial meltwater. These processes are especially prevalent within fast-flowing ice streams, with erosion rates up to 4.8 mm yr^{-1} calculated beneath the present-day Greenland Ice Sheet (Cowton et al., 2012) and estimated mean erosion rates of 0.6 - 0.8 mm yr^{-1} at the bed of fast flowing ice streams in the Barents Sea during the Late Pleistocene (Laberg et al., 2012). Depositional landforms are created when eroded material is left behind by the cessation of dynamic ice sheet processes. These are typically associated to deglaciation phases, when ice is thinning and retreating, leaving behind entrained basal, englacial and supraglacial sediments.

Due to the immense geomorphic capabilities of ice sheets, evidence for the most recent advance and decay of an ice sheet system tends to be best preserved, as each subsequent glaciation modifies or erases the geomorphology created by the former. Also, the geomorphic record tends to be biased towards the most erosive components of an ice sheet, or those that deposit large quantities of sediments. As a consequence, processes that are not efficient at shaping the landscape are likely to be underrepresented. Geomorphologically based reconstructions have driven significant advances in understanding of palaeo-ice sheet advance and retreat over Fennoscandia (Kleman and Hattestrand, 1999; Sejrup et al., 2000; Mangerud, 2004; Stroeven et al., 2016) and the Barents Sea (Andreassen et al., 2007, 2008; Laberg et al., 2010; Winsborrow et al., 2010; Vorren et al., 2011). The Barents Sea is an ideal site for geomorphological study of LGM palaeo-ice sheet behaviour, since the seabed lacks significant postglacial modification. Ice build-up to, and retreat from, the Last Glacial Maximum (LGM) period (~22 ka B.P.) modified the landscape, leaving behind sedimentological and geomorphological evidence of its activity, and facilitating reconstructions of past ice sheet behaviour over large spatial and temporal scales using diagnostic assemblages of glacial landforms.

1.2 Aims, objectives and study sites

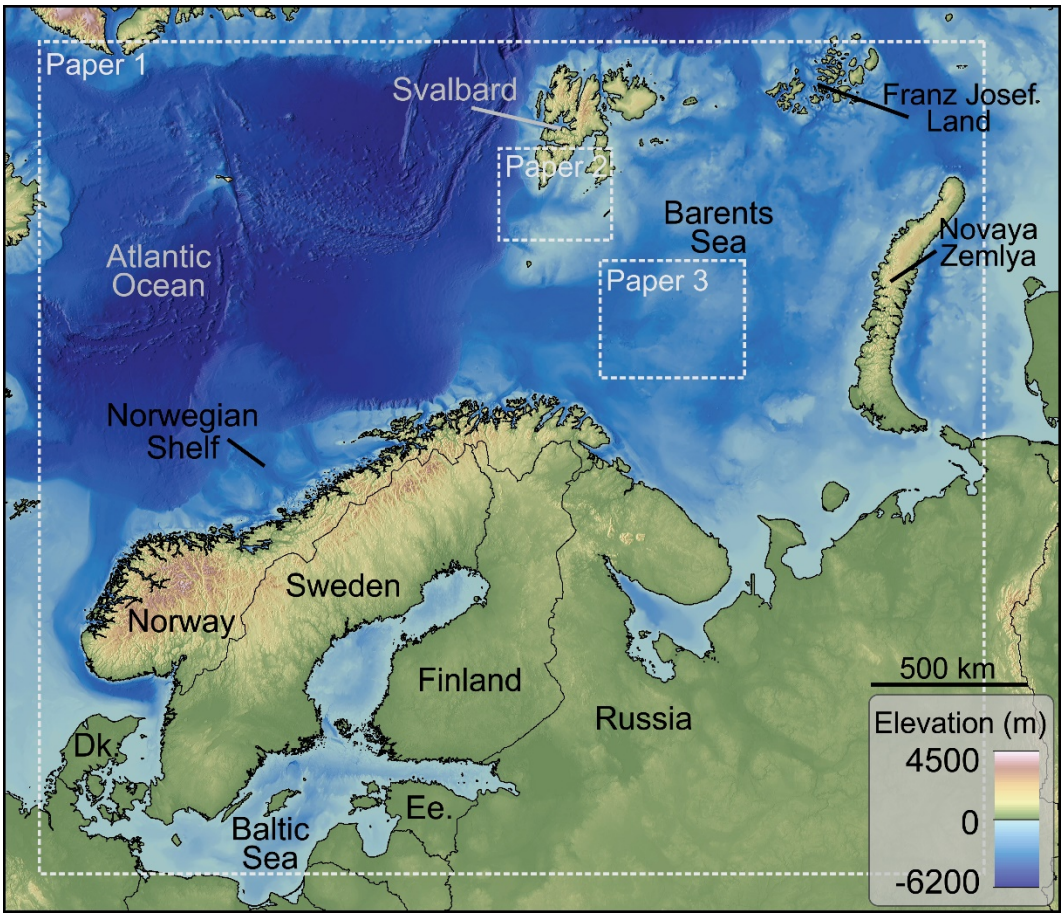

Figure 3: Overview of regions studied in this thesis. Paper 1 is a study of subglacial drainage beneath the Fennoscandian and Barents Sea palaeo-ice sheets. Paper 2 focusses on ice-marginal geomorphology in outer Storfjordrenna, a cross-shelf bathymetric trough south of Svalbard. Paper 3 focusses on meltwater geomorphology in the central sectors of the Barents Sea.

The aim of this doctoral thesis is to investigate the subglacial drainage of the BSIS & FIS using a combination of approaches, and constrain potential impacts on ice dynamics. A range of temporal and spatial scales, along with various ice sheet settings are investigated (Fig. 3). Paper 1 encompasses ice sheet scale hydrology over an entire glaciation, modelling the evolution of subglacial hydraulic pressure potential over the build-up and decay of the Fennoscandian and Barents Sea ice sheets from 37-10 ka B.P. (Section 2.1). Paper 2 focusses on shorter temporal and smaller spatial scales, studying ice marginal landforms in Storfjordrenna, south of Svalbard (Fig. 3) to investigate processes related to subglacial meltwater-influenced ice margin retreat and deposition (Section 2.2). Finally, Paper 3 uses bathymetric datasets to reconstruct the evolution of subglacial hydrological networks and their influence on ice dynamics in the central Barents Sea (Fig. 3; Section 2.3).

Figure 4: The Last Glacial Maximum (LGM) ice extent maxima over Fennoscandia and the Barents Sea is drawn in white (Patton et al., 2017). The locations and flow directions of major palaeo-ice streams are drawn as white arrows. Lt. = Lithuania; Lv. = Latvia; Ee. = Estonia; HT = Hinlopen Trough; KvT= Kvitøya trough; FVT = Franz Victoria Trough; SF = Storfjordrenna; DR= Djuprenna; VF/TD =Vestfjorden/Traenadjupet. Figure taken from Shackleton et al. 2018.

The Barents Sea is a shallow, epicontinental sea that was repeatedly glaciated over the Late Quaternary period (Vorren et al., 1988; Dahlgren et al., 2005), and is today characterised by shallow banks and deep troughs (Fig. 3). The Barents Sea Ice Sheet (BSIS) was drained by ice streams operating within bathymetric troughs (Fig. 4), the largest of which in Bjørnøyrenna, the St. Anna Trough, Franz Victoria Trough, Hinlopen Trough, and Storfjordrenna all terminated at the continental shelf break during peak glaciation (Fig. 4) (e.g. Andreassen et al., 2007; Vorren et al., 2011). The BSIS was marine based, with ice grounded mostly below sea level, making it sensitive to climatic fluctuations and sea level rise, especially where ice rests on retrograde bed slopes (Katz and Worster, 2010; Jamieson et al., 2012; Favier et al., 2014). The contemporary West Antarctic Ice Sheet (WAIS) shares similar characteristics with the Late Weichselian BSIS (Andreassen and Winsborrow, 2009) making it a good palaeo-analogue and useful indicator of the potential response of marine-based ice sheets to current and future changes in climate.

Contrastingly, the Fennoscandian Ice Sheet (FIS) was mostly terrestrially-based (Fig. 4), with high topographic relief along western Scandinavia and relatively flat terrain across southern Finland. This ice sheet was drained by ice streams operating in the present-day Gulf of Bothnia, the Norwegian Channel and along the Norwegian continental shelf (e.g. Sejrup et al., 2000; Ottesen et al., 2005; Greenwood et al., 2017). During the LGM, ice expansion and merging of the FIS with the BSIS, led to a multi-domed, dynamic ice sheet over Eurasia, spanning a range of glaciologic, geographic and topographic settings, with extensive terrestrial and marine margins.

1.3 Methods and data

1.3.1 Subglacial hydraulic potential reconstruction (Paper 1)

The flow of water at the beds of glaciers and ice sheets is influenced by the gravitational pull from differences in elevation, and the impact of the overlying ice sheet on hydraulic pressure (Shreve, 1972). Overlying ice sheet thicknesses and isostatically corrected bed topographies can therefore be used to calculate gradients in hydraulic pressure potential (ϕ):

$$\phi = \rho_w g z_b + F\rho_i g(z_s - z_b), \quad (1)$$

where ρ_w is the density of water (1000 kg m^{-3}); g is the acceleration due to gravity (9.81 m s^{-2}); z_b is the bed elevation; ρ_i is the density of ice (917 kg m^{-3}); z_s is the height of the ice sheet surface. The flotation factor (F) is the ratio between subglacial water pressure and the ice overburden pressure, and varies temporally and spatially according to meltwater inputs, drainage system character, basal ice temperature, and the underlying substrate (Clarke, 2005; Andrews et al., 2014). In this thesis, modelled ice sheet surfaces and isostatic adjustment output from an established coupled climate/ice flow model (Auriac et al., 2016; Patton et al., 2016, 2017) are utilized to reconstruct subglacial hydraulic potential at the bed of the Fennoscandian and Barents Sea ice sheets, from initial ice build-up around 37 ka B.P through to full deglaciation at 10 ka B.P. Reconstructing spatio-temporal changes in hydraulic potential reveals insights into long-term evolution of subglacial drainage routing and potential locations for subglacial lakes at the bed.

1.3.2 Geomorphologically based reconstruction (Papers 2 and 3)

The landforms left behind by the erosive and depositional processes of ice advance and decay can be used to reconstruct their past behaviour, given adequate knowledge of the processes that form them (cf. Kleman et al., 2006). This thesis reconstructs processes occurring at the bed and margins of palaeo-ice masses, and investigates how subglacial hydrology might have developed over the course of a glaciation, and its influence on ice-dynamic behaviour. Ice marginal landform assemblages mapped from seabed bathymetry and subsurface data in outer-Storfjordrenna provide insights into subglacial conditions and ice margin processes during initial deglaciation of the Storfjordrenna Ice stream (Section 2.2). In the central sectors of the Barents Sea Ice Sheet, meltwater landforms are used to reconstruct subglacial drainage throughout ice-maximum phases of the ice sheets development and through to its final retreat stages (Section 2.3).

High-resolution swath bathymetry surveys were undertaken in Storfjordrenna during 2013 and 2014 research cruises on-board the R/V Helmer Hanssen. Datasets were acquired using a hull-mounted Kongsberg Simrad 30 kHz EM300 multibeam echosounder and processing was done in Neptune software. The data were corrected to include sound-velocity profiles, and anomalous data was removed, before being gridded using QPS Fledermaus software to a horizontal resolution of

15 x 15 m. Bathymetric datasets were used to create solar relief shaded visualisations, which were used for manual mapping of glacial geomorphology at the seabed using the Fledermaus software and Esri ArcGIS v.10. Bathymetric data used to investigate the central Barents Sea was collected using a Kongsberg EM170 and EM2040 onboard the R/V G.O. Sars, and was processed and supplied by the Geological Survey of Norway (NGU) MAREANO programme.

Subsurface profiles were acquired in Storfjordrenna using a hull-mounted Edgetech 3300 – HM CHIRP sub-bottom sediment profiler, with 4 x 4 transducer array operating at 4 kW, transmitting an FM pulse, linearly swept over a full spectrum frequency range (1.5 kHz to 9 kHz over 40 ms). Data were processed and interpreted using the Kingdom Suite v.8.8 software. A sound wave velocity of 1500 m s^{-1} through seawater is assumed, and also used for subsurface travel of waves due to the relatively shallow nature of sedimentary deposits, thus providing a minimum estimate for the thickness of sedimentary units. 2D seismic profiles were also acquired in Storfjordrenna, using a Generator-Injector airgun operating in harmonic mode, with a total volume of 30 in^3 to generate seismic shots at a rate of 3 s. A hydrophone cable (16 m long, single-channel streamer) was used to record two-way travel time for the reflected seismic signal. Navigation correction, bandpass filtering and amplitude corrections were applied in DelphSeismic software and the data were visualised and interpreted using Petrel v.2014.1 software.

2.0 Summary of research papers

2.1 Paper 1

"Subglacial water storage and drainage beneath the Fennoscandian and Barents Sea ice sheets"

C. Shackleton, H. Patton, A. Hubbard, M. Winsborrow, J. Kingslake, M. Esteves, K. Andreassen, S. Greenwood. 2018. *Quaternary Science Reviews* **201**:13-28.

In this paper, long-term subglacial drainage development beneath an evolving ice sheet is investigated. Previously published, numerically modelled ice-sheet reconstructions of the Eurasian ice sheet are utilized to model potential subglacial meltwater drainage routes and predict the locations of subglacial lakes beneath the Fennoscandian and Barents Sea ice sheets. This analysis is performed at 1000-year intervals, during the build-up to, and retreat from, the Last Glacial Maximum (37-10 ka B.P.). Subglacial hydraulic potential surfaces are generated at discrete time-slices using modelled ice-sheet surfaces and isostatically corrected bed topographies. Gradients in hydraulic potential drive the flow of basal water, and so drainage routes are predicted by routing water down the maximum gradient in hydraulic potential. Subglacial lakes sites are identified by filling sites of hydraulic potential minima to their lip, with up to 3500 subglacial lakes predicted beneath the two ice sheets during ice maximum conditions. Asynchronous ice sheet growth over areas of flat relief in northeast Europe results in up to 100 km^3 more water stored within subglacial lakes during ice build-up compared to retreat, for similar ice sheet areal extents. To assess the validity of results, predicted subglacial drainage routing and subglacial lakes are assessed against empirical evidence for palaeo-meltwater drainage. This reveals potential sources and sinks for subglacial water either side of large subglacial channel networks in the Gulf of Bothnia, and good agreement with mapped subglacial lakes and channels in the central Barents Sea. The migration of ice-marginal meltwater outlets as the ice sheet decayed informs sites of focussed freshwater and sediment discharge, and maps of hydraulic potential minima persisting throughout the ice sheet evolution define potential targets for field-based investigations in search of palaeo-subglacial lakes and preserved sediments.

Author contributions:

CS designed the study together with HP and MW, and undertook the analysis, writing, figure making and editing. HP and AH supplied the model output used to calculate subglacial hydraulic potential surfaces. SG and ME provided mapping in the Gulf of Bothnia and central Barents Sea. All co-authors were involved in the discussion of the results and editing of the manuscript.

2.2 Paper 2

"Ice margin retreat and grounding-zone dynamics during initial deglaciation of the Storfjordrenna Ice Stream, western Barents Sea"

C. Shackleton, M. Winsborrow, K. Andreassen, R. Lucchi, L.R. Bjarnadóttir. 2019. *In Review, Boreas.*

This study investigates a retreating palaeo-ice margin, based on geomorphological mapping from high-resolution multibeam bathymetric datasets and subsurface data (2D seismic and CHIRP) acquired in outer Storfjordrenna, south of Svalbard. Data was acquired during two expeditions of the Centre for Arctic Gas Hydrate, Environment and Climate (CAGE) using the R/V Helmer Hanssen in 2013 and 2014. Geophysical data reveal ice marginal landforms including grounding zone deposits and an array of iceberg ploughmarks, created during initial retreat of the Storfjordrenna Ice Stream from its ice-maximum position at the continental shelf edge. Spatial clustering of distinct populations of iceberg ploughmarks indicate locally diverse controls on iceberg calving, which led to the production of deep-drafted, single-keeled icebergs at the northern sector of the former ice margin, and multi-keeled, tabular icebergs at the southern sector. Ice-proximal fans on the western flank of the grounding zone deposits indicate that meltwater conduits and ice marginal meltwater plumes were active during retreat, potentially contributing to the observed pattern of iceberg calving by undercutting and incising the ice margin. The heavily keel-scoured seafloor of outer Storfjordrenna indicates that ice retreat from the continental shelf break was characterised by rapid ice-margin break-up via large calving events. It is suggested that early retreat from the continental shelf edge in the northern sector of the ice stream was facilitated by retrograde bedslopes and proximal ice sources over Spitsbergen, whereas the southern sector of the ice stream remained grounded at the shelf edge for longer, delivering sediment-laden meltwater and building the continental slope. The grounding zone deposits documented in this study represent the first major still-stand in ice margin retreat from the continental shelf edge. 2D seismic profiles reveal three bedrock ridges, which, together with the protruding tip of southern Spitsbergen, provide basal and lateral pinning points for stabilization of the retreating ice margin.

Author contributions:

The data were acquired by KA and CS, who also designed the study together with MW. CS undertook the mapping, analysis, writing, figure making and editing. All co-authors were involved in the discussion of the results and editing of the manuscript.

2.3 Paper 3

Transitions in subglacial drainage and influences on glacial dynamics in the central Barents Sea, reconstructed from assemblages of meltwater landforms

> C. Shackleton, M. Winsborrow, H. Patton, M. Esteves, L. Bjarnadóttir, K. Andreassen, 2019. *Manuscript in preparation.*

In this study, the high-resolution MAREANO multibeam bathymetric dataset from the central Barents Sea is used to map subglacial meltwater landforms and refine existing geomorphological mapping on Thor-Iversenbanken, a shallow bank that formed an influential sector of the Barents Sea Ice Sheet (BSIS) bed in different stages of its development. Assemblages of eskers, meltwater channels and tunnel valleys are detected throughout the central Barents Sea, indicating that this region was a focus for meltwater throughout ice advance and retreat. The various drainage systems documented here operated at differing spatial and temporal scales, and formed in contrasting phases of the ice sheets evolution. Based on the geomorphological mapping and cross-cutting relationships, relative timing constraints are placed on the formation of the various meltwater landforms. A succession of meltwater drainage landforms is observed, evidencing meltwater flow through subglacial conduits incised into the ice sheet bed, with shifts in channel activity/inactivity resulting in a vast network of braided meltwater channels on the floor of wide tunnel valleys. Basins upstream of large tunnel valleys are inferred to be the site of palaeo-subglacial lakes, and cyclic filling and drainage of these are suggested to have impacted the development of the subglacial drainage system and downstream ice dynamics. During the later stages of ice retreat, meltwater conduits incised into basal ice within a limited distance of the retreating ice margin are evidenced by eskers superimposed onto the floors and banks of tunnel valleys. The morphology and organisation of eskers into closely-spaced parallel ridges suggests that the basal drainage systems operating during the late-deglacial stages were charged by supraglacial meltwater sources.

Author contributions:

CS designed the study together with MW, HP and ME. Geomorphological mapping was undertaken by CS and ME, with some published mapping provided by LB. CS undertook the analysis, writing, figure making and editing. All co-authors were involved in the discussion of the results and editing of the manuscript.

3.0 Synthesis

Through the combined application of geomorphologically based reconstruction, geophysical investigation of the seabed subsurface, and modelling of subglacial hydraulic pressure potential, this thesis contributes to an increased understanding of subglacial hydrology, grounding line dynamics, and ice sheet behaviour. A wide range of spatial and temporal scales of meltwater processes have been investigated: at the ice sheet scale over an entire glaciation (Paper 1), at the grounding line of a retreating ice margin (Paper 2), and over a region of the ice bed that experienced both ice maximum and deglacial stages of the ice sheet (Paper 3). The following sections examine the contributions that this thesis makes to scientific knowledge of subglacial hydrology and concludes with suggestions for future work.

3.1 Operational scales of subglacial drainage processes

Observations of present-day subglacial drainage systems have enhanced our understanding of subglacial hydrology and impacts on ice flow (e.g. Stearns et al., 2008; Gulley et al., 2012b; Andrews et al., 2014; Fricker et al., 2014; Smith et al., 2017). However, these insights are limited to observational time periods, which, relative to the operational time-scales of ice sheet evolution, are decidedly short-term. Despite the fragmentation of the landform record and uncertain timescales of landform creation (Kehew et al., 2012; Greenwood et al., 2016), the deglaciated beds of palaeo-ice sheets offer insights into subglacial hydrology over longer and more relevant time periods. This thesis advances understanding of the timescales of subglacial drainage processes by predicting the long-term behaviour of subglacial water storage and drainage in response to fluctuations in modelled ice sheet surfaces (Paper 1) and detangling a composite record of meltwater drainage landforms in the central Barents Sea that represent a range of subglacial drainage processes operational over contrasting timescales (Paper 3). Furthermore, it is shown that meltwater outlets operated at the ice margin during retreat of the Storfjordrenna Ice Stream, and were confined to the northern and southern sectors of the former ice margin (Paper 2).

Hydraulic potential modelling (Paper 1) predicts the routing of subglacial meltwater during ice sheet build-up and retreat, indicating potential locations of water storage at the bed to form subglacial lakes. The ephemeral nature of many subglacial lakes predicted in this study suggests that storage and release of basal water may have been sensitive to the shifting geometry of overlying ice, especially where subglacial lakes are predicted in topographically smoother areas of the bed, in the central/northern Barents Sea, and throughout Sweden and Finland (Paper 1; Fig. 3). These unstable sites of subglacial water storage are likely to drain with minor shifts in the geometry of overlying ice, leading to short-lived but significant influxes of meltwater to the subglacial drainage system and downstream ice stream beds. Contrastingly, predicted sites of large or clustered subglacial lakes that remain stable throughout ice sheet evolution are likely to have had a longer lasting influence on palaeo-ice dynamics. Particularly stable subglacial lakes are predicted in the

Gulf of Bothnia and Baltic Sea (Paper 1; Fig. 3b), corresponding well to empirical observations of high meltwater fluxes through this region (Greenwood et al., 2016b). Although not captured in our large-scale modelling approach, these subglacial lakes may have periodically filled, drained and exchanged water on timescales of months to years, similar to those detected beneath present day ice streams in Antarctica (Smith et al., 2009).

The seafloor in the central Barents Sea (Paper 3) contains meltwater landforms that represent subglacial drainage systems operating at various temporal and spatial scales, and in contrasting phases of ice sheet development. This thesis presents a composite map of meltwater landforms in the central Barents Sea (Paper 3; Fig. 9), with reconstructions of the geomorphically dominant subglacial drainage modes as the ice sheet developed (Paper 3; Fig. 10). Meltwater channels and tunnel valleys represent long-term drainage of subglacial water through this region, with channels potentially utilized over multiple glacial cycles. The braided and anastomosing structure of tunnel valleys indicates fluctuating meltwater supply to the drainage system which may have occurred seasonally, or intermittently due to fill and drain cycles of upstream subglacial water stores. The occurrence of eskers along the banks and channel floor of large meltwater channels and tunnel valleys informs a switch to meltwater incised into basal ice within R-Channels during the later stages of deglaciation. These landforms also indicate continued subglacial drainage towards the ice margin as it retreated through Sentralbankrenna and onto Thor-Iversenbanken. Here it is concluded that eskers are the geomorphic imprint of short-lived flooding events, with conduits possibly charged by influxes from supraglacial water sources. This indicates that the subglacial domain can be directly affected by climatic changes and inter-annual variations occurring at the surface of the ice sheet, as observed at outlet glaciers in Greenland (Bartholomew et al., 2011; Sole et al., 2011).

3.2 Factors influencing subglacial drainage patterns

Given the impacts of subglacial drainage on the ice sheet system, it is important to determine the factors influencing how water behaves at the ice-bed interface. Modelling the long-term development of subglacial drainage routing and water storage (Paper 1) reveals preferred locations for subglacial lakes at the beds of the BSIS and FIS. For the same areal extent, up to two times more water is stored within predicted subglacial lakes at the FIS bed during ice advance than during retreat (Paper 1; Fig. 5). This vast difference in water storage capacity is attributed to ice expansion into topographically smoother areas of the bed, with easterly migration of FIS ice domes into the flatter sectors of eastern Fennoscandia (Patton et al., 2017). Coupled with the steeper surface slopes of the retreating ice sheet, this may have promoted shallower, less stable subglacial lakes, with potential impacts on basal water availability and regulation of fast ice flow. In contrast, easterly migration of the BSIS into topographically rougher sectors of the eastern Barents Sea led to greater numbers of subglacial lakes predicted at the bed during the deglaciation phase, with only minor oscillations in water storage capacity during ice retreat (Paper 1; Fig. 5). This study highlights the

sensitivity of basal water storage to the shifting geometry of overlying ice and migration into areas of divergent topographic relief.

At the margin of the Storfjordrenna Ice Stream, ice proximal fans at the northern and southern sectors of the former grounding line indicate sediment deposition out of ice marginal meltwater plumes (Paper 2). It is inferred that the observed pattern of ice proximal fan deposits is caused by meltwater sourced from different sectors of the ice sheet, being routed either side of relatively thicker ice in the centre of the trough as the ice margin was grounded in outer-Storfjordrenna. Correspondingly, the hydraulic potential modelling predicts several drainage outlets at the ice margin in Storfjordrenna (Paper 1; Figure 8), which drain catchments that remain distinct throughout deglaciation, draining separate subglacial environments over Svalbard to the north, and the interior BSIS to the east and south. The modelling predicts that the largest meltwater drainage catchments outlet into northern Storfjordrenna, which is supported by observations of the largest ice proximal fan deposits in the north (Paper 2; Fig. 4).

Meltwater landforms in the central Barents Sea (Paper 3) indicate that large volumes of subglacial meltwater were routed towards and stored on Thor-Iversenbanken, potentially facilitated by the relatively flat ice sheet surface and extensive catchment area during ice maximum conditions, with ice draw-down towards Sentralbankrenna. During deglaciation, water supply from supraglacial sources is inferred based on esker morphology and distributions (Paper 3), and the pattern of basal drainage may have been influenced by the distribution of supraglacial lakes, moulins and surface crevasses. Also, Thor-Iversenbanken was in close proximity to inferred ice divides that migrated during deglaciation (Patton et al., 2016, 2017; Piasecka et al., 2016), and shifting of subglacial catchment boundaries may have led to re-routing of meltwater between catchments. With easterly migrating ice divides, the catchment boundary for the Sentralbankrenna glacial system expands into the eastern Barents Sea, potentially providing higher fluxes of meltwater to the ice-stream bed during deglaciation.

3.3 Subglacial drainage impacts on the ice sheet system and beyond

Studies from contemporary glaciers and ice sheets show that subglacial drainage system development is linked to changes in basal effective pressure and ice flow speed in Greenland (Sole et al., 2011), and subglacial lake drainage events correspond to increased flow in Antarctica (Stearns et al., 2008). Modelling of water exchange and drainage from subglacial lakes at the bed of Antarctic ice streams suggests that the development from distributed to channelized drainage systems may regulate basal water pressures and impact local and regional ice dynamics (Carter et al., 2017). The papers presented in this thesis indicate that subglacial meltwater played an important role across diverse sectors of the Fennoscandian and Barents Sea ice sheets and at various stages of advance and decay. Hydraulic potential modelling (Paper 1) indicates a large number of possible

sites for subglacial lake formation at the beds of the Fennoscandian and Barents Sea ice sheets. These sites occur in the onset zones and at the beds of major palaeo-ice streams, often in clusters (Paper 1; Fig. 3), suggesting the potential for water exchange and drainage system modulation, with impacts on local and regional ice flow.

The geomorphology of the central Barents Sea region (paper 3) indicates that it was a focus for meltwater routing, and that the BSIS had extensive drainage systems at its base. Geomorphologically based reconstructions indicate highly dynamic ice sheet behaviour in this region, with fast-flowing ice streams undergoing switches in flow speed and direction (Rüther et al., 2011; Winsborrow et al., 2012; Piasecka et al., 2016). Large, braided tunnel valleys and meltwater channels evidence high-discharge meltwater conduits feeding into the bed of the Sentralbankrenna Ice Stream, providing abundant meltwater to facilitate basal sliding in this region. Additionally, cyclic filling and draining of subglacial lakes is inferred as a source of periodic water injection into downstream subglacial drainage systems, with the potential for regulating basal lubrication and subglacial sediment shear strengths, contributing to ice flow variability in Sentralbankrenna.

This thesis also shows that subglacial hydrology impacted grounding line dynamics, sediment delivery to the ice margin, and the proglacial environment. The hydraulic potential modelling (Paper 1) predicts the locations of freshwater and sediment delivery to the evolving FIS and BSIS ice margin, and the migration of drainage routes and outlets as the ice sheets developed. Meltwater outlets are important controls on proglacial landscape evolution, contributing to the building and instability of sediments on the continental slope (Lucchi et al., 2012), while also influencing local ocean circulation (Slater et al., 2015). The modelling indicates where sediments and freshwater may have been focussed as the ice sheet retreated, with the largest inputs expected along the Norwegian Channel, in northern Bjørnøyrenna, the White Sea, and Baltic Sea (Paper 1; Fig. 8).

Ice marginal geomorphology in outer-Storfjordrenna (Paper 2) indicates that subglacial meltwater outlets delivered freshwater and sediments to the ice margin, and distinct patterns of iceberg calving may have been influenced by outlet locations particularly to the north of the former ice margin as it was grounded in outer-Storfjordrenna. Freshwater fluxes at modern sub-marine ice margins are shown to influence ice margin mass loss through convective-driven melting and undercutting of the calving face (Jenkins, 2011; Chauché et al., 2014). Sediment delivery over the grounding line and settling out of ice marginal meltwater plumes deposited distinct ice proximal fans at the northern and southern flanks of grounding zone deposits (Paper 2; Fig. 4). These landforms are characteristic of meltwater-dominated marine-terminating ice streams, and add to a growing body of evidence for ice stream margin stillstands in this region during deglaciation, with grounding line dynamics and deposition heavily influenced by subglacial meltwater (Bjarnadóttir et al., 2013; Esteves et al., 2017).

3.4 Future work

The work presented in this thesis highlights the importance of subglacial hydrology beneath the LGM ice sheets across Fennoscandia and the Barents Sea. However, analysing composite geomorphological records formed by meltwater processes that occur at contrasting temporal and spatial scales requires a greater understanding of the formation mechanisms of landforms. Also, given the low preservation potential of subglacial lakes in the landform record, modelling approaches to predicting subglacial lake locations at both deglaciated and modern ice beds might be the most efficient way to locate potential sites for further study. A key output of the hydraulic potential modelling work are maps of persistently predicted locations for subglacial lakes beneath the evolving ice sheets (Paper 1, Fig. 3). These sites are widespread across Fennoscandia and the northern Barents Sea, and are useful targets for future investigations in search of geomorphological and sedimentological evidence of palaeo-subglacial lakes.

While the deglaciated beds of former ice streams are comparatively well-studied, further geophysical investigation of inter-ice stream regions and shallower banks is required to fully determine the role that upstream hydrology plays in regulating surrounding and downstream ice dynamics. Increased data collection in the Barents Sea region has already revealed abundant meltwater features where they were previously thought to be absent (Clark and Walder, 1994), highlighting the importance of geomorphic mapping studies based on high-resolution geophysical datasets. Some meltwater landforms are beyond the resolution of existing digital elevation models in data-poor regions, and further mapping will help to reconstruct a more complete overview of the palaeo-ice sheet system. Additionally, subsurface profiles over key landforms in the central Barents Sea region would help to resolve the formation of more complex, composite landforms such as the braided tunnel valley systems, and landforms with limited geomorphological expression on the seabed such as subglacial lakes.

Despite the observed correlation between increases in meltwater input and increases in ice flow speed at contemporary ice sheets (Sole et al., 2011; Stearns et al., 2008), the mechanisms behind switches in subglacial drainage mode and feedbacks on ice dynamics are still largely unknown (Greenwood et al., 2016a). Observations at contemporary ice sheets and glaciers are therefore crucial to understanding diurnal, seasonal, and decadal development of subglacial drainage. On longer timescales, subglacial hydrological modelling fully-coupled to an evolving ice beds are required to fully understand the influence of meltwater on basal sliding, improving simulations of palaeo-ice advance and retreat over the Barents Sea and Fennoscandia, as well as improving forecast models of contemporary ice sheet response to changes in climate. The abundance of undisturbed evidence for glacial and meltwater processes makes the central Barents Sea an ideal case-study for empirical testing of model results.

4.0 References

Alley, R.B., 1989. Water-pressure coupling of sliding and bed deformation: 1. Water system. *J. Glaciol.* 35, 108–118.

Anderson, R.S., Hallet, B., Walder, J., Aubry, B.F., 1982. Observations in a cavity beneath grinnell glacier. *Earth Surf. Process. Landforms* 7, 63–70. doi:10.1002/esp.3290070108

Andreassen, K., Laberg, J.S., Vorren, T.O., 2008. Seafloor geomorphology of the SW Barents Sea and its glaci-dynamic implications. *Geomorphology* 97, 157–177. doi:10.1016/j.geomorph.2007.02.050

Andreassen, K., Odegaard, C.M., Rafaelsen, B., 2007. Imprints of former ice streams, imaged and interpreted using industry three-dimensional seismic data from the south-western Barents Sea. *Geol. Soc. London, Spec. Publ.* 277, 151–169. doi:10.1144/GSL.SP.2007.277.01.09

Andreassen, K., Winsborrow, M.C.M., 2009. Signature of ice streaming in Bjørnøyrenna, Polar North Atlantic, through the pleistocene and implications for ice-stream dynamics. *Ann. Glaciol.* 50, 17–26. doi:10.3189/172756409789624238

Andrew G. Fountain, 1994. Borehole water-level variations and implications for the subglacial hydraulics of South Cascade Glacier, Washington State, V.S.A. *J. Glaciol.* 40, 293–304.

Andrews, L.C., Catania, G.A., Hoffman, M.J., Gulley, J.D., Lüthi, M.P., Ryser, C., Hawley, R.L., Neumann, T.A., 2014. Direct observations of evolving subglacial drainage beneath the Greenland Ice Sheet. *Nature* 514, 80–83. doi:10.1038/nature13796

Arnold, N., Sharp, M., 2002. Flow variability in the Scandinavian ice sheet: Modelling the coupling between ice sheet flow and hydrology. *Quat. Sci. Rev.* 21, 485–502. doi:10.1016/S0277-3791(01)00059-2

Auriac, A., Whitehouse, P.L., Bentley, M.J., Patton, H., Lloyd, J.M., Hubbard, A., 2016. Glacial isostatic adjustment associated with the Barents Sea ice sheet: A modelling inter-comparison. *Quat. Sci. Rev*. 147, 122–135. doi:10.1016/j.quascirev.2016.02.011

Bartholomew, I., Nienow, P., Mair, D., Hubbard, A., King, M.A., Sole, A., 2010. Seasonal evolution of subglacial drainage and acceleration in a Greenland outlet glacier. *Nat. Geosci.* 3, 408–411. doi:10.1038/ngeo863

Bartholomew, I., Nienow, P., Sole, A., Mair, D., Cowton, T., Palmer, S., Wadham, J., 2011. Supraglacial forcing of subglacial drainage in the ablation zone of the Greenland ice sheet. *Geophys. Res. Lett.* 38, 1–5. doi:10.1029/2011GL047063

Bell, R.E., Studinger, M., Fahnestock, M.A., Shuman, C.A., 2006. Tectonically controlled subglacial lakes on the flanks of the Gamburtsev Subglacial Mountains, East Antarctica. *Geophys. Res. Lett.* 33. doi:10.1029/2005GL025207

Bennett, M.R., 2003. Ice streams as the arteries of an ice sheet: Their mechanics, stability and significance. *Earth-Science Rev.* 61, 309–339. doi:10.1016/S0012-8252(02)00130-7

Bjarnadóttir, L.R., Rüther, D.C., Winsborrow, M.C.M., Andreassen, K., 2013. Grounding-line dynamics during the last deglaciation of Kveithola, W Barents Sea, as revealed by seabed geomorphology and shallow seismic stratigraphy. *Boreas* 42, 84–107. doi:10.1111/j.1502-3885.2012.00273.x

Boulton, G.S., Caban, P.E., Van Gijssel, K., 1995. Groundwater Flow Beneath Ice Sheets : Part I - Patterns. *Quaterny Sci. Rev.* 14, 545–562. doi:10.1016/0277-3791(95)00039-r

Boulton, G.S., Dobbie, K.., Zatsepin, S., 2001. Sediment deformation beneath glaciers and its coupling to the subglacial hydraulic system. *Quat. Int.* 86, 3–28. doi:10.1016/S1040-6182(01)00048-9

Boulton, G.S., Lunn, R., Vidstrand, P., Zatsepin, S., 2007. Subglacial drainage by groundwater–channel coupling, and the origin of esker systems: part II—theory and simulation of a modern system. *Quat. Sci. Rev.* 26, 1091–1105. doi:10.1016/j.quascirev.2007.01.006

Carter, S.P., Fricker, H.A., Siegfried, M.R., 2017. Antarctic subglacial lakes drain through sediment-floored canals: Theory and model testing on real and idealized domains. *Cryosph*. 11, 381–405. doi:10.5194/tc-2016-74

Carter, S.P., Fricker, H.A., Siegfried, M.R., 2013. Evidence of rapid subglacial water piracy under Whillans Ice Stream, West Antarctica. *J. Glaciol.* 59, 1147–1162. doi:10.3189/2013JoG13J085

Chauché, N., Hubbard, A., Gascard, J.-C., Box, J.E., Bates, R., Koppes, M., Sole, A., Christoffersen, P., Patton, H., 2014. Ice–ocean interaction and calving front morphology at two west Greenland tidewater outlet glaciers. *Cryosph*. 8, 1457–1468. doi:10.5194/tc-8-1457-2014

Clark, P.U., Walder, J.S., 1994. Subglacial drainage, eskers, and deforming beds beneath the Laurentide

and Eurasian ice sheets. *Geol. Soc. Am. Bull. 1*06, 304–314. doi:10.1130/0016-7606(1994)106<0304:SDEADB>2.3.CO;2
Clarke, G.K.C., 2005. Subglacial Processes. *Annu. Rev. Earth Planet.* Sci. 33, 247–276. doi:10.1146/annurev.earth.33.092203.122621
Clarke, G.K.C., Collins, S.G., Thompson, D.E., 1984. Flow, thermal structure, and subglacial conditions of a surge-type glacier. *Can. J. Earth Sci.* 21, 232–240. doi:10.1139/e84-024
Clason, C. C., Applegate, P. J., Holmlund, P., 2014. Modelling Late Weichselian evolution of the Eurasian ice sheets forced by surface meltwater-enhanced basal sliding. *J. Glaciol.* 60(219), 29–40. doi: 10.3189/2014JoG13J037.
Cowton, T., Nienow, P., Bartholomew, I., Sole, A., Mair, D., 2012. Rapid erosion beneath the Greenland ice sheet. *Geology* 40, 343–346. doi:10.1130/G32687.1
Cowton, T., Nienow, P., Sole, A., Wadham, J., Lis, G., Bartholomew, I., Mair, D., Chandler, D., 2013. Evolution of drainage system morphology at a land-terminating Greenlandic outlet glacier. *J. Geophys. Res. Earth Surf.* 118, 29–41. doi:10.1029/2012JF002540
Creyts, T.T., Schoof, C.G., 2009. Drainage through subglacial water sheets. *J. Geophys. Res. Earth Surf.* 114, 1–18. doi:10.1029/2008JF001215
Dahlgren, K.I.T., Vorren, T.O., Stoker, M.S., Nielsen, T., Nygård, A., Sejrup, H.P., 2005. Late Cenozoic prograding wedges on the NW European continental margin: Their formation and relationship to tectonics and climate. *Mar. Pet. Geol.* 22, 1089–1110. doi:10.1016/j.marpetgeo.2004.12.008
De Fleurian, B., Werder, M.A., Beyer, S., Brinkerhoff, D.J., Delaney, I., Dow, C.F., Downs, J., Gagliardini, O., Hoffman, M.J., Hooke, R.L., Seguinot, J., Sommers, A.N., 2018. SHMIP The subglacial hydrology model intercomparison Project. *J. Glaciol.* 1–20. doi:10.1017/jog.2018.78
Doyle, S.H., Hubbard, B., Christoffersen, P., Young T J, Hofstede, C., Bougamont M, Box J E, Hubbard A, 2018. Physical Conditions of Fast Glacier Flow: 1 . Measurements From Boreholes Drilled to the Bed of Store Glacier, West Greenland. *J. Geophys. Res. Earth Surf.* 123.
Esteves, M., Bjarnadóttir, L.R., Winsborrow, M.C.M., Shackleton, C.S., Andreassen, K., 2017. Retreat patterns and dynamics of the Sentralbankrenna glacial system, Central Barents Sea. *Quat. Sci. Rev.* 169, 131–147. doi:10.1016/j.quascirev.2017.06.004
Favier, L., Durand, G., Cornford, S.L., Gudmundsson, G.H., Gagliardini, O., Gillet-Chaulet, F., Zwinger, T., Payne, A.J., Le Brocq, A.M., 2014. Retreat of Pine Island Glacier controlled by marine ice-sheet instability. *Nat. Clim. Chang.* doi:10.1038/nclimate2094
Fountain, A.G., 1993. Geometry and flow conditions of subglacial water at South Cascade Glacier, Washington State, USA; an analysis of tracer injections. *J. Glaciol.* 39, 143–156. doi:10.1017/S0022143000015793
Fountain, A.G., 1992. Subglacial water flow inferred from stream measurements at South Cascade Glacier, Washington, U.S.A. *J. Glaciol.* 38, 51–64.
Fowler, A., Walder, J.S., 1994. Channelized subglacial drainage over a deformable bed. *J. Glaciol*. 40, 3–15.
Fricker, H.A., Carter, S.P., Bell, R.E., Scambos, T., 2014. Active lakes of recovery ice stream, East Antarctica: A bedrock-controlled subglacial hydrological system. *J. Glaciol.* 60, 1015–1030. doi:10.3189/2014JoG14J063
Fricker, H.A., Scambos, T., Bindschadler, R., Padman, L., 2007. An active subglacial water system in West Antarctica mapped from space. Science (80-.). 315, 1544–1548. doi:10.1126/science.1136897
Greenwood, S.L., Clason, C.C., Helanow, C., Margold, M., 2016a. Theoretical, contemporary observational and palaeo-perspectives on ice sheet hydrology: Processes and products. *Earth-Science Rev.* 155, 1–27. doi:10.1016/j.earscirev.2016.01.010
Greenwood, S.L., Clason, C.C., Jakobsson, M., 2016b. Ice-flow and meltwater landform assemblages in the Gulf of Bothnia. *Geol. Soc. London Mem.* 46, 321–324. doi:10.1144/M46.163
Greenwood, S.L., Clason, C.C., Nyberg, J., Jakobsson, M., Holmlund, P., 2017. The Bothnian Sea ice stream: early Holocene retreat dynamics of the south-central Fennoscandian Ice Sheet. *Boreas* 46, 346–362. doi:10.1111/bor.12217
Gulley, J., Benn, D.I., 2007. Structural control of englacial drainage systems in Himalayan debris-covered glaciers. *J. Glaciol.* 53, 399–412. doi:10.3189/002214307783258378
Gulley, J.D., Benn, D.I., Screaton, E., Martin, J., 2009. Mechanisms of englacial conduit formation and their implications for subglacial recharge. *Quat. Sci. Rev.* 28, 1984–1999.

doi:10.1016/j.quascirev.2009.04.002
Gulley, J.D., Grabiec, M., Martin, J.B., Jania, J., Catania, G., Glowacki, P., 2012a. The effect of discrete recharge by moulins and heterogeneity in flow-path efficiency at glacier beds on subglacial hydrology. *J. Glaciol.* 58, 926–940. doi:10.3189/2012JoG11J189
Gulley, J.D., Walthard, P., Martin, J., Banwell, A.F., Benn, D.I., Catania, G., 2012b. Conduit roughness and dye-trace breakthrough curves: Why slow velocity and high dispersivity may not reflect flow in distributed systems. *J. Glaciol.* 58, 915–925. doi:10.3189/2012JoG11J115
Hanna, E., Navarro, F.J., Pattyn, F., Domingues, C.M., Fettweis, X., Ivins, E.R., Nicholls, R.J., Ritz, C., Smith, B., Tulaczyk, S., Whitehouse, P.L., Zwally, H.J., 2013. Ice-sheet mass balance and climate change. *Nature*. doi:10.1038/nature12238
Hart, J.K., Rose, K.C., Clayton, A., Martinez, K., 2015. Englacial and subglacial water flow at Skálafellsjökull, Iceland derived from ground penetrating radar, in situ Glacsweb probe and borehole water level measurements. *Earth Surf. Process. Landforms* 40, 2071-2083. doi:10.1002/esp.3783
Hewitt, I.J., 2011. Modelling distributed and channelized subglacial drainage: the spacing of channels. *J. Glaciol.* 57, 302–314. doi:10.3189/002214311796405951
Hubbard, B.P., Sharp, M.J., Willis, I.C., Nielsen M K, Smart C C, 1995. Borehole water-level variations and the structure of the subglacial hydrological system of Haut Glacier d'Arolla, Valais, Switzerland. *J. Glaciol.* 41, 572–583.
Iken, A., 1981. The effect of the subglacial water pressure on the sliding velocity of a glacier in an idealized numerical model. *J. Glaciol*. 27, 407–421. doi:10.3198/1981JoG27-97-407-421
Iken, A., Bindschadler, R.A., 1986. Combined Measurements of Sub Glacial Water Pressure and Surface Velocity of Findelengletscher, Switzerland: Conclusions About Drainage System and Sliding Mechanism. *J. Glaciol.* 32, 101–119.
Iken, A., Echelmeyer, K., Harrison, W., Funk, M., 1993. Mechanisms of fast flow in Jakobshavn Isbrae, West Greenland: Part I. Measurements of temperature and water level in deep boreholes. J. Glaciol. 39. doi:10.1017/S0022143000015689
Jamieson, S.S.R., Vieli, A., Livingstone, S.J., Ó Cofaigh, C., Stokes, C., Hillenbrand, C.-D., Dowdeswell, J.A., 2012. Ice-stream stability on a reverse bed slope. *Nat. Geosci.* 5, 799–802. doi:10.1038/NGEO1600
Jansson, P., 1995. Water pressure and basal sliding on Storglaciaren, northern Sweden. *J. Glaciol*. 41, 232–240. doi:10.1017/S0022143000016130
Jenkins, A., 2011. Convection-Driven Melting near the Grounding Lines of Ice Shelves and Tidewater Glaciers. *J. Phys. Oceanogr.* 41, 2279–2294. doi:10.1175/JPO-D-11-03.1
Joughin, I., Alley, R.B., Holland, D.M., 2012. Ice-sheet response to oceanic forcing. *Science* 338, 1172–6. doi:10.1126/science.1226481
Kamb, B., 2001. Basal Zone of the West Antarctic Ice Streams and its Role in Lubrication of Their Rapid Motion, in: Alley, R.B., Bindschadler, R.A. (Eds.), TheWest Antarctic Ice Sheet: Behaviour and Environment. *American Geophysical Union,* 157–199. doi:10.1029/AR077p0157
Kamb, B., 1987. Glacier Surge Mechanism Based on Linked Cavity Configuration of the Basal Water Conduit System. *J. Geophys. Res*. 92, 9083–9100.
Kamb, B., Raymond C F, Harrison W D, Engelhardt, H., Echelmeyer, K., Humphrey, N., Brugman, M.M., Pfeffer, T., 1985. Glacier Surge Mechanism: 1982-1983 Surge of Variegated Glacier, Alaska. *Science* 227, 469–479.
Katz, R.F., Worster, M.G., 2010. Stability of ice-sheet grounding lines. *Proc. R. Soc. A Math. Phys. Eng. Sci.* 466, 1597–1620. doi:10.1098/rspa.2009.0434
Kehew, A., Piotrowski, J., Jørgensen, F., 2012. Tunnel valleys: Concepts and controversies — A review. *Earth-Science Rev.* 113, 33–58. doi:10.1016/j.earscirev.2012.02.002
Kleman, J., Hattestrand, C., 1999. Frozen-bed Fennoscandian and Laurentide ice sheets during the Last Glacial Maximum. *Nature* 402, 63–66. doi:10.1038/47005
Kleman, J., Hättestrand, C., Stroeven, A.P., Jansson, K.N., Angelis, H. De, Borgstrom, I., 2006. Reconstruction of palaeo-ice sheets — inversion of their glacial geomorphological record. *Glacier Sci. Environ. Chang.* 192–198.
Kuhn, G., Hillenbrand, C.-D., Kasten, S., Smith, J.A., Nitsche, F.O., Frederichs, T., Wiers, S., Ehrmann, W., Klages, J.P., Mogollon, J.M., 2017. Evidence for a palaeo-subglacial lake on the Antarctic continental shelf. *Nat. Commun.* 8, 15591. doi:10.1038/ncomms15591

Laberg, J.S., Andreassen, K., Knies, J., Vorren, T.O., Winsborrow, M.C.M., 2010. Late Pliocene – Pleistocene development of the Barents Sea Ice Sheet. *Geol. Soc. Am.* 38, 107–110. doi:10.1130/G30193.1

Laberg, J.S., Andreassen, K., Vorren, T.O., 2012. Late cenozoic erosion of the high-latitude southwestern barents sea shelf revisited. *Bull. Geol. Soc. Am.* 124, 77–88. doi:10.1130/B30340.1

Laberg, J.S., Vorren, T.O., 1995. Late Weichselian Submarine Debris Flow Deposits On the Bear-island-trough-mouth-fan. *Mar. Geol.* 127, 45–72.

Livingstone, S.J., Clark, C.D., Piotrowski, J.A., Tranter, M., Bentley, M.J., Hodson, A., Swift, D.A., Woodward, J., 2012. Theoretical framework and diagnostic criteria for the identification of palaeo-subglacial lakes. *Quat. Sci. Rev.* 53, 88–110. doi:10.1016/j.quascirev.2012.08.010

Lucchi, R.G., Pedrosa, M.T., Camerlenghi, A., Urgeles, R., De Mol, B., Rebesco, M., 2012. Recent Submarine Landslides on the Continental Slope of Storfjorden and Kveithola Trough-Mouth Fans (North West Barents Sea), in: In: Yamada, Y., Kawamura, K., Ikehara, K., Ogawa, Y., Urgeles, R.,Mosher, D., Chaytor, J., Strasser, M. (Eds.), Submarine Mass Movements and Their Consequences. Advances in Natural and Technological Hazards Research, *Springer Science Book Series,* 31. pp. 735–745. doi:10.1007/978-94-007-2162-3

Mangerud, J., 2004. Ice sheet limits in Norway and on the Norwegian continental shelf. *Dev. Quat. Sci.* 2, 271–294. doi:10.1016/S1571-0866(04)80078-2

Mangerud, J., Jakobsson, M., Alexanderson, H., Astakhov, V., Clarke, G.K.C., Henriksen, M., Hjort, C., Krinner, G., Lunkka, J.P., Möller, P., Murray, A., Nikolskaya, O., Saarnisto, M., Svendsen, J.I., 2004. Ice-dammed lakes and rerouting of the drainage of northern Eurasia during the Last Glaciation. *Quat. Sci. Rev.* 23, 1313–1332. doi:10.1016/j.quascirev.2003.12.009

Marshall, S.J., Clarke, G.K.C., 1999. Modelling North American freshwater runoff through the last glacial cycle. *Quat. Res.* 52, 300–315. doi:10.1006/qres.1999.2079

Nitsche, F.O., Gohl, K., Larter, R.D., Hillenbrand, C.D., Kuhn, G., Smith, J.A., Jacobs, S., Anderson, J.B., Jakobsson, M., 2013. Paleo ice flow and subglacial meltwater dynamics in Pine Island Bay, West Antarctica. *Cryosph.* 7, 249–262. doi:10.5194/tc-7-249-2013

Oswald, G.K.A., Gogineni, S.P., 2008. Recovery of subglacial water extent from Greenland radar survey data. *J. Glaciol.* 54, 94–106. doi:10.3189/002214308784409107

Ottesen, D., Dowdeswell, J.A., Rise, L., 2005. Submarine landforms and the reconstruction of fast-flowing ice streams within a large Quaternary ice sheet: The 2500-km-long Norwegian-Svalbard margin (57-80N). *Bull. Geol. Soc. Am.* 117, 1033–1050. doi:10.1130/B25577.1

Patton, H., Hubbard, A., Andreassen, K., Auriac, A., Whitehouse, P.L., Stroeven, A.P., Shackleton, C., Winsborrow, M.C.M., Heyman, J., Hall, A.M., 2017. Deglaciation of the Eurasian ice sheet complex. *Quat. Sci. Rev.* 169, 148–172. doi:10.1016/j.quascirev.2017.05.019

Patton, H., Hubbard, A., Andreassen, K., Winsborrow, M.C.M., Stroeven, A.P., 2016. The build-up, configuration, and dynamical sensitivity of the Eurasian ice-sheet complex to Late Weichselian climatic and oceanic forcing. *Quat. Sci. Rev.* 153, 97–121. doi:10.1016/j.quascirev.2016.10.009

Piasecka, E.D., Winsborrow, M.C.M., Andreassen, K., Stokes, C.R., 2016. Reconstructing the retreat dynamics of the Bjørnøyrenna Ice Stream based on new 3D seismic data from the central Barents Sea. *Quat. Sci. Rev.* 151, 212–227. doi:10.1016/j.quascirev.2016.09.003

Piotrowski, J.A., 1997. Subglacial hydrology in north-western Germany during the last glaciation: Groundwater flow, tunnel valleys and hydrological cycles. *Quat. Sci. Rev.* 16, 169–185. doi:10.1016/S0277-3791(96)00046-7

Powell, R.D., 1990. Glacimarine processes at grounding-line fans and their growth to ice-contact deltas. *Geol. Soc. London, Spec. Publ.* 53, 53–73. doi:10.1144/GSL.SP.1990.053.01.03

Pritchard, H.D., Arthern, R.J., Vaughan, D.G., Edwards, L.A., 2009. Extensive dynamic thinning on the margins of the Greenland and Antarctic ice sheets. *Nature* 461, 971–5. doi:10.1038/nature08471

Röthlisberger, H., 1972. Water Pressure in Intra- and Subglacial Channels. *J. Glaciol.* 11, 177–203. doi:10.1017/S0022143000022188

Rüther, D.C., Mattingsdal, R., Andreassen, K., Forwick, M., Husum, K., 2011. Seismic architecture and sedimentology of a major grounding zone system deposited by the Bjørnøyrenna Ice Stream during Late Weichselian deglaciation. *Quat. Sci. Rev.* 30, 2776–2792. doi:10.1016/j.quascirev.2011.06.011

Sejrup, H.P., Larsen, E., Landvik, J., King, E.L., Haflidason, H., Nesje, a., 2000. Quaternary glaciations in southern Fennoscandia: Evidence from southwestern Norway and the northern North Sea region.

Quat. Sci. Rev. 19, 667–685.
Sharp, M., Richards, K., Willis, I., Arnold, N., Nienow, P., Lawson, W., Tison, J.-L., 1993. Geometry, bed topography and drainage system structure of the haut glacier d'Arolla, Switzerland. *Earth Surf. Process. Landforms* 18, 557–571. doi:10.1002/esp.3290180608
Shaw, J., 2002. The meltwater hypothesis for subglacial bedforms. *Quat. Int.* 90, 5–22. doi:10.1016/S1040-6182(01)00089-1
Shreve, R.L., 1972. The movement of water in glaciers. *J. Glaciol.* 11, 205–214.
Siegfried, M.R., Fricker, H.A., Carter, S.P., Tulaczyk, S., 2016. Episodic ice velocity fluctuations triggered by a subglacial flood in West Antarctica. *Geophys. Res. Lett*. 43, 2640–2648. doi:10.1002/2016GL067758
Simkins, L.M., Anderson, J.B., Greenwood, S.L., Gonnermann, H.M., Prothro, L.O., Ruth, A., Halberstadt, W., Stearns, L.A., Pollard, D., Deconto, R.M., 2017. Anatomy of a meltwater drainage system beneath the ancestral East Antarctic ice sheet. *Nat. geo* 10, 691–698. doi:10.1038/NGEO3012
Slater, D.A., Nienow, P.W., Cowton, T.R., Goldberg, D.N., Sole, A.J., 2015. Effect of near-terminus subglacial hydrology on tidewater glacier submarine melt rates. *Geophys. Res. Lett.* 42, 2861–2868. doi:10.1002/2014GL062494
Smith, B.E., Fricker, H.A., Joughin, I.R., Tulaczyk, S.M., 2009. An inventory of active subglacial lakes in Antarctica detected by ICESat (2003-2008). *J. Glaciol.* 55, 573–595. doi:10.3189/002214309789470879
Smith, B.E., Gourmelen, N., Huth, A., Joughin, I., 2017. Connected subglacial lake drainage beneath Thwaites Glacier, West Antarctica. *Cryosph*. 11, 451–467. doi:10.5194/tc-11-451-2017
Sole, A.J., Mair, D.W.F., Nienow, P.W., Bartholomew, I.D., King, M.A., Burke, M.J., Joughin, I., 2011. Seasonal speedup of a Greenland marine-terminating outlet glacier forced by surface melt-induced changes in subglacial hydrology. *J. Geophys. Res. Earth Surf.* 116, 1–11. doi:10.1029/2010JF001948
Stearns, L.A., Smith, B.E., Hamilton, G.S., 2008. Increased flow speed on a large East Antarctic outlet glacier caused by subglacial floods. *Nat. Geosci.* 1, 827–831. doi:10.1038/ngeo356
Stocker, T.F., Qin, D., Plattner, G.-K., Tignor, M., Allen, S.K., Boschung, J., Nauels, A., Xia, Y., Bex, V., Midgley, P.., 2013. IPCC, 2013: Climate Change 2013: The Physical Science Basis. Contribution of Working Group 1 to the Fifth Assessment Report of the Intergovernmental Panel on Climate Change. *Cambridge University Press.*
Stroeven, A.P., Hättestrand, C., Kleman, J., Heyman, J., Fabel, D., Fredin, O., Goodfellow, B.W., Harbor, J.M., Jansen, J.D., Olsen, L., Caffee, M.W., Fink, D., Lundqvist, J., Rosqvist, G.C., Strömberg, B., Jansson, K.N., 2016. Deglaciation of Fennoscandia. *Quat. Sci. Rev.* 147, 91–121. doi:10.1016/j.quascirev.2015.09.016
Toucanne, S., Soulet, G., Freslon, N., Silva Jacinto, R., Dennielou, B., Zaragosi, S., Eynaud, F., Bourillet, J.F., Bayon, G., 2015. Millennial-scale fluctuations of the European Ice Sheet at the end of the last glacial, and their potential impact on global climate. *Quat. Sci. Rev.* 123, 113–133. doi:10.1016/j.quascirev.2015.06.010
Vaughan, D.G., Comiso, J.C., Allison, I., Carrasco, J., Kaser, G., Kwok, R., Mote, P., Murray, T., Paul, F., Ren, J., Rignot, O., Steffen, K., Zhang, T., 2013. IPCC, 2013: Climate Change, The Physical Science Basis. Contribution of Working Group I to the Fifth Assessment Report of the Intergovernmental Panel on Climate Change. doi:10.1017/CBO9781107415324.012
Vorren, T.O., Laberg, J.S., 1997. Trough mouth fans — palaeoclimate and ice-sheet monitors. *Quat. Sci. Rev.* 16, 865–881. doi:10.1016/S0277-3791(97)00003-6
Vorren, T.O., Landvik, J., Andreassen, K., Laberg, J.S., 2011. Glacial History of the Barents Sea Region, 1st ed, Quaternary Glaciations - Extent and Chronology. *Elsevier Inc.* doi:10.1016/B978-0-444-53447-7.00027-1
Vorren, T.O., Lebesbye, E., Andreassen, K., Larsen, K.-B., 1988. Glacigenic seidments on a passive continental margin as exemplified by the barents Sea. *Mar. Geol.* 85, 251–272.
Weertman, J., 1972. General theory of water flow at the base of a glacier or ice sheet. *Rev. Geophys.* 10, 287–333.
Werder, M.A., Hewitt, I.J., Schoof, C.G., Flowers, G.E., 2013. Modeling channelized and distributed subglacial drainage in two dimensions. *J. Geophys. Res. Earth Surf.* 118, 2140–2158. doi:10.1002/jgrf.20146
Winberry, J.P., Anandakrishnan, S., Alley, R.B., 2009. Seismic observations of transient subglacial water-

flow beneath MacAyeal Ice Stream, West Antarctica. *Geophys. Res. Lett.* 36, 1–5. doi:10.1029/2009GL037730

Wingham, D.J., Siegert, M.J., Shepherd, A., Muir, A.S., 2006. Rapid discharge connects Antarctic subglacial lakes. *Nature* 440, 1033–1036. doi:10.1038/nature04660

Winsborrow, M.C.M., Andreassen, K., Corner, G.D., Laberg, J.S., 2010. Deglaciation of a marine-based ice sheet: Late Weichselian palaeo-ice dynamics and retreat in the southern Barents Sea reconstructed from onshore and offshore glacial geomorphology. *Quat. Sci. Rev.* 29, 424–442. doi:10.1016/j.quascirev.2009.10.001

Winsborrow, M.C.M., Stokes, C.R., Andreassen, K., 2012. Ice-stream flow switching during deglaciation of the southwestern Barents Sea. *Bull. Geol. Soc. Am.* 124, 275–290. doi:10.1130/B30416.1

Paper 1

Subglacial water storage and drainage beneath the Fennoscandian and Barents Sea ice sheets

Calvin Shackleton, Henry Patton, Alun Hubbard, Monica Winsborrow, Jonathan Kingslake, Mariana Esteves, Karin Andreassen, Sarah Greenwood. 2018.

Quaternary Science Reviews **201**: 13-28.

Quaternary Science Reviews 201 (2018) 13–28

Contents lists available at ScienceDirect

Quaternary Science Reviews

journal homepage: www.elsevier.com/locate/quascirev

Subglacial water storage and drainage beneath the Fennoscandian and Barents Sea ice sheets

Calvin Shackleton [a, *], Henry Patton [a], Alun Hubbard [a, b], Monica Winsborrow [a], Jonathan Kingslake [c], Mariana Esteves [a], Karin Andreassen [a], Sarah L. Greenwood [d]

[a] CAGE - Centre for Arctic Gas Hydrate, Environment and Climate, Department of Geosciences, UiT the Arctic University of Norway, 9037, Tromsø, Norway
[b] Department of Geography and Earth Science, Aberystwyth University, Wales, SY23 3DB, UK
[c] Lamont-Doherty Earth Observatory, Columbia University, Palisades, NY, 10964, USA
[d] Department of Geological Sciences, Stockholm University, Stockholm, 106 91, Sweden

ARTICLE INFO

Article history:
Received 5 July 2018
Received in revised form
8 October 2018
Accepted 8 October 2018

Keywords:
Subglacial lakes
Basal hydrology
Meltwater drainage
Fennoscandian ice sheet
Barents sea ice sheet
Eurasian ice sheet complex
Late weichselian
Last glacial maximum
Glacial geology
Glaciation

ABSTRACT

Subglacial hydrology modulates how ice sheets flow, respond to climate, and deliver meltwater, sediment and nutrients to proglacial and marine environments. Here, we investigate the development of subglacial lakes and drainage networks beneath the Fennoscandian and Barents Sea ice sheets over the Late Weichselian. Utilizing an established coupled climate/ice flow model, we calculate high-resolution, spatio-temporal changes in subglacial hydraulic potential from ice sheet build-up (~37 ka BP) to complete deglaciation (~10 ka BP). Our analysis predicts up to 3500 potential subglacial lakes, the largest of which was 658 km^2, and over 70% of which had surface areas <10 km^2, comparable with subglacial lake-size distributions beneath the Antarctic Ice Sheet. Asynchronous evolution of the Fennoscandian Ice Sheet into the flatter relief of northeast Europe affected patterns of subglacial drainage, with up to 100 km^3 more water impounded within subglacial lakes during ice build-up compared to retreat. Furthermore, we observe frequent fill/drain cycles within clusters of subglacial lakes at the onset zones and margins of ice streams that would have affected their dynamics. Our results resonate with mapping of large subglacial channel networks indicative of high-discharge meltwater drainage through the Gulf of Bothnia and central Barents Sea. By tracking the migration of meltwater drainage outlets during deglaciation, we constrain locations most susceptible to focussed discharge, including the western continental shelf-break where subglacial sediment delivery led to the development of major trough-mouth fans. Maps of hydraulic potential minima that persist throughout the Late Weichselian reveal potential sites for preserved subglacial lake sediments, thereby defining useful targets for further field-investigation.

1. Introduction

The presence and behaviour of water at the interface between an ice mass and its substrate exerts a fundamental control over many aspects of ice sheet behaviour. Lubrication of the ice-bed interface and subglacial sediment shear strengths are regulated by subglacial water pressure, driving ice flow variability over diurnal and seasonal time-scales (Alley, 1989; Boulton et al., 2001; Weertman, 1972). Refreezing of meltwater at the bed and the resultant release of latent heat also warms and softens basal and englacial ice, leading to enhanced deformation (Arnold and Sharp, 2002; Bell et al., 2014). Subglacial water availability also plays a key role in regulating ice flow, by controlling the distribution of high traction zones (sticky spots) via basal freeze-on (Sergienko and Hulbe, 2011; Trommelen et al., 2014; Winsborrow et al., 2016), and water piracy between neighbouring catchments (Anandakrishnan and Alley, 1997; Carter et al., 2013; Lindbäck et al., 2015). Furthermore, freshwater fluxes exiting sub-marine ice margins directly modulate the rate of mass loss beneath ice shelves and at calving faces through convective-driven melting (Chauché et al., 2014; Jenkins, 2011; Xu et al., 2012). Critically though, changes in ice sheet geometry also strongly influence subglacial hydrological behaviour; even minor changes in ice thickness in areas of low relief can lead to rerouting of basal water flow

* Corresponding author.
E-mail address: calvin.s.shackleton@uit.no (C. Shackleton).

https://doi.org/10.1016/j.quascirev.2018.10.007
0277-3791/

(Vaughan et al., 2008).

Subglacial lakes are an important component of the subglacial drainage system, and have been studied extensively despite their extreme inaccessibility (Wright and Siegert, 2012). Geophysical and modelling investigations of subglacial lakes and hydrology beneath contemporary ice sheets (Carter et al., 2017; Dowdeswell and Siegert, 2003; Fricker et al., 2007; Hubbard et al., 2004; Lindbäck et al., 2015; Wingham et al., 2006), along with modelling and sedimentary/geomorphic studies of palaeo-subglacial lakes (Christoffersen et al., 2008; Esteves et al., *In Review;* Livingstone et al., 2013a, 2016; Kuhn et al., 2017), has led to improved understanding of their formation, longevity and influence on ice sheet dynamics. Episodic filling and drainage of subglacial lakes (e.g. Winberry et al., 2009) has been directly linked to accelerations in ice stream velocity (Carter et al., 2013; Stearns et al., 2008) and modifications to background stick-slip cycles in Antarctica (Siegfried et al., 2016). Moreover, internally modulated filling/drainage cycles (Smith et al., 2017; Stearns et al., 2008; Wingham et al., 2006) reveals that subglacial hydrology impacts on ice velocity and mass balance independently of climate forcing. Hence, it is important to consider the mechanisms driving long and short-term behaviour of subglacial lakes and their influence on basal drainage when assessing the current and future stability of ice masses globally.

Palaeo-ice sheets provide an opportunity to investigate the evolution of subglacial hydrological processes over millennial time scales. The Eurasian Ice Sheet Complex (EISC) was the third largest ice mass globally after the Antarctic and the North American ice sheets during the last glaciation, and was comprised of the Celtic Ice Sheet (CIS), the Fennoscandian Ice Sheet (FIS) and the Barents Sea Ice Sheet (BSIS). During the Last Glacial Maximum (LGM), the margins of the EISC reached the continental shelf break along most of the northern and western borders of the Barents Sea, Norway, and the British Isles (Fig. 1). In this study, we focus on the Fennoscandian and Barents Sea sectors of the EISC: independent ice sheet centres which contrasted in their glaciologic, geographic and topographic setting. The majority of the BSIS was grounded below sea level, thereby providing a useful palaeo-analogue for the marine-based West Antarctic Ice Sheet. Conversely, the FIS was largely terrestrial-based, draining ice from the Scandes Mountains to its eastern and southern margins, though with substantial marine terminating-sectors and outlets off the present-day Norwegian and Danish coasts.

Shreve's (1972) subglacial hydraulic potential analysis has been widely applied to infer basal water storage and drainage characteristics beneath both contemporary and palaeo-ice sheets and glaciers, at timescales ranging from days to tens of thousands of years (Alley, 1989; Banwell et al., 2013, 2012; Chu et al., 2016; Le Brocq et al., 2009; Lindbäck et al., 2015; Livingstone et al., 2013a, 2013b; Pattyn, 2008; Sharp et al., 1993; Siegert, 2000; Siegert et al., 2007; Smith et al., 2017; Tulaczyk et al., 2000; Vaughan et al., 2008; Wright et al., 2008; Arnold and Sharp, 2002; Evatt et al., 2006; Gudlaugsson et al., 2017; Patton et al., 2017a). In this study, we use modelled ice sheet surfaces (Patton et al., 2016, 2017a) and associated isostatic perturbations to reconstruct and investigate the temporal and spatial evolution of potential subglacial drainage routes and subglacial lakes beneath the FIS and BSIS during the build-up to, and retreat from, the LGM. Furthermore, through combined examination of the empirical record, we analyse the potential impacts associated with water routing and storage beneath the ice sheets during deglaciation.

2. Methods

2.1. Model output and data

Patton et al. (2016; 2017a) present a first-order thermomechanical model reconstruction of the evolving EISC throughout the Late Weichselian, constrained and validated against a diverse suite of empirical data (Patton et al., 2017a) and independent glacial isostatic adjustment modelling (Auriac et al., 2016). The ice-flow model is fully described in Hubbard (2006) and consists of a first-order approximation of the Stokes equations, which include longitudinal stress gradients that become increasingly important across steep relief and basal conditions that drive fast-flow (Hubbard, 2000). For the Eurasian domain, the 3D model was

Fig. 1. The Fennoscandian and Barents Sea sectors of the Eurasian Ice Sheet complex. Last Glacial Maximum (LGM) ice extent is drawn in white (Patton et al., 2017a), major troughs are named and the flow directions of their associated palaeo-ice streams are indicated with arrows. Present-day lakes are drawn in blue. Lt. = Lithuania; Lv. = Latvia; Ee. = Estonia; HT = Hinlopen Trough; KvT = Kvitøya trough; FVT = Franz Victoria Trough; SF = Storfjordrenna; DR = Djuprenna; VF/TD = Vestfjorden/Traenadjupet.

applied to a finite-difference grid based on the GEBCO_2014 GRID filtered to a resolution of 10 km, with isostatic loading implemented using an elastic lithosphere/relaxed asthenosphere scheme (Le Meur and Huybrechts, 1996). The first order rheology has been validated against ISMIP-HOM benchmark experiments (Pattyn et al., 2008) and used to successfully reconstruct palaeo-ice sheets across Iceland, Britain and Patagonia (Hubbard et al., 2005, 2006; 2009; Kuchar et al., 2012; Patton et al., 2013a, 2013b; 2017b). Surface mass balance is determined by a positive degree-day scheme, with both temperature and precipitation adjusting to the evolving ice sheet surface according to prescribed lapse rates derived from multiple regression analyses of modern meteorological observations. Perturbations in climate forcing are scaled against the NGRIP $\partial^{18}O$ ice-core record (Andersen et al., 2004) and sea level forcing applied from a global eustatic reconstruction (Waelbroeck et al., 2002). In this study, we develop the analysis presented by Patton et al. (2017a), and use modelled ice sheet geometry and isostatic adjustments based on output from their model, applied to a resampled (500 m) and filtered GEBCO_2014 Grid (version 20150318, www.gebco.net), to calculate subglacial hydraulic potential over the Late Weichselian glaciation.

2.2. Hydraulic potential calculation

The flow of water at the bed of glaciers and ice sheets is driven by gradients in hydraulic pressure potential (ϕ), which according to Shreve (1972) is a function of the elevation potential and water pressure:

$$\phi = \rho_w g z_b + F\rho_i g(z_s - z_b), \quad (1)$$

Where ρ_w is the density of water (1000 kg m^{-3}); g is the acceleration due to gravity (9.81 m s^{-2}); z_b is the bed elevation; ρ_i is the density of ice (917 kg m^{-3}); z_s is the height of the ice sheet surface. The flotation factor (F) is the ratio between subglacial water pressure and the ice overburden pressure, and varies temporally and spatially according to meltwater inputs, drainage system character, basal ice temperature, and the underlying substrate (Andrews et al., 2014; Clarke, 2005).

Boreholes drilled to the bed of the Greenland Ice Sheet reveal a range of subglacial water pressures generally above 90% of the ice overburden pressure. Spatially and temporally averaged (over at least a full melt season) measurements within boreholes of 94.8–96.7% (Doyle et al., 2018); 88–94%; 82–92%; ~100% (Meierbachtol et al., 2013); 85–94% (Thomsen et al., 1991); and 80–110% (Wright et al., 2016) of the overburden are reported, with a mean value of 92.41%. Based on this we adopt an F-value of 0.925, while recognizing that this is a generalisation of the relationship between ice overburden pressure and mean, long-term subglacial water pressure. Banwell et al. (2013) suggest, based on the relationship between modelled run-off and measured proglacial discharge in Greenland, that a value of 0.925 is realistic when averaged over a full melt season. Likewise, Lindbäck et al. (2015) use values ranging from 0.5 to 1.1 to investigate hydrological sensitivities but find a value of 0.925 to be optimal for part of the western sector of the Greenland Ice Sheet.

Equation (1) implicitly demonstrates that ice surface slopes exert ~10-times stronger control on subglacial water flow than basal topography. However, ice sheet surface slopes are generally low and basal slopes can exceed that of the surface by an order of magnitude, and therefore remain a strong influence on the routing and storage of subglacial water, particularly in regions characterised by rugged basal topography. Flow routing tools in the ArcHydro toolbox for ArcGIS 10.5 assume that the steepest gradient in hydraulic potential constrains water flow direction at a given point in eight possible directions. The flow direction of each cell is combined to yield optimal hydrological flowpaths and thereby the predicted drainage network. This method is suitable for the prediction of arborescent channel networks, as the flow routing tools calculate the most efficient path to route water from areas of high to low hydraulic potential. Potential subglacial lake locations are identified by filling local minima in modelled hydraulic potential to their spill point. Subglacial lakes with an area ≤ 2 km^2 are filtered out from the analysis to reduce the impact of interpolation artefacts on results. The capacity for water storage at the bed at each time slice is calculated using the volume to which hydraulic potential requires adjusting to remove the hydraulic potential minima and hence, maximum subglacial lake volume is estimated under the assumption of bank-full conditions. Modelled subglacial drainage maps are generated for discrete time slices at 100-year intervals from 37 to 10 ka BP, and the persistence of hydraulic features is determined by tracking and collating the locations of modelled drainage features through time.

2.3. Methodological and data limitations

Equation (1) couples subglacial water routing to modelled ice sheet thickness and surface gradients in a generalised manner, and furthermore, this approach ignores the reciprocal impact of subglacial water on ice flow. Basal water flow and pressure varies in time and space in response to a multitude of factors including ice sheet characteristics, the nature of the substrate, and meltwater delivery, all of which impact on basal lubrication (Christoffersen et al., 2018; Johnson and Fastook, 2002) and ice flow (Iken, 1981). Also, subglacial water pressure is likely to be much lower close to the ice margin where ice is thinner, and our chosen value for the flotation factor is less representative in this sector where channelized systems may dominate, leading to less reliable predictions of subglacial drainage (Gulley et al., 2012). Meierbachtol et al. (2013) find that conduit pressures of less than 70% of the ice overburden pressure are limited to <10 km from the ice margin, and that subglacial pressures increase to the overburden pressure (i.e. F approaches 1) further into the interior as ice thickness and hydrostatic pressure increases.

Furthermore, coupling feedbacks between the base of the ice sheet and subglacial drainage system are not accounted for, such as lack of basal friction and ice surface flattening over subglacial lakes, and local fluctuations in thermal regime and melt rate. The drainage features modelled in this study are therefore described as potential subglacial routes and lakes and should be considered representative of large-scale patterns of basal drainage. Additionally, conditions that determine subglacial drainage system morphology are absent from this method, including underlying geology, water supply, and sediment load. Limitations for the approach also include the reliability of modelled ice sheet output for calculating hydraulic potential, and interpolation errors in the topography data. An analysis of subglacial lake predictions for an LGM timeslice and the associated GEBCO_2014 source data used for hydraulic potential calculations is presented in Table S1. Furthermore, the digital elevation model (DEM) used for our calculations contains post-glacial sediments and erosion surfaces along with present-day lakes, all of which introduce potential sources of error. Some of these errors can be mitigated by applying a 3×3 gaussian filter to the bed DEM and by masking out present-day lakes where appropriate.

2.4. Model sensitivity

A suite of sensitivity experiments was conducted to assess the relative importance of the key parameters influencing the total areal extent of predicted subglacial lakes and the degree to which

their spatial extents intersect with the optimum experiment (Table 1). To test the sensitivity of subglacial lakes to changes in water pressure, an experiment using the LGM ice sheet surface (21 ka BP) was conducted, varying the flotation factor (F) using values 0.7, 0.8, 0.925 and 1.0. Model sensitivity to bed roughness was also assessed through varying degrees of bed filtering; the unfiltered GEBCO_2014 DEM, and the results of 1, 2, and 3 passes of a 3×3 gaussian filter were used to yield progressive bed smoothing before the hydraulic potential calculation was applied. Sensitivity to modelled basal temperatures was assessed by masking subglacial lake predictions in areas of the bed below −1.5, −0.75, and 0 °C (relative to the pressure melting point) and comparing to the optimum experiment without a basal temperature filter. To assess predicted subglacial lake sensitivity to uncertainties in ice model physics, the hydraulic potential analysis was applied under different LGM ice thicknesses, generated using a range of deformation/viscosity (A_0) parameters (Patton et al., 2016). This empirical flow enhancement coefficient is a conventional adaption of Glen's flow law, used to encompass the effects of crystal anisotropy and impurities on bulk ice deformation (Cuffey and Paterson, 2010). The most significant result of modifying strain rates is that softer ice tends to flow faster, resulting in a lower aspect ratio ice sheet and shallower long-profiles of glaciers, while stiffer ice produces thicker glaciers and ice sheets with steeper profiles.

3. Results

3.1. Subglacial drainage routing

The modelled subglacial drainage system is organised into linear or dendritic channel networks, which flow in radial patterns from the main ice sheet accumulation centres (Fig. 2a–i). Alongside this radial pattern, topographic features direct large drainage systems along major troughs or around subglacial obstacles. The most extensive subglacial drainage catchments are constrained by their surrounding and underlying topography, and are concentrated beneath palaeo-ice streams such as those occupying the Baltic, Bjørnøyrenna and St. Anna troughs (Figs. 1 and 2). Linear drainage systems close to the ice margins mostly ignore even large-scale topographic features, such as the mountains of Novaya Zemlya, the southern tip of Finland, and present northern coastline of Estonia (Fig. 2d–g) during modelled ice maximum conditions. Extensive and well-connected drainage systems are predicted with increased frequency under ice maximum conditions (Fig. 2c–g), while the dominance of smaller, linear drainage systems is common when ice sheets are smaller and thinner (Fig. 2a,b,h,i).

Some drainage systems are insensitive to fluctuations in ice sheet geometry and remain stable through time. For example, once established, the drainage routes and outlets predicted under the ice streams flowing over the mid-Norwegian shelf (Fig. 1), Hinlopen trough (Fig. 1: HT), and Kvitøya trough east of Svalbard (Fig. 1: KvT) remain stable and persist throughout the latter stages of the glaciation (Fig. 2b–g). The present-day Baltic Sea and Gulf of Bothnia host the longest potential drainage network from source to outlet, attaining lengths over 1600 km, and draining the subglacial environment of fast-flowing ice in the Baltic Sea (Fig. 2a–i). This extensive catchment is already active by 30 ka BP and drains subglacial water from terrestrial Sweden and Finland (Fig. 2a). During the modelled build up to LGM conditions, outlet locations remain relatively stable, draining into north-east and coastal Poland at maximum southern ice margin extents (Fig. 2c–f), and shifting northwards to drain into the southern Baltic Sea basin and on into the Gulf of Bothnia as the ice stream retreats (Fig. 2g–i).

In the Barents Sea, ice accumulation centres over the islands of Svalbard and Franz Josef Land result in radial drainage during initial ice build-up (Fig. 2a), which is partly funnelled by Storfjordrenna, Bjørnøyrenna, the Franz Victoria Trough, St. Anna Trough, and the surrounding more intricate topographic channels. The modelled ice centres merge and shift southwards towards the central Barents Sea as the ice sheet grows, causing a 90-degree shift in flow direction, shown in the transition between Fig. 2a and b and Fig. 2c and d. Bjørnøyrenna hosts the most expansive and hydraulically well-connected drainage system, with a marine-terminating catchment extending from the continental shelf edge into central parts of the Barents Sea (Fig. 2e–g), more than 900 km from source to outlet. As the BSIS retreats through Bjørnøyrenna, drainage routes and outlets migrate eastwards in connection with the shifting ice domes (Fig. 2g and h). The Bjørnøyrenna, Storfjordrenna and north Norwegian Coast Parallel trough catchments experience considerable shifts in marine-terminating drainage outlet locations with changing ice sheet geometry. During ice maximum conditions beginning around 24 ka BP, these three vast catchments drain directly into the Polar North Atlantic, focussed along the western Barents Sea shelf break (Fig. 2c). This ends abruptly following the retreat of the ice margin from the shelf break (after 17 ka BP), after which the outlets are more distributed, draining into the much shallower western Barents Sea (Fig. 2g) and ultimately draining into the central and south-eastern Barents Sea following the break-up of the Fennoscandian-Barents Sea ice saddle (Fig. 2h).

3.2. Potential subglacial lakes

Local hydraulic potential minima, indicative of potential subglacial lakes, are widespread across the beds of the FIS and BSIS. Many subglacial lake locations are regularly predicted in regions of high relief, such as western Novaya Zemlya, Franz Josef Land, Svalbard, the Norwegian coast and across central Scandinavia (Fig. 2a–i; 3a,b). Furthermore, relatively large clusters of subglacial lakes tend to be predicted under thick ice and in inner ice sheet regions, including the central and northern Barents Sea, central Sweden and Finland, the Baltic, and in the Gulf of Bothnia (Fig. 2). In these central areas, predicted subglacial lake locations follow the shifting ice domes, especially in the Barents Sea, where easterly migration is accompanied by an increase in the number and size of region occupied by subglacial lakes in the east of the Barents Sea. As ice thickens between the FIS and BSIS, subglacial lakes are predicted with increased frequency in the southern Barents Sea, especially beneath the thickest ice towards the central sectors (Fig. 2a–g). Subglacial lakes nearer the ice margins are more likely to be found where topography is particularly pronounced, for example, close to the present-day coastlines of northwest Norway and western Novaya Zemlya, and around Svalbard and Franz Josef Land (Fig. 2).

Fig. 3 maps subglacial lake persistence, measured as the duration of their presence as a percentage of the total time that each location was ice covered. Many remain stable in the northern Barents Sea (Fig. 3a), Gulf of Bothnia, Baltic Sea and over central Scandinavia and coastal Norway (Fig. 3b), with larger and deeper subglacial lakes commonly persisting for over 80% of the time that ice was present. Our results show that subglacial lakes are more persistent in areas of rugged topography such as Franz Josef Land, Svalbard, and the western Norwegian fjords (Fig. 3a, b), and in the stoss sides of major ice-bed topographic obstacles, for example, along the western coast of Novaya Zemlya (Fig. 3a) and the north Estonian coast (Fig. 3b); such topographically-controlled lakes are particularly resilient to changes in ice sheet geometry. Widespread occurrence of potential subglacial lake locations is also predicted in less topographically influenced areas, for example in the relatively flat areas of the northern Barents Sea, surrounding Sentralbankrenna (Fig. 3a), and particularly large examples in the Gulf

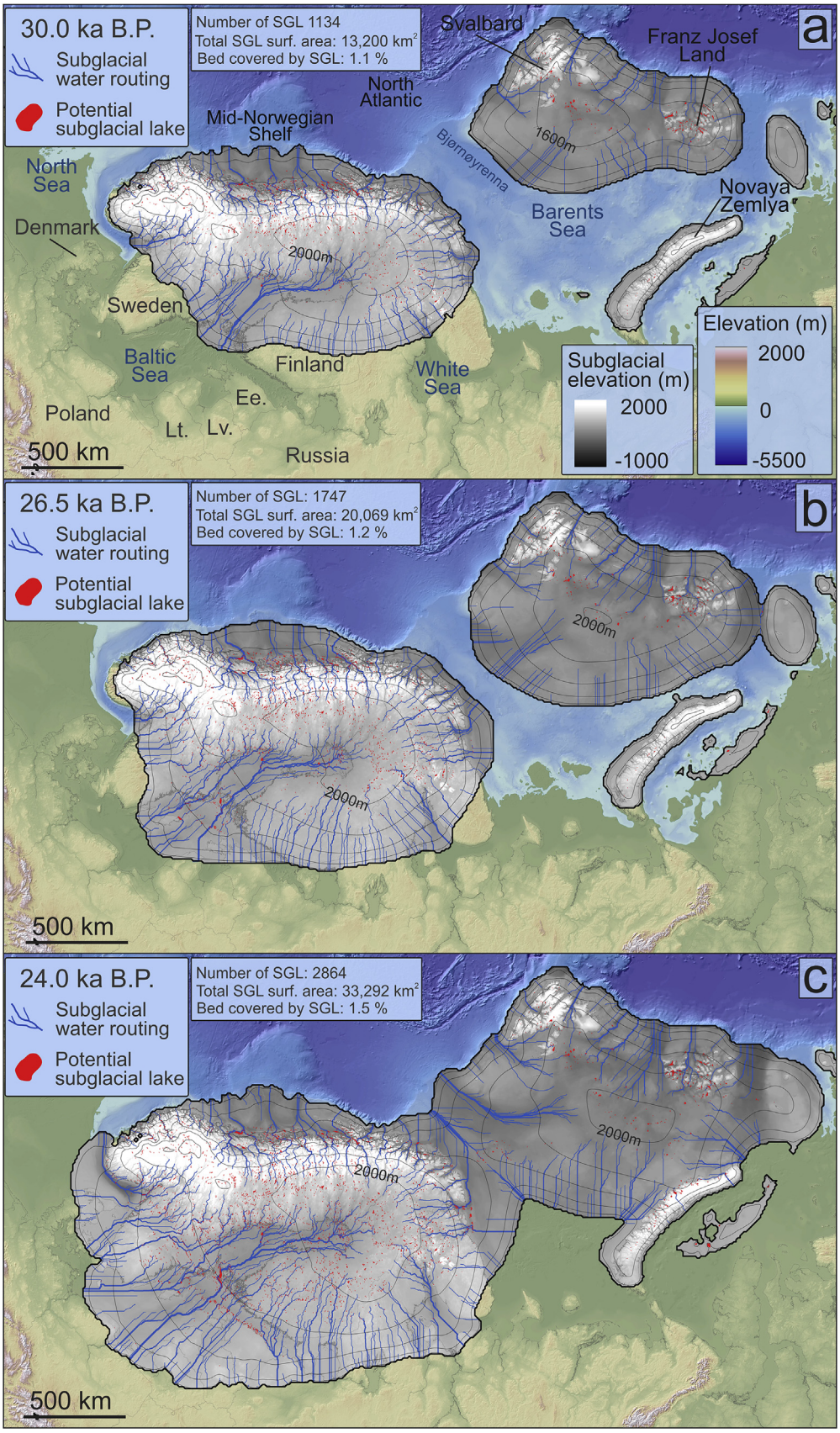

Fig. 2. Subglacial hydrological evolution of the FIS and BSIS, as snapshots of hydrology in the build up to the LGM (**a-c**), during the LGM (**d-f**) and during ice retreat (**g-i**). The Strahler stream order method of calculating downstream connectivity was applied to the predicted water routes and stream width is proportional to this. Subglacial topography is coloured in greyscale, and ice-sheet surface slope is indicated by contours at 400 m intervals. The coastline evolves in response to changes in isostatic loading and fluctuations in eustatic sea level; the present-day coastline is shown to aid spatial reference. Subglacial lakes and drainage routing in the Norwegian Channel at 22.7 ka BP were calculated in conjunction with simulated ice covering the British Isles. SGL = Subglacial lake; Lt. = Lithuania; Lv. = Latvia; Ee. = Estonia.

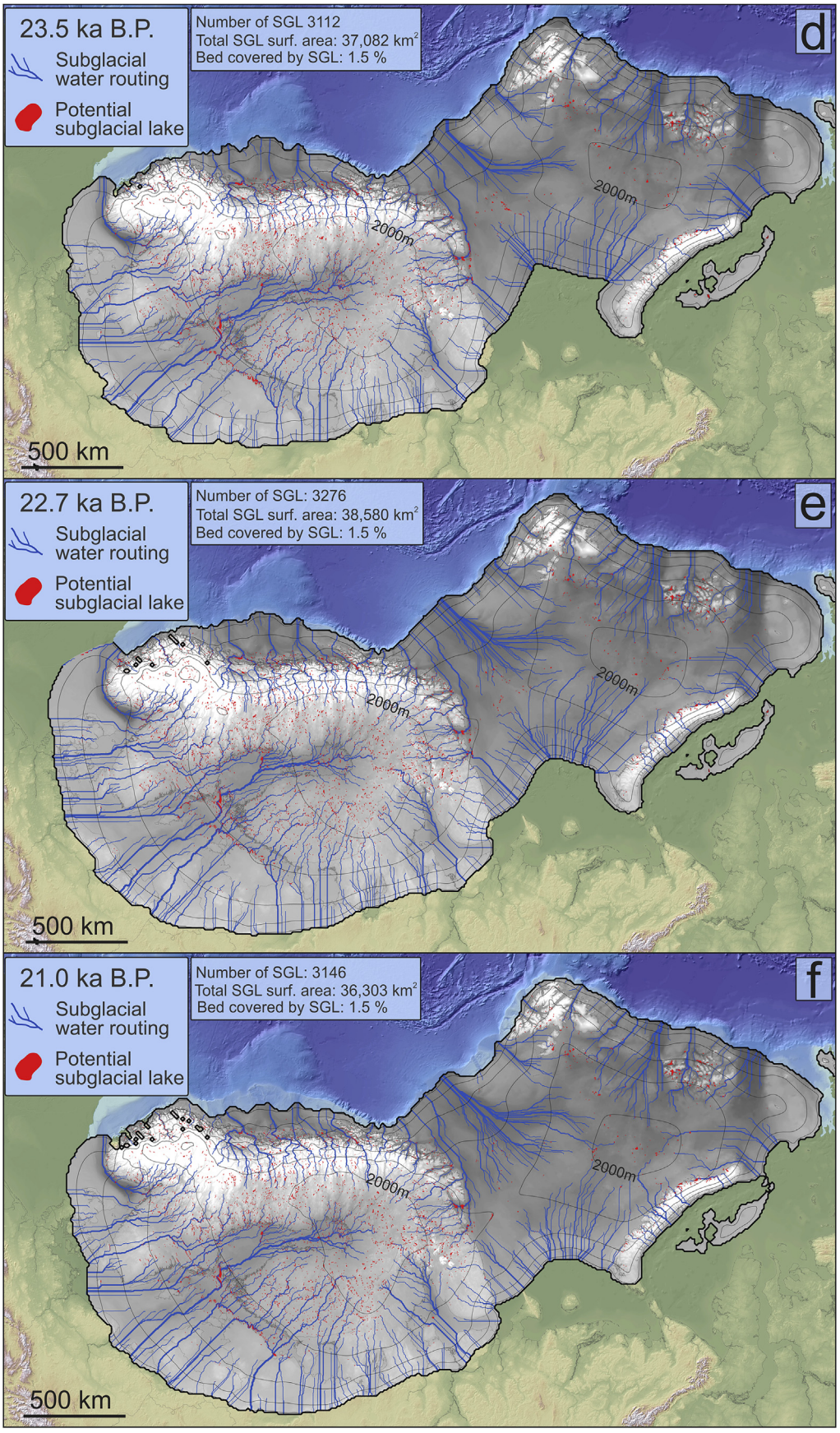

Fig. 2. (*continued*).

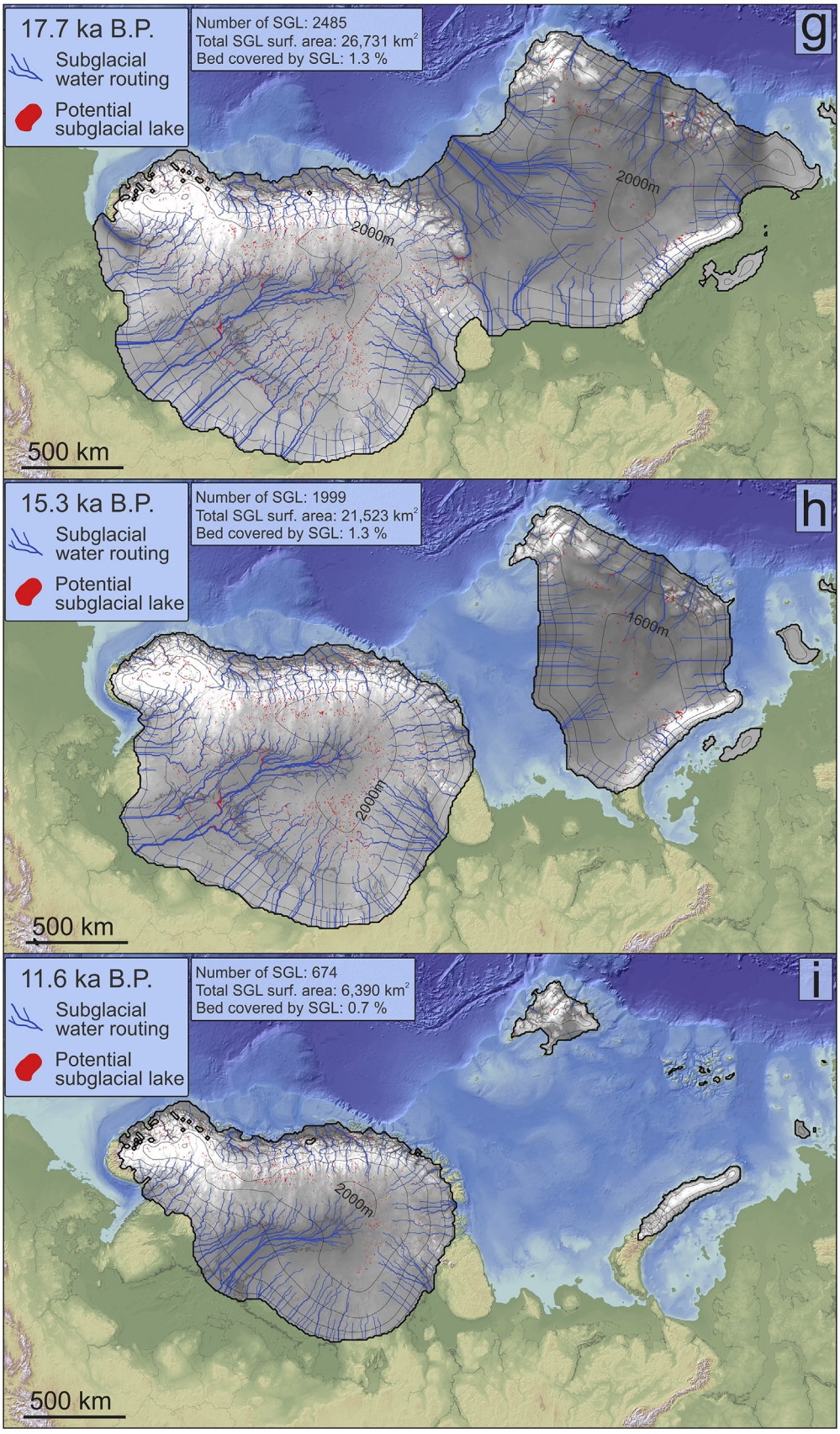

Fig. 2. (*continued*).

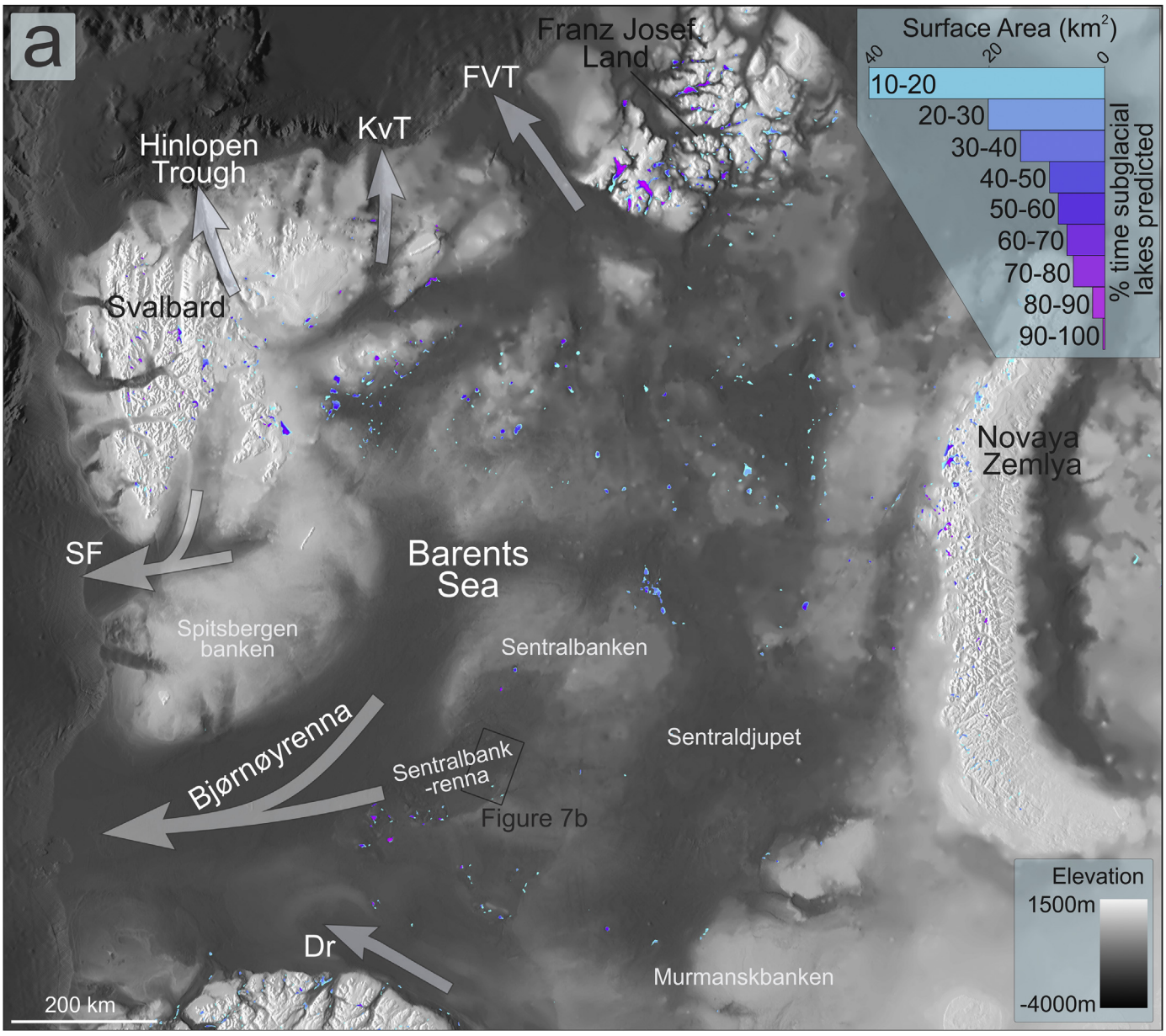

Fig. 3. Subglacial lake persistency shows the percentage of time that subglacial lakes formed while ice covered in (**a**) the Barents Sea and (**b**) Fennoscandia. The surface area of the different persistency classes is also plotted. The omitted category of 1–10% persistency covers surface areas of 22,166 km^2 over Fennoscandia, and 17,869 km^2 for the Barents Sea region. BIS = Baltic Ice Stream; NC = Norwegian Channel; Dr = Djuprenna; FVT = Franz Victoria Trough; KvT = Kvitøya trough; SF = Storfjordrenna; Vf/Td = Vestfjorden/Traenadjupet.

of Bothnia (Fig. 3b). Some areas lack subglacial lakes, including the relatively shallow areas of Spitsbergenbanken and Murmanskbanken (Fig. 3a), and in the floors of several large troughs including Bjørnøyrenna, the Franz Victoria Trough, Sentraldjupet, and the Norwegian Channel (Fig. 3a, b).

The number of predicted subglacial lakes increases as the ice sheet builds up to its LGM extent (Fig. 4a), with the highest lake count of 3449 (>2 km^2) occurring at 22.9 ka BP, followed by stepped decreases in lake numbers. A temporary increase in both the number of subglacial lakes (Fig. 4a) and volume of water stored within them (Fig. 4b) at the FIS bed occurs immediately before 15 ka BP, following a short re-advance phase and ice surface flattening in the Baltic Sea during overall deglaciation. Fewer lakes are predicted at the bed of the BSIS, peaking later than that of the FIS, with a lingering plateau in lake numbers and water storage through deglaciation (Fig. 4a, b). The relative proportion of the FIS subglacial environment covered by lakes increases from 0.4% around 10 ka BP to a peak of 1.3% at 22.9 ka BP. During the lead-up to, and throughout ice-maximum conditions around 24 ka BP, bed coverage by subglacial lakes increases (Fig. 4c) and broadly follows the fluctuating areal extent of the FIS. The BSIS had less of its bed occupied by potential subglacial lakes (Fig. 4c), between 0.1 and 0.4% and with only minor fluctuations over the course of the glaciation. Estimated amounts of water stored within subglacial lakes at the bed of the FIS are much greater during ice build-up than during retreat (Fig. 5), with >100 km^3 difference for the same ice sheet areal extent. Storage of water at the bed of the BSIS (Fig. 5) peaks twice during ice build-up around 34 ka BP and 26 ka BP with more linear reductions and minor oscillations in water storage capacity throughout retreat.

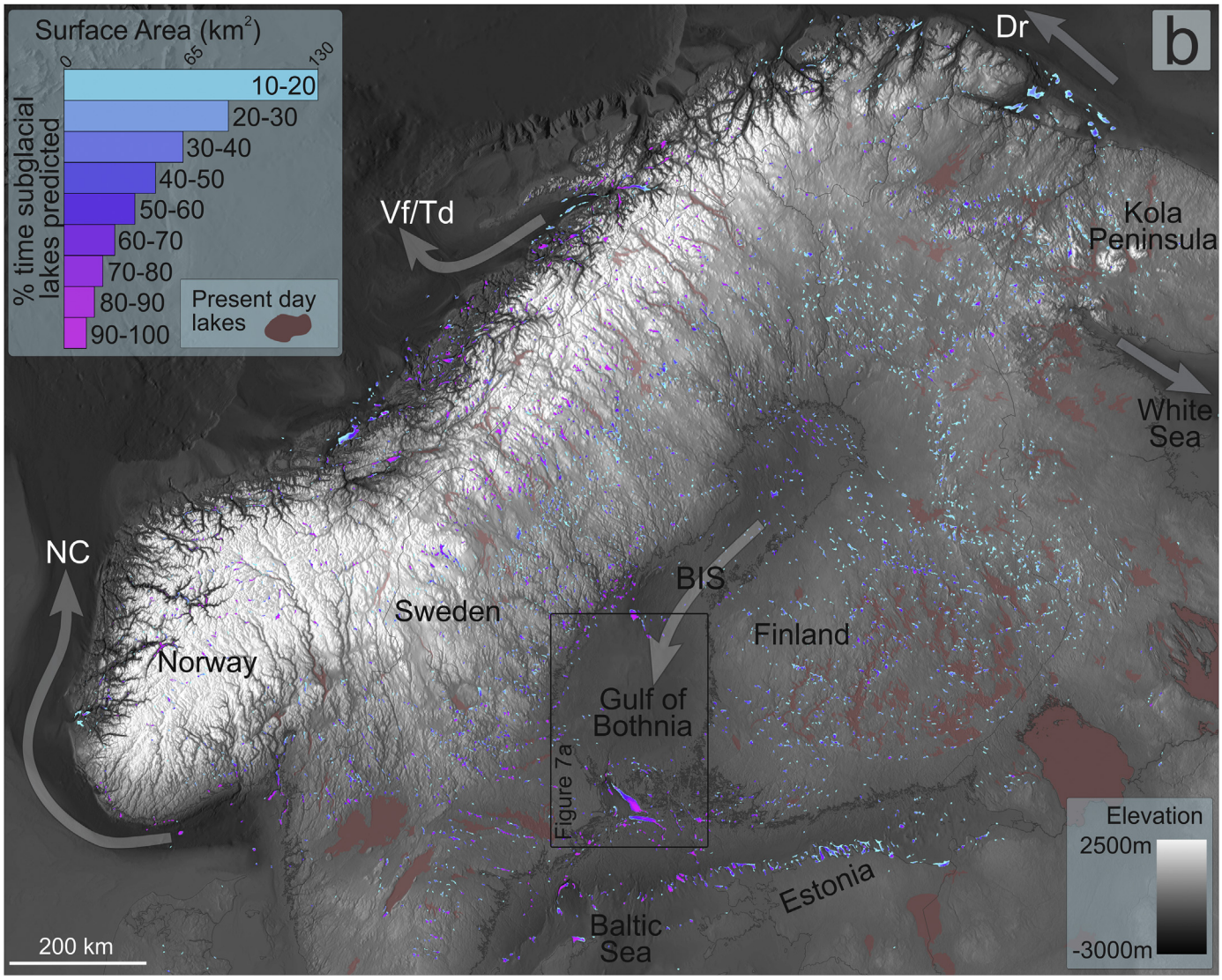

Fig. 3. (*continued*).

3.3. Sensitivity analysis

An analysis of the relative importance of key parameters influencing the hydraulic potential modelling (maps presented in Fig. S1) reveals that the greatest sensitivity and difference in subglacial lake coverage is in response to changes in the flotation criterion (Table 1), with an approximately 168,900 km^2 difference in total subglacial lake area between the lowest and highest F-value perturbations. Despite a relatively high range in total subglacial lake area, the spatial correspondence (percentage of subglacial lake

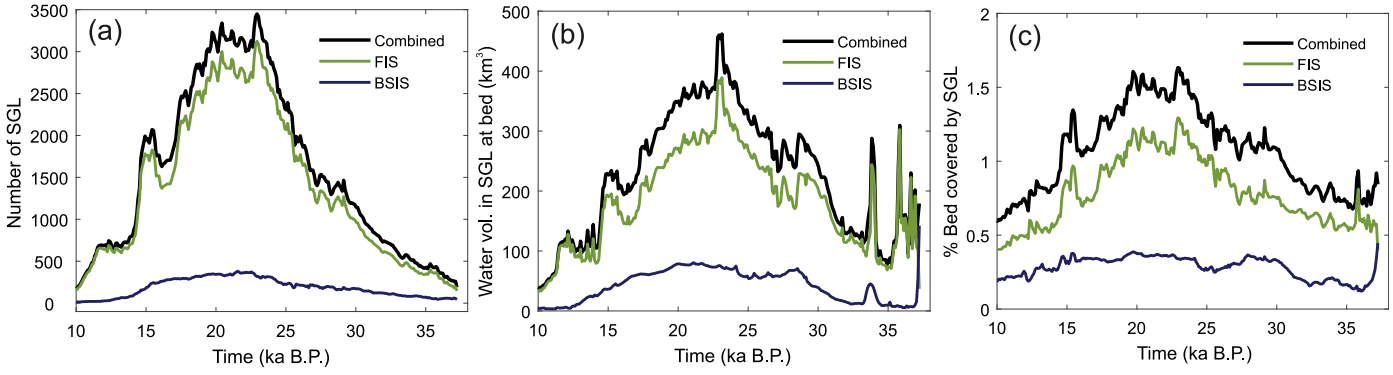

Fig. 4. (**a**) Total number of potential subglacial lakes, (**b**) estimated total volumes of water stored within subglacial lakes, and (**c**) the percentage of the bed occupied by subglacial lakes, for the BSIS, FIS, and combined from 37–10 ka BP.

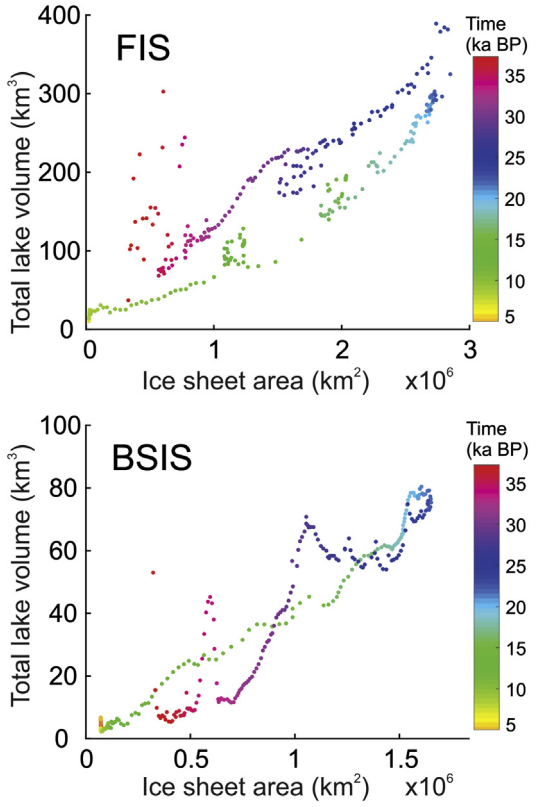

Fig. 5. Estimated total volume of water stored within subglacial lakes beneath the FIS and BSIS plotted against ice sheet areal extent. Points are coloured chronologically. A small number of timeslices with total water storage volumes greater than 100 km^3 for the BSIS are omitted in order to better present the overall trends in the data.

area intersecting with the optimum results) between the sensitivity results and optimum experiment remains high, especially for lower F-values. Additionally, the tendency for drainage routes to remain separate, and not merge close to the ice margins (e.g. in Bjørnøyrenna, Fig. 2e) is a symptom of the prescribed high value for the flotation criterion, and therefore increased importance of the ice surface on drainage routing, coupled with steep surface slopes close to the margin.

Subglacial lakes are less sensitive to small-scale perturbations in bed roughness and basal temperatures, with total area differences of 27,500 km^2 and 25,400 km^2 respectively between the highest and lowest sensitivity parameters. Spatial correspondence between subglacial lakes is consistently high between the different bed roughness sensitivity parameters, however, much lower spatial correspondence occurs when results below the pressure melting point are masked out (Table 1). Perturbations in ice flow (deformation/viscosity) parameters yield the smallest spatial extent differences at 12,100 km^2, and strong spatial correspondence with the optimum experiment suggests that the locations of predicted subglacial lakes remains consistent despite ice surface fluctuations. Based on the mostly high spatial correspondence between the optimum experiment and the sensitivity analysis results, we suggest that the locations of predicted subglacial lakes are robust, and that differences in areal coverage are largely driven by fluctuations in the sizes of individual subglacial lakes. Large, deep subglacial lakes are likely to be consistently predicted despite the various perturbations, and will dominate the trends in lake metrics.

4. Discussion

Based on the estimation of subglacial hydraulic potential beneath the Fennoscandian and Barents Sea ice sheets, we reconstruct the evolution of subglacial drainage pathways and potential subglacial lake locations through the Late Weichselian. Our reconstructions find potential subglacial lakes to be abundant beneath the former ice sheets, and here the influences on their distribution are discussed and comparison made with empirical evidence for past subglacial hydrology. Finally, we discuss the potential implications that the drainage reconstructions have on ice flow dynamics and beyond the ice margin.

4.1. Influences on subglacial lakes and their distribution

Hydraulic potential gradients are driven by the interplay between bed topography and modelled ice sheet thickness and surface slope. Throughout the glaciation the relationship between, and relative importance of, these drivers change primarily due to fluctuations in ice thickness, ice-divide and margin positions, and surface slopes. Stepped decreases in subglacial lake numbers beneath the FIS during deglaciation (Fig. 4a) are driven by intermittent ice margin retreat/stability, and retreat from areas of high basal roughness (Patton et al., 2017a), which are common across its former bed. The sharp fall in the number of potential subglacial lakes at 18 ka BP, followed by an increase approaching 15 ka BP (Fig. 4a), occurs due to margin retreat in the Baltic and overall

Table 1
Total potential subglacial lake area occupying the bed under an LGM (21 ka BP) timeslice following perturbations in the flotation factor (F), bed filtering (Bf), bed temperature masks below the pressure melting point (Bt) and ice flow enhancement factor perturbations (A_0). *optimum experiment.

Sensitivity parameter	Total subglacial lake area (km^2)	Area intersecting with optimum (%)
F = 0.7	177,902	88
F = 0.8	108,269	92
F = 0.925*	36,303	100
F = 1	9018	42
Bf x 0	57,793	97
Bf x 1*	36,303	100
Bf x 2	32,935	92
Bf x 3	30,315	86
Bt = no mask*	36,303	100
Bt ≤ −1.5 °C	20,202	58
Bt ≤ −0.75 °C	17,601	51
Bt ≤ 0 °C	10,891	31
A_0 = 5	48,144	76
A_0 = 25	39,279	91
A_0 = 50*	36,303	100
A_0 = 75	36,026	94

thinning, followed by a re-advance phase and ice thickening (Fig. 2). Beneath the BSIS, late ice-dome migration into more topographically rugged eastern sectors of the Barents Sea, and thick ice flowing towards and over the mountains of Novaya Zemlya (Fig. 2) drive the later peak and plateau in subglacial lake numbers (Fig. 4a).

Lake-area frequency distribution for the combined FIS and BSIS throughout their build-up and retreat (Fig. 6a) shows that the majority of predicted subglacial lakes are smaller than 10 km^2 with modal size between 4.3 and 6.8 km^2, similar to those predicted under LGM configurations of the Antarctic Ice Sheet (AIS) (Livingstone et al., 2013b), and those geophysically detected beneath the contemporary AIS (Wright and Siegert, 2012). FIS bed coverage by subglacial lakes is generally above 1% during the LGM (Fig. 4c), and the peak of 1.3% at 22.9 ka BP is comparable to 1.2% of the bed area predicted beneath the present-day Greenland Ice Sheet (Livingstone et al., 2013b). Higher numbers and a greater portion of the bed covered by lakes beneath the FIS again are likely driven by a higher subglacial bed roughness when compared to the BSIS, which had large portions underlain by relatively smooth bed (Fig. 1). Moreover, the flat surface of present-day lakes in the DEM precludes the prediction of subglacial lakes in these basins, and so in reality the percentage of the ice bed occupied by subglacial lakes for the FIS is likely to have been considerably greater given the abundance of present-day lakes (covering >100,000 km^2; www.ngdc.noaa.gov) across Fennoscandia (Fig. 3b).

The differences in potential subglacial lake coverage between the FIS and BSIS could also be explained by the post-glacial draping of marine sediments and sparse coverage and accuracy of bathymetric data in the Barents Sea, compared to the resolution, accuracy, and density of terrestrial data that cover the former FIS bed. However, the large, smooth troughs characteristic of the Barents Sea were inherited from earlier glaciations and underwent intense erosion during the lead-up to the LGM, and therefore were glacially smoothed prior to the inferred period of meltwater activity. Present sedimentation rates in the Barents Sea are generally low at c. 2–5 cm ka^{-1}, increasing to 15–20 cm ka^{-1} in near coastal areas (Elverhøi et al., 1989). Predicted subglacial lake numbers could potentially be higher with the provision of more accurate bathymetric and terrestrial data, although the total water storage capacity of subglacial lakes at the bed is unlikely to be significantly affected by DEM resolution or Holocene sediment draping.

For comparable ice sheet dimensions the volume of water stored within subglacial lakes at the bed of the FIS is up to twice as much (>100 km^3 greater) during ice build-up than during retreat (Fig. 5). This occurs despite a uniform relationship between ice-sheet area and the area of the bed occupied by lakes (Fig. 6b). However, subglacial lakes inherited from previous ice sheet configurations could persist through changes in ice-sheet geometry due to the positive feedback effect of ice-surface flattening above subglacial lakes reinforcing their stability (Livingstone et al., 2013b). This effect is not captured in our approach due to the absence of dynamic ice-hydrological coupling within the ice-sheet model, and so the disparity between water volumes stored within subglacial lakes beneath the advancing and retreating FIS is likely to have been lower. Nevertheless, the migration of FIS ice domes into the flatter sectors of eastern Fennoscandia led to lower volumes of water storage during deglaciation. It is also likely that subglacial lakes were deeper and more abundant during ice build-up, as the steeper surface slopes of a retreating ice sheet promote shallower, less stable subglacial lakes, with the potential for impacting on the rate of ice retreat through hydraulically driven modulation of ice velocties.

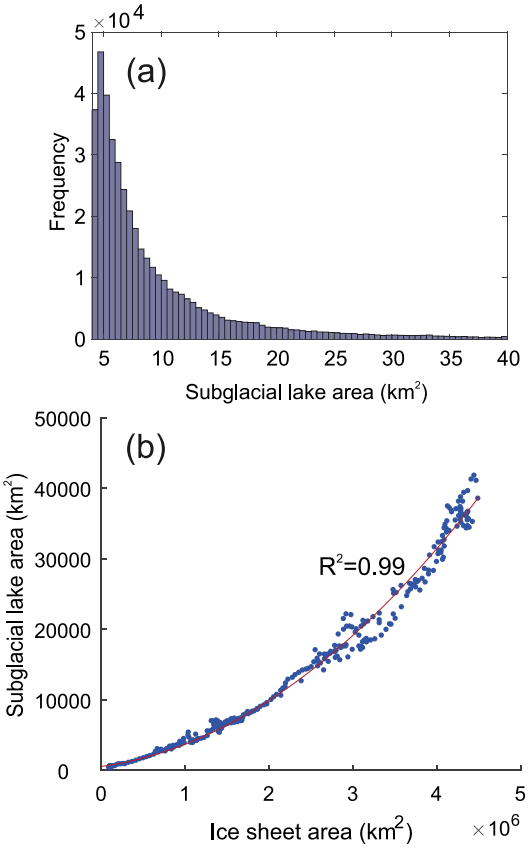

Fig. 6. (**a**) Subglacial lake size-frequency histogram for all lakes predicted through the Late Weichselian glaciation. (**b**) Total subglacial lake area plotted against ice sheet area.

4.2. *Affinity with the empirical record*

The geomorphological record of subglacial hydrology is influenced by the geology of the former ice-bed, and is likely to be biased towards the most erosive and persistent hydraulic activity. The preservation potential for evidence of subglacial lakes is low, especially for small, fast-circulation lakes which exist only on short time scales and account for a large proportion of the predicted subglacial lakes in this study (Fig. 3a, b). However, recent work identifying the geomorphological and sedimentological records of subglacial lakes and downstream landforms such as meltwater channels and eskers has successfully reconstructed former hydraulic conditions (Kuhn et al., 2017; Livingstone et al., 2015, 2012; Livingstone and Clark, 2016; Simkins et al., 2017), in particular those related to rapid, high-discharge drainage events. In the Barents Sea and Fennoscandia recent empirial studies (Bjarnadóttir et al., 2014; Esteves et al., 2017, *In Review;* Greenwood et al., 2016, 2017) enable the assessment of our predicted routing and lake locations against the palaeo-record of subglacial meltwater activity.

Our analysis reveals that the Gulf of Bothnia was a focal point for the routing and storage of subglacial meltwater over much of the last glaciation; a result that resonates strongly with the empirical record. Large, persistent subglacial lakes are predicted in the northwestern and southern Gulf of Bothnia (Fig. 3b), along with water routing through the area throughout ice occupancy (Fig. 2a–i). Between the predicted subglacial lakes (Fig. 7a), a suite of subglacial meltwater landforms are observed, including eskers and meltwater channels up to 4 km wide (Clason et al., 2016; Greenwood et al., 2017, 2016). High energy and high discharge meltwater systems are invoked to explain the observed channel features (Greenwood et al., 2016), and a large, periodically draining subglacial lake

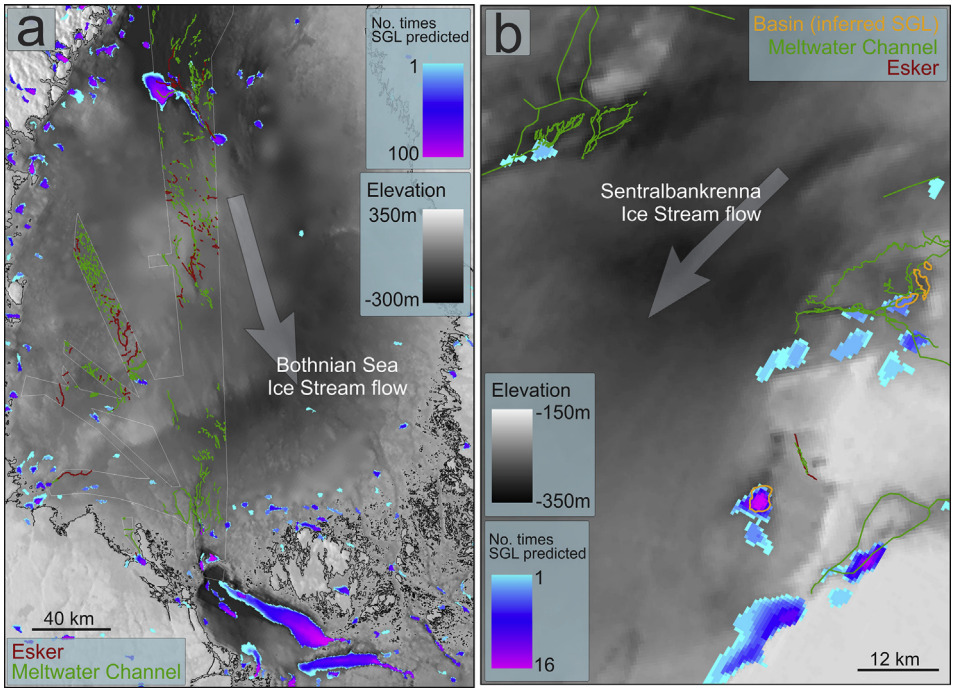

Fig. 7. Potential subglacial lakes predicted in this study compared to published mapping of subglacial meltwater geomorphology in (**a**) the Gulf of Bothnia (Greenwood et al., 2017, 2016) and (**b**) the central Barents Sea (Bjarnadóttir et al., 2017; Esteves et al., In Review, 2017). The outline of the bathymetric dataset upon which the mapping in the Gulf of Bothnia is based is drawn in white. Ice stream flow direction arrows are drawn based on the published reconstructions of ice flow.

proposed upstream of the drainage features (Greenwood et al., 2017) is supported by our results (Fig. 7a). A source of periodic or steady water injections to the clearly dynamic subglacial hydraulic system through this area is provided by the high number of subglacial lakes predicted here (Fig. 7a). Further, sudden large inputs of water to the drainage systems might lead to hydraulic overcapacity, initiating the formation of R-channels which infill with sediments to leave behind eskers following the decreases in discharge associated with complete drainage of a subglacial lake or termination of a flood event. The large number of eskers across Fennoscandia (Stroeven et al., 2016) may be related to the propensity of the landscape for subglacial lake formation as a source of time-varying meltwater fluxes. Compatibly, eskers are associated to the areas downstream of subglacial lakes beneath the North American palaeo-ice sheet (Livingstone et al., 2016).

Geomorphological and sedimentological investigations in the central Barents Sea also reveal several clusters of interconnected palaeo-subglacial lakes, meltwater channels, and eskers (Bjarnadóttir et al., 2017; Esteves et al., 2017, *In Review*). We predict subglacial lakes in several sites of mapped basins that are upstream of, and interlinking, large meltwater channels that feed into the Sentralbankrenna Ice Stream bed (Fig. 7b). It is suggested that the subglacial hydrology of this region was characterised by fill/drain cycles and periodic outburst flooding from hypothesised subglacial lakes (Bjarnadóttir et al., 2017; Esteves et al., 2017; *In Review*), compatible with the clusters of lakes predicted in this study. The lower number of times subglacial lakes are predicted at sites in the central Barents Sea compared to those in the Gulf of Bothnia (Fig. 7) tentatively suggests that their stability was susceptible to fluctuations in the configuration of overlying ice. Wider analysis of the association between meltwater geomorphology and predicted lakes gives confidence to reconstructions of subglacial hydrology and its impacts on ice flow. Inversely, sites of persistent subglacial lakes (Fig. 3a, b; Fig. 7a,b) are also more likely to contain geomorphological evidence of hydraulic activity and might make good candidates for geophysical/sedimentological surveys in search of palaeo-subglacial lakes.

4.3. Impacts of subglacial hydrology on ice dynamics

Subglacial lakes have been detected at the onset of ice streams in Antarctica (Bell et al., 2007; Fricker et al., 2007), and directly influence ice flow velocities through drainage events (Stearns et al., 2008) which can occur periodically due to natural instability (Evatt et al., 2006; Pattyn, 2008; Wingham et al., 2006). Hydraulically connected clusters of subglacial lakes modify basal stick-slip behaviour, and are associated with hydrologically-induced sticky-spots and effective pressure modulation through regulation of meltwater supply to the bed (Siegfried et al., 2016; Smith et al., 2017). A large number of both persistent and short-lived subglacial lakes are predicted at the onset of and draining into the beds of Fennoscandian and Barents Sea ice streams, including those occupying the Franz Victoria Trough, Sentralbankrenna, Djuprenna (Fig. 3a), Vestfjorden/Traenadjupet, and the Baltic (Fig. 3b). Although our approach lacks coupling between subglacial meltwater and ice dynamics, the abundance of predicted subglacial lakes connected to these modelled ice streams show the potential for impacts on ice dynamics by regulating meltwater supply to the bed, and clusters of predicted lake locations indicate the potential for interconnected subglacial lake systems analogous to those observed beneath contemporary ice sheets (Smith et al., 2017; Wingham et al., 2006) and at deglaciated beds (Nitsche et al., 2013; Simkins et al., 2017). Furthermore, a reduced capacity for water storage at the bed of retreating ice sheets, as demonstrated here for the FIS during deglaciation (Fig. 5), could limit the effect of periodic modifications to ice-flow through subglacial lake filling and draining. This would promote a more moderate response to increasing/decreasing meltwater inputs and associated impacts on ice flow.

Previous studies demonstrate that FIS flow, and consequently

ice thickness, is highly sensitive to basal meltwater (Arnold and Sharp, 2002; Clason et al., 2014; Gudlaugsson et al., 2017), and predictions of large, highly persistent lakes in the rugged topography of Fennoscandia and eastern Novaya Zemlya (Gudlaugsson et al., 2017) are in general agreement with our predictions. Our results demonstrate a greater frequency of less-persistent subglacial lakes especially in the Barents Sea and eastern Fennoscandia (Fig. 3a, b) which are prone to drainage with small shifts in ice geometry. Clason et al. (2016) suggest that ice flow and grounding line retreat through the Bothnian Sea was influenced by surface meltwater enhanced basal sliding, which is supported by evidence for high-discharge subglacial meltwater conduits (Greenwood et al., 2017, 2016). A propensity for subglacial lake formation in the Gulf of Bothnia and surrounding areas (Fig. 4b) suggests that surface meltwater penetrating to the bed could have been stored in subglacial lakes and released on varying timescales, further modulating the stability and dynamic activity of the ice stream. Similarly, given the evidence for high-discharge subglacial meltwater systems in the central Barents Sea (Bjarnadóttir et al., 2017; Esteves et al., 2017), it is likely that ice flow of the Sentralbankrenna Ice Stream, and the neighbouring Bjørnøyrenna Ice Stream (Fig. 1), would have been regulated by the filling and draining of the subglacial lakes predicted in their onset zones (Fig. 7b). Evidence for highly dynamic ice stream activity is recorded in the geomorphology of their former beds, with cross-cutting sets of megascale glacial lineations indicating numerous switches in flow direction during the LGM (Piasecka et al., 2016). Furthermore, grounding zone wedges containing evidence for ice-marginal subglacial meltwater discharge suggest cycles of ice margin retreat, stability, and re-advance influenced by sustained basal hydrological activity during overall retreat (Bjarnadóttir et al., 2014; Esteves et al., 2017; Newton and Huuse, 2017).

The routing of water also has implications for the dynamics of overlying ice, as shallow surface slopes render subglacial water routing extremely sensitive to minor shifts in ice sheet geometry. These areas are susceptible to rerouting of drainage towards or away from individual catchments, with the potential for hydraulic regulation of fast ice flow, as has been observed in present-day Antarctica and Greenland (Anandakrishnan and Alley, 1997; Carter et al., 2013; Lindbäck et al., 2015; Vaughan et al., 2008). Empirical based reconstructions of ice stream dynamics in Bjørnøyrenna suggest frequent major switches in ice flow directions during the LGM (Piasecka et al., 2016) and surging behaviour during retreat (Andreassen et al., 2014; Bjarnadóttir et al., 2014) which, in combination with shifting ice divides, may have been driven by fluctuating meltwater routing and lake fill/drain cycles given the high number of subglacial lake clusters predicted at the onset of, and in the tributaries to the former ice stream. This is supported by evidence for vast subglacial meltwater networks and interlinked subglacial lakes surrounding the Sentralbankrenna tributary ice stream (Bjarnadóttir et al., 2014; Esteves et al., 2017, *In Review*). Geomorphic evidence is generally in agreement with our modelling results which predict highly dynamic drainage systems with the potential for upstream subglacial lakes feeding into drainage systems with significant temporal and spatial variations in water routing.

4.4. Potential impacts beyond the ice margin

The locations of subglacial drainage outlets are transient and migrate in response to changes in ice margin position, ice sheet

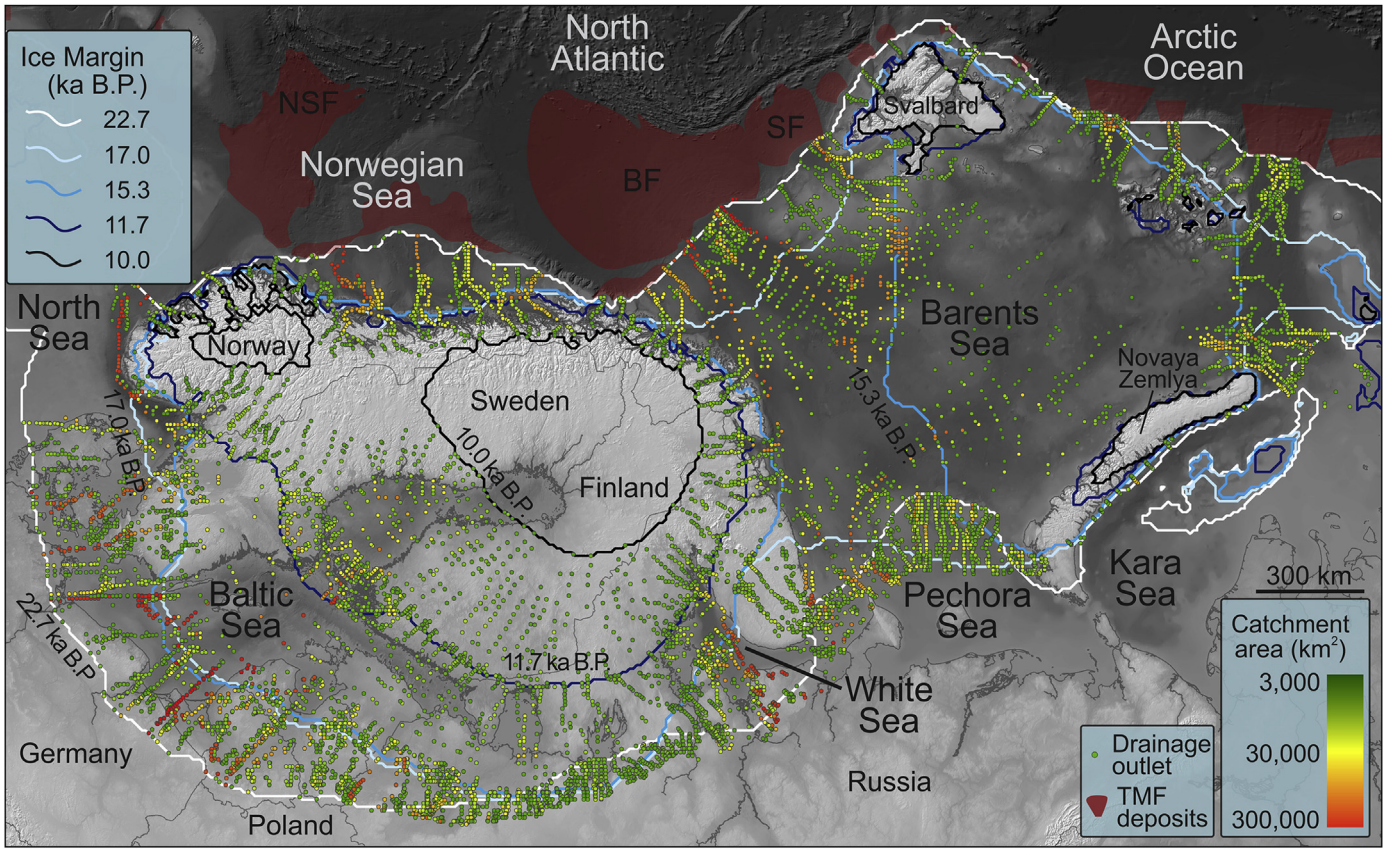

Fig. 8. Subglacial catchment outlet migration between maximum ice extent conditions (22.7 ka BP) and 10 ka BP at 100-year intervals. The outlets are coloured according to the size of their associated catchment on a logarithmic scale. Outlets for small catchments (<3000 km^2) have been removed. The extents of major trough mouth fan deposits are shown in red. BF = Bjørnøyrenna Fan; NSF = North Sea Fan; SF = Storfjordrenna Fan. Ice margin extents are derived from the ice sheet model (Patton et al., 2017a).

configuration and geometry, and shifts in proximity to/contact with the oceans which, in turn, are influenced by eustatic sea-level changes and ice stream discharge. Fig. 8 maps subglacial drainage outlets, colour coded by catchment size, between maximum ice extent at 22.7 ka BP and through to full deglaciation at 10 ka BP. Given the large catchment size of some predicted subglacial drainage systems (a maximum of 327,000 km^2 beneath the Baltic Sea Ice Stream and 224,000 km^2 beneath the Bjørnøyrenna Ice Stream) it is likely that they were responsible for concentrated sediment deposition and focussed inputs of cold, fresh water to the oceans and Eurasian continent, especially during deglaciation.

Sudden drops in subglacial water storage capacity, for example at 23 ka BP and 15 ka BP (Fig. 4b), result in over 100 km^3 of freshwater input to the subglacial system fed from subglacial lakes alone, which is subsequently routed towards the margins. Outlet positions and subglacial catchment sizes are therefore important when considering the influence of retreating ice sheets on proglacial landscape evolution and where glacially eroded sediments are transported and deposited. Additionally, the estimated combined volume of water stored within subglacial lakes at the beds of the FIS and BSIS ranges from 36 to 462 km^3 (Fig. 4b), highlighting the important function of subglacial lakes as both a perennial store and source of freshwater, dependent on ice-sheet geometry. In comparison, estimated total volumes of water stored beneath the FIS and BSIS (Fig. 5) are less than the ~1000 km^3 predicted beneath LGM configurations of the North American Ice Sheet (Livingstone et al., 2013a) and considerably less than the 9000–16,000 km^3 estimated beneath the contemporary AIS (Wright and Siegert, 2012).

Nearly half of the total LGM ice sheet configuration terminated in marine outlets (Fig. 8), which subsequently increased through deglaciation. The strongest concentrations of meltwater and sediment delivery to marine-terminating sectors occurred at the continental shelf break west of Bjørnøyrenna, towards the Bjørnøyrenna Trough Mouth Fan (TMF; Fig. 8), the largest glacial sediment depocentre in the Arctic (Vorren et al., 2011). Outlets draining catchments approaching 300,000 km^2 are predicted consistently here throughout ice margin retreat (Fig. 8), and these would have been the primary source of sediments to the upper slope, and potentially to enhanced deposition conducive to slope failures (e.g. Lucchi et al., 2012, 2013), thereby influencing slope stability. Furthermore, discharge of meltwater with a high concentration of suspended sediments may flow hyperpycnally along the seabed and initiate turbidity currents (Piper and Normark, 2009), thereby directly contributing to both the quantity and architecture of proglacial marine sediments accumulated within TMFs.

The TMF associated with the neighbouring Storfjordrenna Ice Stream contains well-documented sedimentological evidence for intensive meltwater plume activity (Llopart et al., 2015). Distinct meltwater signals between three hypothesised sub-ice stream lobes here (Pedrosa et al., 2011) is supported by the outlet positions and distinct migration paths predicted in this study (Fig. 8). Stable drainage outlets of substantial size might also have contributed to three partly merged sediment depocenters off the mid-Norwegian Shelf (Fig. 8), although material from the most southern depocentre (and largest catchment area outlets) has been removed by mass slides in Storegga (Dahlgren et al., 2005). Where major catchments outlet onto terrestrial regions, they contributed to the formation of large proglacial lakes and river networks (Patton et al., 2017a). Large catchment outlets in the Baltic leading up to the Younger Dryas (11.7 ka BP) are also accordant with the initiation of and precursors to the Baltic Ice Lake around 14.2 ka BP (Mangerud et al., 2004).

5. Conclusions

Through the application of well-constrained ice sheet modelling output, we demonstrate the abundance of potential sites for subglacial lake formation and drainage pathways beneath the Fennoscandian and Barents Sea ice sheets through the Last Glacial Maximum (37–10 ka BP). During peak glaciation c. 22.7 ka BP up to 3500 subglacial lake locations are predicted, accounting for 38,580 km^2 of the subglacial domain. Throughout deglaciation, predicted subglacial lake locations resonate with recent geomorphological mapping, evidencing pronounced water fluxes beneath both ice sheets, and indicating that subglacial meltwater played a major role in governing dynamic and rapid ice-sheet retreat. Several cluster-sites of potential subglacial lakes are predicted at the onset of, and in the banks surrounding, the Bjørnøyrenna, Franz-Victoria Trough, Baltic Sea, and Norwegian Coast Parallel palaeo-ice streams, suggesting these ice-sheet catchments were susceptible to hydraulic regulation. Lower volumes of water impounded beneath the FIS during ice retreat demonstrates the potential for shallower, unstable subglacial lakes under its retreating ice geometry, with implications for the supply of meltwater to the bed and impacts on ice flow surrounding, and downstream of, major Fennoscandian subglacial lakes.

Transient model outputs reveal the migration paths of subglacial catchment outlets, from which concentrations of sediments and freshwater exited the ice sheet system. While the ice margin lay adjacent to the continental shelf edge, these shifting outlets would have contributed to the build-up and architecture of sediments within the adjacent trough mouth fans, the most significant of which lay beneath the Bjørnøyrenna ice stream with a catchment reach of >900 km. Subglacial lake persistency maps integrated over the full Late Weichselian glaciation reveal multiple sites for long-lived, and potentially preserved, subglacial lakes. These locations represent key targets for further geophysical/sedimentological investigations.

Acknowledgements

This research is part of the Centre for Arctic Gas Hydrate, Environment and Climate and was supported by the Research Council of Norway through its Centres of Excellence funding scheme grant No. 223259. The ice sheet modelling outputs used were also supported by the PetroMaks project “Glaciations in the Barents Sea area (GlaciBar)” (grant No. 200672). We thank two anonymous reviewers for their constructive feedback on the manuscript.

Appendix A. Supplementary data

Supplementary data to this article can be found online at https://doi.org/10.1016/j.quascirev.2018.10.007.

References

Alley, R.B., 1989. Water-pressure coupling of sliding and bed deformation: 1. Water system. J. Glaciol. 35, 108–118.

Anandakrishnan, S., Alley, R.B., 1997. Stagnation of ice stream C, west Antarctica by water piracy. Geophys. Res. Lett. 24, 265. https://doi.org/10.1029/96GL04016.

Andersen, K.K., Azuma, N., Barnola, J.M., Bigler, M., Biscaye, P., Caillon, N., Chappellaz, J., Clausen, H.B., Dahl-Jensen, D., Fischer, H., Flückiger, J., Fritzsche, D., Fujii, Y., Goto-Azuma, K., Grønvold, K., Gundestrup, N.S., Hansson, M., Huber, C., Hvidberg, C.S., Johnsen, S.J., Jonsell, U., Jouzel, J., Kipfstuhl, S., Landais, A., Leuenberger, M., Lorrain, R., Masson-Delmotte, V., Miller, H., Motoyama, H., Narita, H., Popp, T., Rasmussen, S.O., Raynaud, D., Rothlisberger, R., Ruth, U., Samyn, D., Schwander, J., Shoji, H., Siggard-Andersen, M.L., Steffensen, J.P., Stocker, T., Sveinbjörnsdóttir, A.E., Svensson, A., Takata, M., Tison, J.L., Thorsteinsson, T., Watanabe, O., Wilhelms, F., White, J.W.C., 2004. High-resolution record of Northern Hemisphere climate

extending into the last interglacial period. Nature 431, 147–151. https://doi.org/10.1038/nature02805.
Andreassen, K., Winsborrow, M.C.M., Bjarnadóttir, L.R., Rüther, D.C., 2014. Ice stream retreat dynamics inferred from an assemblage of landforms in the northern Barents Sea. Quat. Sci. Rev. 92, 246–257. https://doi.org/10.1016/j.quascirev.2013.09.015.
Andrews, L.C., Catania, G.A., Hoffman, M.J., Gulley, J.D., Lüthi, M.P., Ryser, C., Hawley, R.L., Neumann, T.A., 2014. Direct observations of evolving subglacial drainage beneath the Greenland Ice Sheet. Nature 514, 80–83. https://doi.org/10.1038/nature13796.
Arnold, N., Sharp, M., 2002. Flow variability in the Scandinavian ice sheet: modelling the coupling between ice sheet flow and hydrology. Quat. Sci. Rev. 21, 485–502. https://doi.org/10.1016/S0277-3791(01)00059-2.
Auriac, A., Whitehouse, P.L., Bentley, M.J., Patton, H., Lloyd, J.M., Hubbard, A., 2016. Glacial isostatic adjustment associated with the Barents Sea ice sheet: a modelling inter-comparison. Quat. Sci. Rev. 147, 122–135. https://doi.org/10.1016/j.quascirev.2016.02.011.
Banwell, A.F., Arnold, N.S., Willis, I.C., Tedesco, M., Ahlstrøm, A.P., 2012. Modeling supraglacial water routing and lake filling on the Greenland Ice Sheet. J. Geophys. Res. Earth Surf. 117, F04012. https://doi.org/10.1029/2012JF002393.
Banwell, A.F., Willis, I.C., Arnold, N.S., 2013. Modeling subglacial water routing at Paakitsoq, W Greenland. J. Geophys. Res. Earth Surf. 118, 1282–1295. https://doi.org/10.1002/jgrf.20093.
Bell, R.E., Paden, J., Tinto, K., Das, I., Wolovick, M., Chu, W., Creyts, T.T., Frearson, N., Abdi, A., Paden, J.D., 2014. Deformation, warming and softening of Greenland's ice by refreezing meltwater. Nat. Geosci. 7, 497–502. https://doi.org/10.1038/ngeo2179.
Bell, R.E., Studinger, M., Shuman, C.A., Fahnestock, M.A., Joughin, I., 2007. Large subglacial lakes in East Antarctica at the onset of fast-flowing ice streams. Nature 455, 904–907. https://doi.org/10.1038/nature05554.
Bjarnadóttir, L.R., Winsborrow, M.C.M., Andreassen, K., 2017. Large subglacial meltwater features in the central Barents Sea. Geology 45, 1–45. https://doi.org/10.1111/bor.12142.
Bjarnadóttir, L.R., Winsborrow, M.C.M., Andreassen, K., 2014. Deglaciation of the central Barents Sea. Quat. Sci. Rev. 92, 208–226. https://doi.org/10.1016/j.quascirev.2013.09.012.
Boulton, G.S., Dobbie, K., Zatsepin, S., 2001. Sediment deformation beneath glaciers and its coupling to the subglacial hydraulic system. Quat. Int. 86, 3–28. https://doi.org/10.1016/S1040-6182(01)00048-9.
Carter, S.P., Fricker, H.A., Siegfried, M.R., 2017. Antarctic subglacial lakes drain through sediment-floored canals: theory and model testing on real and idealized domains. Cryosphere 11, 381–405. https://doi.org/10.5194/tc-2016-74.
Carter, S.P., Fricker, H.A., Siegfried, M.R., 2013. Evidence of rapid subglacial water piracy under whillans ice stream, west Antarctica. J. Glaciol. 59, 1147–1162. https://doi.org/10.3189/2013JoG13J085.
Chauché, N., Hubbard, A., Gascard, J.-C., Box, J.E., Bates, R., Koppes, M., Sole, A., Christoffersen, P., Patton, H., 2014. Ice–ocean interaction and calving front morphology at two west Greenland tidewater outlet glaciers. Cryosphere 8, 1457–1468. https://doi.org/10.5194/tc-8-1457-2014.
Christoffersen, P., Tulaczyk, S., Wattrus, N.J., Peterson, J., Quintana-Krupinski, N., Clark, C.D., Sjunneskog, C., 2008. Large subglacial lake beneath the Laurentide Ice Sheet inferred from sedimentary sequences. Geology 36, 563–566. https://doi.org/10.1130/G24628A.1.
Christoffersen, P., Pettersson, R., Hubbard, A., Doyle, S.H., Grigsby, S., 2018. Cascading lake drainage on the Greenland Ice Sheet triggered by tensile shock and fracture. Nat. Commun. 9, 1064. https://doi.org/10.1038/s41467-018-03420-8.
Chu, W., Creyts, T.T., Bell, R.E., 2016. Rerouting of subglacial water flow between neighboring glaciers in West Greenland. J. Geophys. Res. 121, 925–938. https://doi.org/10.1002/2015JF003705.
Clarke, G.K.C., 2005. Subglacial processes. Annu. Rev. Earth Planet Sci. 33, 247–276. https://doi.org/10.1146/annurev.earth.33.092203.122621.
Clason, C.C., Applegate, P.J., Holmlund, P., 2014. Modelling Late Weichselian evolution of the Eurasian ice sheets forced by surface meltwater-enhanced basal sliding. J. Glaciol. 60, 29–40. https://doi.org/10.3189/2014JoG13J037.
Clason, C.C., Greenwood, S.L., Selmes, N., Lea, J.M., Jamieson, S.S.R., Nick, F.M., Holmlund, P., 2016. Controls on the early Holocene collapse of the Bothnian Sea ice stream. J. Geophys. Res. Earth Surf. 121, 2494–2513. https://doi.org/10.1002/2016JF004050.
Cuffey, K.M., Paterson, W.S.B., 2010. The Physics of Glaciers, fourth ed. Butterworth-Heinemann, Oxford.
Dahlgren, K.I.T., Vorren, T.O., Stoker, M.S., Nielsen, T., Nygård, A., Sejrup, H.P., 2005. Late Cenozoic prograding wedges on the NW European continental margin: their formation and relationship to tectonics and climate. Mar. Petrol. Geol. 22, 1089–1110. https://doi.org/10.1016/j.marpetgeo.2004.12.008.
Dowdeswell, J.A., Siegert, M.J., 2003. The physiography of modern Antarctic subglacial lakes. Global Planet. Change 35, 221–236. https://doi.org/10.1016/S0921-8181(02)00128-5.
Doyle, S.H., Hubbard, B., Christoffersen, P., Young, T.J., Hofstede, C., Bougamont, M., Box, J.E., Hubbard, A., 2018. Physical conditions of fast glacier flow: 1 . Measurements from boreholes drilled to the bed of store glacier, west Greenland. J. Geophys. Res. Earth Surf. 123.
Elverhøi, A., Pfirman, S.L., Solheim, A., Larssen, B.B., 1989. Glaciomarine sedimentation in epicontinental seas exemplified by the northern Barents Sea. Mar. Geol. 85, 225–250. https://doi.org/10.1016/0025-3227(89)90155-2.
Esteves, M., Bjarnadóttir, L.R., Winsborrow, M.C.M., Shackleton, C.S., Andreassen, K., 2017. Retreat patterns and dynamics of the Sentralbankrenna glacial system, central Barents Sea. Quat. Sci. Rev. 169, 131–147. https://doi.org/10.1016/j.quascirev.2017.06.004.
Esteves, M., Rüther, D., Winsborrow, M.C.M., Livingstone, S.J., Shackleton, C.S., Andreassen, K., Hong, W.-L. and Knies, J. In Review. An Interconnected Palaeo-subglacial Lake System in the Central Barents Sea.
Evatt, G., Fowler, A., Clark, C., Hulton, N.R., 2006. Subglacial floods beneath ice sheets. Philos. Trans. R. Soc. London A Math. Phys. Eng. Sci. 364.
Evatt, G.W., Fowler, A.C., Clark, C.D., Hulton, N.R.J., 2006. Subglacial floods beneath ice sheets. Philos. Trans. A. Math. Phys. Eng. Sci. 364, 1769–1794. https://doi.org/10.1098/rsta.2006.1798.
Fricker, H.A., Scambos, T., Bindschadler, R., Padman, L., 2007. An active subglacial water system in West Antarctica mapped from space. Science 315, 1544–1548. https://doi.org/10.1126/science.1136897.
Greenwood, S.L., Clason, C.C., Jakobsson, M., 2016. Ice-flow and meltwater landform assemblages in the Gulf of Bothnia. Geol. Soc. London Mem. 46, 321–324. https://doi.org/10.1144/M46.163.
Greenwood, S.L., Clason, C.C., Nyberg, J., Jakobsson, M., Holmlund, P., 2017. The Bothnian Sea ice stream: early Holocene retreat dynamics of the south-central Fennoscandian Ice Sheet. Boreas 46, 346–362. https://doi.org/10.1111/bor.12217.
Gudlaugsson, E., Humbert, A., Andreassen, K., Clason, C.C., Kleiner, T., Beyer, S., 2017. Eurasian ice-sheet dynamics and sensitivity to subglacial hydrology. J. Glaciol. 63, 556–564. https://doi.org/10.1017/jog.2017.21.
Gulley, J.D., Grabiec, M., Martin, J.B., Jania, J., Catania, G., Glowacki, P., 2012. The effect of discrete recharge by moulins and heterogeneity in flow-path efficiency at glacier beds on subglacial hydrology. J. Glaciol. 58, 926–940. https://doi.org/10.3189/2012JoG11J189.
Hubbard, A., 2000. The verification and significance of three approaches to longitudinal stresses in high-resolution models of glacier flow. Geogr. Ann. Ser. A Phys. Geogr. 82, 471–487. https://doi.org/10.1111/j.0435-3676.2000.00135.x.
Hubbard, A., Lawson, W., Anderson, B., Hubbard, B., Blatter, H., 2004. Evidence for subglacial ponding across taylor glacier, dry valleys, Antarctica. Ann. Glaciol. 39, 79–84.
Hubbard, A., Hein, A.S., Kaplan, M.R., Hultun, N.R.J., Glasser, N., 2005. A modelling reconstruction of the last glacial maximum ice sheet and its deglaciation in the vicinity of the northern Patagonia icefield, South America. Geogr. Ann. 87, 375–391.
Hubbard, A., 2006. The validation and sensitivity of a model of the Icelandic ice sheet. Quat. Sci. Rev. 25 (17–18), 2297–2313.
Hubbard, A., Sugden, D., Dugmore, A., Norddahl, H., Pétursson, H.G., 2006. A modelling insight into the Icelandic Last Glacial Maximum ice sheet. Quat. Sci. Rev. 25, 2283–2296. https://doi.org/10.1016/j.quascirev.2006.04.001.
Hubbard, A., Bradwell, T., Golledge, N., Hall, A., Patton, H., Sugden, D., Cooper, R., Stoker, M., 2009. Dynamic cycles, ice streams and their impact on the extent, chronology and deglaciation of the British–Irish ice sheet. Quat. Sci. Rev. 28, 758–776. https://doi.org/10.1016/j.quascirev.2008.12.026.
Iken, A., 1981. The effect of the subglacial water pressure on the sliding velocity of a glacier in an idealized numerical model. J. Glaciol. 27, 407–421. https://doi.org/10.3198/1981JoG27-97-407-421.
Jenkins, A., 2011. Convection-driven melting near the grounding lines of ice shelves and tidewater glaciers. J. Phys. Oceanogr. 41, 2279–2294. https://doi.org/10.1175/JPO-D-11-03.1.
Johnson, J., Fastook, J.L., 2002. Northern Hemisphere glaciation and its sensitivity to basal melt water. Quat. Int. 95, 65–74. https://doi.org/10.1016/S1040-6182(02)00028-9.
Kuhn, G., Hillenbrand, C.-D., Kasten, S., Smith, J.A., Nitsche, F.O., Frederichs, T., Wiers, S., Ehrmann, W., Klages, J.P., Mogollon, J.M., 2017. Evidence for a palaeo-subglacial lake on the Antarctic continental shelf. Nat. Commun. 8, 15591. https://doi.org/10.1038/ncomms15591.
Kuchar, J., Milne, G., Hubbard, A., Patton, H., Bradley, S., Shennan, I., Edwards, R., 2012. Evaluation of a numerical model of the British – Irish ice sheet using relative sea-level data: implications for the interpretation of trimline observations. J. Quat. Sci. 27, 597–605. https://doi.org/10.1002/jqs.2552.
Le Brocq, A.M., Payne, A.J., Siegert, M.J., Alley, R.B., 2009. A subglacial water-flow model for West Antarctica. J. Glaciol. 55, 879–888. https://doi.org/10.1063/1.2756072.
Le Meur, E., Huybrechts, P., 1996. A comparison of different ways of dealing with isostasy: examples from modelling the Antarctic ice sheet during the last glacial cycle. Ann. Glaciol. 23, 309–317. https://doi.org/10.013/epic.12717.d001.
Lindbäck, K., Pettersson, R., Hubbard, A.L., Doyle, S.H., van As, D., Mikkelsen, A.B., Fitzpatrick, A.A., 2015. Subglacial water drainage, storage, and piracy beneath the Greenland Ice Sheet. Geophys. Res. Lett. 42, 7606–7614. https://doi.org/10.1002/2015GL065393.
Livingstone, S.J., Clark, C.D., 2016. Morphological properties of tunnel valleys of the southern sector of the Laurentide Ice Sheet and implications for their formation. Earth Surf. Dyn. 4, 567–589. https://doi.org/10.5194/esurf-4-567-2016.
Livingstone, S.J., Clark, C.D., Piotrowski, J.A., Tranter, M., Bentley, M.J., Hodson, A., Swift, D.A., Woodward, J., 2012. Theoretical framework and diagnostic criteria for the identification of palaeo-subglacial lakes. Quat. Sci. Rev. 53, 88–110. https://doi.org/10.1016/j.quascirev.2012.08.010.
Livingstone, S.J., Clark, C.D., Tarasov, L., 2013a. Modelling North American palaeo-subglacial lakes and their meltwater drainage pathways. Earth Planet Sci. Lett. 375, 13–33. https://doi.org/10.1016/j.epsl.2013.04.017.
Livingstone, S.J., Clark, C.D., Woodward, J., Kingslake, J., 2013b. Potential subglacial

lake locations and meltwater drainage pathways beneath the Antarctic and Greenland ice sheets. Cryosphere 7, 1721–1740. https://doi.org/10.5194/tc-7-1721-2013.
Livingstone, S.J., Storrar, R.D., Hillier, J.K., Stokes, C.R., Clark, C.D., Tarasov, L., 2015. An ice-sheet scale comparison of eskers with modelled subglacial drainage routes. Geomorphology 246, 104–112. https://doi.org/10.1016/j.geomorph.2015.06.016.
Livingstone, S.J., Utting, D.J., Ruffell, A., Clark, C.D., Pawley, S., Atkinson, N., Fowler, A.C., 2016. Discovery of relict subglacial lakes and their geometry and mechanism of drainage. Nat. Commun. 7 https://doi.org/10.1038/ncomms11767.
Llopart, J., Urgeles, R., Camerlenghi, A., Lucchi, R.G., Rebesco, M., De Mol, B., 2015. Late quaternary development of the storfjorden and kveithola trough mouth fans, northwestern Barents Sea. Quat. Sci. Rev. 129, 68–84. https://doi.org/10.1016/j.quascirev.2015.10.002.
Lucchi, R.G., Camerlenghi, A., Rebesco, M., Colmenero-hidalgo, E., Sierro, F.J., Sagnotti, L., Urgeles, R., Melis, R., Morigi, C., Barcena, M.A., Giorgetti, G., Villa, G., Persico, D., Flores, J.A., Rigual-Hernandez, A.S., Pedrosa, M.T., Macri, P., Caburlotto, A., 2013. Postglacial sedimentary processes on the Storfjorden and Kveithola trough mouth fans : significance of extreme glacimarine sedimentation. Global Planet. Change 111, 309–326.
Lucchi, R.G., Pedrosa, M.T., Camerlenghi, A., Urgeles, R., De Mol, B., Rebesco, M., 2012. Recent submarine landslides on the continental slope of storfjorden and kveithola trough-mouth fans (north west Barents Sea). In: Yamada, Y., Kawamura, K., Ikehara, K., Ogawa, Y., Urgeles, R., Mosher, D., Chaytor, J., Strasser, M. (Eds.), Submarine Mass Movements and Their Consequences. Advances in Natural and Technological Hazards Research, vol. 31. Springer Science Book Series, pp. 735–745. https://doi.org/10.1007/978-94-007-2162-3.
Mangerud, J., Jakobsson, M., Alexanderson, H., Astakhov, V., Clarke, G.K.C., Henriksen, M., Hjort, C., Krinner, G., Lunkka, J.P., Möller, P., Murray, A., Nikolskaya, O., Saarnisto, M., Svendsen, J.I., 2004. Ice-dammed lakes and rerouting of the drainage of northern Eurasia during the Last Glaciation. Quat. Sci. Rev. 23, 1313–1332. https://doi.org/10.1016/j.quascirev.2003.12.009.
Meierbachtol, T., Harper, J., Humphrey, N., 2013. Basal drainage system response to increasing surface melt on the Greenland ice sheet. Science 341, 777–779.
Newton, A.M.W., Huuse, M., 2017. Glacial geomorphology of the central Barents Sea: implications for the dynamic deglaciation of the Barents Sea ice sheet. Mar. Geol. 387, 114–131. https://doi.org/10.1016/j.margeo.2017.04.001.
Nitsche, F.O., Gohl, K., Larter, R.D., Hillenbrand, C.D., Kuhn, G., Smith, J.A., Jacobs, S., Anderson, J.B., Jakobsson, M., 2013. Paleo ice flow and subglacial meltwater dynamics in Pine Island Bay, West Antarctica. Cryosphere 7, 249–262. https://doi.org/10.5194/tc-7-249-2013.
Patton, H., Hubbard, A., Glasser, N.F., Bradwell, T., Golledge, N.R., 2013a. The last Welsh Ice Cap: Part 2 - dynamics of a topographically controlled icecap. Boreas 42, 491–510. https://doi.org/10.1111/j.1502-3885.2012.00301.x.
Patton, H., Hubbard, A., Bradwell, T., Glasser, N.F., Hambrey, M.J., Clark, C.D., 2013b. Rapid marine deglaciation: asynchronous retreat dynamics between the Irish Sea Ice Stream and terrestrial outlet glaciers. Earth Surf. Dyn. 1, 53–65. https://doi.org/10.5194/esurf-1-53-2013.
Patton, H., Hubbard, A., Andreassen, K., Winsborrow, M.C.M., Stroeven, A.P., 2016. The build-up, configuration, and dynamical sensitivity of the Eurasian ice-sheet complex to Late Weichselian climatic and oceanic forcing. Quat. Sci. Rev. 153, 97–121. https://doi.org/10.1016/j.quascirev.2016.10.009.
Patton, H., Hubbard, A., Andreassen, K., Auriac, A., Whitehouse, P.L., Stroeven, A.P., Shackleton, C., Winsborrow, M.C.M., Heyman, J., Hall, A.M., 2017a. Deglaciation of the Eurasian ice sheet complex. Quat. Sci. Rev. 169, 148–172. https://doi.org/10.1016/j.quascirev.2017.05.019.
Patton, H., Hubbard, A., Bradwell, T., Schomacker, A., 2017b. The configuration, sensitivity and rapid retreat of the Late Weichselian Icelandic ice sheet. Earth Sci. Rev. 166, 223–245. https://doi.org/10.1016/j.earscirev.2017.02.001.
Pattyn, F., 2008. Investigating the stability of subglacial lakes with a full Stokes ice-sheet model. J. Glaciol. 54, 353–361. https://doi.org/10.3189/002214308784886171.
Pattyn, F., Perichon, L., Aschwanden, A., Breuer, B., de Smedt, B., Gagliardini, O., Gudmundsson, G.H., Hindmarsh, R.C.A., Hubbard, A., Johnson, J.V., Kleiner, T., Konovalov, Y., Martin, C., Payne, A.J., Pollard, D., Price, S., Rückamp, M., Saito, F., Souček, O., Sugiyama, S., Zwinger, T., 2008. Benchmark experiments for higher-order and full-Stokes ice sheet models (ISMIP–HOM). Cryosphere 2, 95–108. https://doi.org/10.5194/tc-2-95-2008.
Pedrosa, M.T., Camerlenghi, A., De Mol, B., Urgeles, R., Rebesco, M., Lucchi, R.G., 2011. Seabed morphology and shallow sedimentary structure of the storfjorden and kveithola trough-mouth fans (north west Barents Sea). Mar. Geol. 286, 65–81. https://doi.org/10.1016/j.margeo.2011.05.009.
Piasecka, E.D., Winsborrow, M.C.M., Andreassen, K., Stokes, C.R., 2016. Reconstructing the retreat dynamics of the Bjørnøyrenna Ice Stream based on new 3D seismic data from the central Barents Sea. Quat. Sci. Rev. 151, 212–227. https://doi.org/10.1016/j.quascirev.2016.09.003.
Piper, D.J.W., Normark, W.R., 2009. Processes that initiate turbidity currents and their influence on turbidites: a marine geology perspective. J. Sediment. Res. 79, 347–362. https://doi.org/10.2110/jsr.2009.046.
Sergienko, O.V., Hulbe, C.L., 2011. "Sticky spots" and subglacial lakes under ice streams of the Siple Coast, Antarctica. Ann. Glaciol. 52, 18–22. https://doi.org/10.3189/172756411797252176.
Sharp, M., Richards, K., Willis, I., Arnold, N., Nienow, P., Lawson, W., Tison, J.-L., 1993. Geometry, bed topography and drainage system structure of the haut glacier d'Arolla, Switzerland. Earth Surf. Process. Landforms 18, 557–571. https://doi.org/10.1002/esp.3290180608.
Shreve, R.L., 1972. The movement of water in glaciers. J. Glaciol. 11, 205–214.
Siegert, M.J., 2000. Antarctic subglacial lakes. Earth Sci. Rev. 50, 29–50. https://doi.org/10.1016/S0012-8252(99)00068-9.
Siegert, M.J., Le Brocq, A., Payne, A.J., 2007. Hydrological connections between Antarctic subglacial lakes, the flow of water beneath the East Antarctic Ice Sheet and implications for sedimentary processes. Glacial Sediment. Process. Prod. 39, 3–10. https://doi.org/10.1002/9781444304435.ch1.
Siegfried, M.R., Fricker, H.A., Carter, S.P., Tulaczyk, S., 2016. Episodic ice velocity fluctuations triggered by a subglacial flood in West Antarctica. Geophys. Res. Lett. 43, 2640–2648. https://doi.org/10.1002/2016GL067758.
Simkins, L.M., Anderson, J.B., Greenwood, S.L., Gonnermann, H.M., Prothro, L.O., Ruth, A., Halberstadt, W., Stearns, L.A., Pollard, D., Deconto, R.M., 2017. Anatomy of a meltwater drainage system beneath the ancestral East Antarctic ice sheet. Nat. geo 10, 691–698. https://doi.org/10.1038/NGEO3012.
Smith, B.E., Gourmelen, N., Huth, A., Joughin, I., 2017. Connected Subglacial lake drainage beneath thwaites glacier, west Antarctica. Cryosphere 11, 451–467. https://doi.org/10.5194/tc-11-451-2017.
Stearns, L.A., Smith, B.E., Hamilton, G.S., 2008. Increased flow speed on a large East Antarctic outlet glacier caused by subglacial floods. Nat. Geosci. 1, 827–831. https://doi.org/10.1038/ngeo356.
Stroeven, A.P., Hättestrand, C., Kleman, J., Heyman, J., Fabel, D., Fredin, O., Goodfellow, B.W., Harbor, J.M., Jansen, J.D., Olsen, L., Caffee, M.W., Fink, D., Lundqvist, J., Rosqvist, G.C., Strömberg, B., Jansson, K.N., 2016. Deglaciation of Fennoscandia. Quat. Sci. Rev. 147, 91–121. https://doi.org/10.1016/j.quascirev.2015.09.016.
Thomsen, H., Olesen, O., Braithwaite, R.J., Boggild, C., 1991. Ice drilling and mass balance at Pakitsoq, Jakobshavn, central West Greenland. Rep. - Geol. Surv. Greenl. 152, 80–84.
Trommelen, M.S., Ross, M., Ismail, A., 2014. Ribbed moraines in northern Manitoba, Canada: characteristics and preservation as part of a subglacial bed mosaic near the core regions of ice sheets. Quat. Sci. Rev. 87 https://doi.org/10.1016/j.quascirev.2014.01.010.
Tulaczyk, S., Kamb, W.B., Engelhardt, H.F., 2000. Basal mechanics of Ice Stream B, west Antarctica: 1. Till mechanics. J. Geophys. Res. 105, 463–481. https://doi.org/10.1029/1999JB900329.
Vaughan, D.G., Corr, H.F.J., Smith, A.M., Pritchard, H.D., Shepherd, A., 2008. Flow-switching and water piracy between rutford ice stream and carlson inlet , west Antarctica. J. Glaciol. 54, 41–48.
Vorren, T.O., Landvik, J., Andreassen, K., Laberg, J.S., 2011. Quaternary Glaciations - Extent and Chronology. Glacial History of the Barents Sea Region, first ed. Elsevier Inc. https://doi.org/10.1016/B978-0-444-53447-7.00027-1.
Waelbroeck, C., Labeyrie, L., Michel, E., Duplessy, J.C., McManus, J.F., Lambeck, K., Balbon, E., Labracherie, M., 2002. Sea-level and deep water temperature changes derived from benthic foraminifera isotopic records. Quat. Sci. Rev. 21, 295–305. https://doi.org/10.1016/S0277-3791(01)00101-9.
Weertman, J., 1972. General theory of water flow at the base of a glacier or ice sheet. Rev. Geophys. 10, 287–333.
Winberry, J.P., Anandakrishnan, S., Alley, R.B., 2009. Seismic observations of transient subglacial water-flow beneath MacAyeal Ice Stream, West Antarctica. Geophys. Res. Lett. 36, 1–5. https://doi.org/10.1029/2009GL037730.
Wingham, D.J., Siegert, M.J., Shepherd, A., Muir, A.S., 2006. Rapid discharge connects Antarctic subglacial lakes. Nature 440, 1033–1036. https://doi.org/10.1038/nature04660.
Winsborrow, M., Andreassen, K., Hubbard, A., Plaza-Faverola, A., Gudlaugsson, E., Patton, H., 2016. Regulation of ice stream flow through subglacial formation of gas hydrates. Nat. Geosci. 9, 370–374. https://doi.org/10.1038/ngeo2696.
Wright, A., Siegert, M., 2012. A fourth inventory of Antarctic subglacial lakes. Antarct. Sci. 24, 1–6. https://doi.org/10.1017/S095410201200048X.
Wright, A.P., Siegert, M.J., Le Brocq, A.M., Gore, D.B., 2008. High sensitivity of subglacial hydrological pathways in Antarctica to small ice-sheet changes. Geophys. Res. Lett. 35, L17504. https://doi.org/10.1029/2008GL034937.
Wright, P.J., Harper, J.T., Humphrey, N.F., Meierbachtol, T.W., 2016. Measured basal water pressure variability of the western Greenland Ice Sheet: implications for hydraulic potential. J. Geophys. Res. Earth Surf. 121, 1134–1147. https://doi.org/10.1002/2016JF003819.Received.
Xu, Y., Rignot, E., Menemenlis, D., Koppes, M., 2012. Numerical experiments on subaqueous melting of Greenland tidewater glaciers in response to ocean warming and enhanced subglacial discharge. Ann. Glaciol. 53, 229–234. https://doi.org/10.3189/2012AoG60A139.

Paper 2

Ice margin retreat and grounding-zone dynamics during initial deglaciation of the Storfjordrenna Ice Stream, western Barents Sea

Calvin Shackleton, Monica Winsborrow, Karin Andreassen, Renata Lucchi, Lilja Bjarnadóttir. 2019.

In review, Boreas

Ice margin retreat and grounding-zone dynamics during initial deglaciation of the Storfjordrenna Ice Stream, western Barents Sea

Calvin Shackleton[1*], Monica C. M. Winsborrow[1], Karin Andreassen[1], Renata G. Lucchi[2], Lilja R. Bjarnadóttir[3]

[1] CAGE - Centre for Arctic Gas Hydrate,Environment and Climate, Department of Geosciences, UiT the Arctic University of Norway, 9037 Tromsø, Norway.
[2] OGS (Istituto Nazionale di Oceanografia e di Geofisca Sperimentale), Sgonico, Italy.
[3] Geological Survey of Norway (NGU), Trondheim, Norway.
[*] calvin.s.shackleton@uit.no

Keywords: Grounding-zone; glacial geomorphology; ice margin; calving; subglacial hydrology; iceberg ploughmarks; meltwater plume; ice stream; Barents Sea; deglaciation

Abstract

Processes occurring at the grounding-zone of marine terminating ice streams are crucial to marginal stability, influencing ice discharge over the grounding-line, and thereby regulating ice sheet mass balance. We present a high-resolution marine geophysical dataset over a ~30 x 40 km area from the former ice stream grounding-zone in Storfjordrenna, a large cross-shelf trough in the western Barents Sea, south of Svalbard. Mapped ice marginal landforms on the outer shelf include a large accumulation of grounding-zone deposits and a diverse population of iceberg ploughmarks, which record the initial retreat and subsequent stabilization of the ice margin during deglaciation of the Late Weichselian Storfjordrenna Ice Stream. Iceberg ploughmark sets suggest diverse controls on iceberg calving locally, which likely led to the production of multi-keeled, tabular icebergs at the southern sector of the former ice margin, and large, single-keeled icebergs in the northern sector. Retreat of the palaeo-ice stream from the continental shelf break was characterised by rapid ice margin break-up via large calving events, evidenced by intensive iceberg scouring on the outer shelf. We suggest that earlier ice stream retreat in the north of Storfjordrenna was facilitated by retrograde bed slopes on the northern shelf. The retreating ice margin stabilized in outer-Storfjordrenna, where the southern tip of Spitsbergen and underlying bedrock ridges provide lateral and basal pinning points. Ice-proximal fans on the western flank indicate that subglacial meltwater conduits were active during deglaciation, forming meltwater plumes at the ice margin. Along the length of the former ice margin, key environmental parameters likely impacted ice margin stability and grounding-zone deposition, and should be taken into consideration when reconstructing recent changes or predicting future changes to the margins of contemporary ice streams.

1.0 Introduction

The greatest ice mass losses from both modern and palaeo-ice masses occur at ocean margins (Pritchard et al., 2009), where ice streams and outlet glaciers interact with the ocean at the transition between grounded and ungrounded ice: the grounding-zone (Stokes and Clark, 2001; Rignot et al., 2011). This zone is a complex area where ice, water and sediments are transferred into the marine environment via pushing, calving and melting (Powell et al., 1996). These processes determine the rate of ice discharge across the grounding zone (Pattyn et al., 2006;

Schoof, 2007; Katz and Worster, 2010) and thus influence the stability of marine-terminating ice margins. Fluctuations may be rapidly propagated upstream, with increases in calving rates triggering ice acceleration, dynamically driven thinning, and enhanced margin retreat (Howat et al., 2007; Nick et al., 2009). The grounding-zone is sensitive to internal glaciological factors, ice dynamics and geometry (Bassis and Jacobs, 2013), marginal glacier hydrology and local sedimentary processes (Powell and Alley, 1997), as well as external environmental factors, such as water depth, bed slope and climatic changes including atmospheric and oceanic temperatures (Moon and Joughin, 2008; Sole et al., 2008). Elucidating the relative importance and magnitude of grounding-zone processes in different settings remains a key challenge to understanding and eventually predicting grounding-zone behaviour.

Investigating the grounding-zones of palaeo-ice streams can provide important insights into long-term grounding-zone behaviour. Accumulations of glacigenic sediments create geomorphological features of distinct size, geometry, and sedimentary structure controlled by depositional, hydrological and glaciological processes occuring at marine ice margins during retreat (Powell, 1990; Ottesen and Dowdeswell, 2006). When ice margins remain stable at a location for some time, the build-up of sediments deposited at the grounding-zone form a range of ice marginal landforms, depending on the dominant mode of deposition. Grounding-zone wedges (GZW), ice-proximal fans, and moraines are observed across glaciated and deglaciated regions (e.g. Powell and Alley, 1997; Horgan et al., 2013; Batchelor and Dowdeswell, 2015), and are used to reconstruct the locations of, and processes occuring at, marine-terminating ice margins. Beyond the ice margin, the keels of icebergs scour seafloor sediments to leave behind iceberg ploughmarks, which are common features in the foreground of contemporary and palaeo marine-terminating outlet glaciers and ice streams (Lien et al., 1989; Dowdeswell et al., 1993; Dowdeswell and Bamber, 2007; Ottesen et al., 2008; Livingstone et al., 2013; Andreassen et al., 2014; Dowdeswell and Hogan, 2014). Here we present a detailed geomorphic study of grounding-zone landforms of the Storfjordrenna palaeo-Ice Stream, a major outlet of the marine-based Barents Sea Ice Sheet (BSIS) (Fig. 1), using high-resolution multibeam bathymetry data, shallow acoustic subsurface Chirp sub-bottom profiles, and 2D seismic profiles to reconstruct calving and grounding-line activity during ice retreat from the continental shelf break through outer-Storfjordrenna.

2.0 Study area

The Storfjordrenna cross-shelf trough is located south of the Svalbard Archipelago in the western Barents Sea, and is up to 420 m deep, 250 km long and 125 km wide at the continental shelf break (Fig. 1a). A trough-mouth fan (TMF) extends westwards from the mouth of the trough, spanning 35,000 km^2 and comprised of 115,000 km^3 of sediments, delivered to the shelf break by ice streams operating in Storfjordrenna over multiple glaciations (Vorren and Laberg, 1997). During the most recent, Late Weichselian glaciation, the Storfjordrenna Ice Stream was grounded at the continental shelf edge (Laberg and Vorren, 1996; Vorren and Laberg, 1997; Pedrosa et al., 2011; Lucchi et al., 2013) and had a drainage basin estimated to

60,000 km^2 (Batchelor and Dowdeswell, 2014), with ice feeding in from the north over Spitsbergen, the islands of Edgeøya, Hopen, Bjørnøya, and the submerged divide along Spitsbergenbanken (Fig. 1) (Landvik et al., 1998; Dowdeswell et al., 2005; Dowdeswell et al., 2010a; Ingólfsson and Landvik, 2013). The vast drainage catchment of the Storfjordrenna Palaeo-Ice Stream spans both terrestrial and shallow to deep marine settings in the Barents Sea, and the ice stream would have been one of the largest ice catchments of the Barents Sea and Svalbard ice sheets, sensitive to climatic and oceanographic changes (Howat et al., 2010).

Relative glaciofluvial sediment volumes observed in cores from the TMF suggest that the northern parts of the ice stream retreated from the shelf break earlier, and the southern sector remained grounded at the shelf break for longer (Pedrosa et al., 2011). Dated foraminifera within hemipelagic sediments in a sediment core (JM02-460-PC) taken over 60 km east from the shelf edge in outer-Storfjordrenna (Fig. 1a), indicate that retreat from the shelf edge began before ca 19.6 cal ka BP (Rasmussen et al. 2007) (Table 1 details radiocarbon dates). Core JM02-460-PC was recovered from the northern parts of the trough, suggesting that the date relates to the early retreat of the northern sector of the ice stream. Bivalve shell fragments found in a core in the inner part of the trough (Fig. 1a) suggest that central Storfjordrenna, over 150 km upstream of the shelf edge, was ice free before ca. 13.9 cal ka BP (Table 1; Łącka et al., 2015). Little is known about the dynamics of the Storfjordrenna Palaeo-Ice Stream and how it deglaciated through the outer trough. The geomorphological features presented here provide insights into the deglaciation of the Storfjordrenna Ice Stream, and contribute to increasing evidence for the geomorphological signatures of marine-terminating palaeo-ice streams.

Core/Location	Uncorrected Age (^{14}C yrs B.P.)	2σ Range (years B.P.)	Median Probability Age (yrs B.P.)	Source	Lat. (°N)	Long. (°S)	Material dated
JM02-460-PC	16,750±110	19,278-19,938	19,608	Rasmussen et al. (2007)	76.05	15.73	*Neogloboquadrina pachyderma* in hemipelagic sediment deposits above till
JM09-020-GC	12,570±60	13,780-14,114	13,947	Łącka et al. (2015)	76.31	19.70	Bivalve shell beneath the upper surface of the subglacial till horizon
JM10-10-GC	10,960±44	12,121-12,562	12,375	Rasmussen and Thomsen (2014)	Georeferenced		Bivalve within mixture of glacimarine and diamictic deposits
Edgøya (Blåfjorddalen)	10,770±110	11,535-12,489	12,025	Landvik et al. (1992)	77.98	22.98	*Mya truncata* within silty marine sands

Table 1: Minimum ages of deglaciation surrounding Storfjordrenna, from radiocarbon AMS dating of sediment cores.

3.0 Materials and methods

We utilize high-resolution swath bathymetry data for geomorphological mapping, covering 1600 km^2 and spanning water depths 300 to 400 m below sea level. Data was collected using a hull-mounted Kongsberg Simrad 30 kHz EM300 multibeam echosounder during two research cruises onboard the R/V Helmer Hanssen in the summers of 2013 and 2014, in outer-Storfjordrenna (Fig. 1b). The bathymetry data was processed in Neptune and gridded in IVS Fledermaus v7 to a horizontal resolution of 15 x 15 m. The Fledermaus software was used to visualize and interpret the data, and landforms were mapped manually in Esri ArcGIS v.10. Two 2D seismic lines were acquired during both research cruises using a Generator-Injector (GI) airgun operating in harmonic mode with total volume of 30 in^3, to generate seismic shots with a shot rate of 3 s. A hydrophone cable (16 m long, single-channel streamer) was used to record the reflected seismic signal. Seismic lines were processed in the DelphSeismic software and visualized and interpreted using Petrel v.2014.1.

Subsurface profiles were acquired in Storfjordrenna using a hull-mounted Edgetech 3300 – HM CHIRP sub-bottom sediment profiler, with 4 x 4 transducer array operating at 4 kW and transmitting an FM pulse, linearly swept over a full spectrum frequency range (1.5 kHz to 9 kHz over 40 ms). Data were processed, viewed and interpreted in the Kingdom Suite v.8.8 software. The velocity of sound waves in seawater is presumed to be 1500 m s^{-1} and due to the relatively shallow nature of the sedimentary features, this velocity is also assumed for subsurface travel of waves. With this assumption we obtain a minimum estimate for the thickness of sedimentary units. Table 1 summarises the ^{14}C ages referred to in the text and in figure 1. All dates were recalibrated using Calib 7.1 (Stuiver and Reimer, 1993) and the MARINE13 calibration curves (Reimer et al., 2013). A ΔR value of 105±24 was applied for local effects on the global reservoir correction in the Arctic (Mangerud et al., 2006).

4.0 Results and interpretation

The bathymetric and subsurface data reveal a complex network of interlinked geomorphological features, which are categorized based on similarities in form, geometry, size, and composition. Here we describe and interpret a large, trough-transverse sedimentary ridge (Figs. 2 and 3; Section 4.1) and an assortment of seafloor grooves (Fig. 4a), which are split into single grooves (Section 4.2) and sets of parallel grooves (Section 4.3).

4.1 Sedimentary wedges and fans: grounding-zone deposits

4.1.1 Observations

The multibeam swath bathymetry shows a 43 km long slope break, 60 km east of the continental shelf edge and orientated approximately north-south, perpendicular to the orientation of the trough and to the direction of former ice flow (Figs. 2 and 3). Shallow acoustic and 2D seismic profiles across the break in slope reveal a uniform, acoustically transparent sedimentary unit with some low-amplitude seaward-dipping reflections but otherwise very few internal reflectors (Figs. 2b-e; 3b,c). Sediment packages with a similar acoustically transparent signature have been described in the neighbouring Kveithola trough

(Rebesco et al.,2011; Bjarnadóttir et al.,2013) and elsewhere in the Barents Sea (Hogan et al., 2010; Andreassen et al., 2014; Bjarnadóttir et al., 2014), and are referred to as an acoustically transparent sediment body (ATB). Forty Chirp sub-bottom profiles and two 2D seismic profiles were utilised to map the western margin of the ATB, and the eastern extent (Fig. 2a) is interpolated between the two seismic profiles (Fig. 3b,c), and three Chirp sub-bottom profiles with sufficient penetration to image observable features.

The ATB has a convex western termination and thickens towards the east, forming an approximate wedge shape up to 120 m thick in the north and up to 25 m thick in the south (Fig. 3b,c). Based on the available sub-surface data, we estimate that it spans a minimum area of 1152 km^2 and extends up to 30 km in the east-west orientation of the trough. In the north, the seafloor west of the ATB is 15 to 20 m deeper than surrounding areas (Fig. 3a), and Pedrosa et al. (2011) show that the depression becomes shallower towards the west, terminating at a ridge on the shelf edge. The ATB margin therefore terminates on a retrograde bed in the north. A buried acoustic reflector is observed in Chirp sub-bottom profiles at the western edge of the ATB (Fig. 2b-e), which varies along its length from being relatively smooth (Fig. 2e), to containing sharp undulations (buried grooves: Fig. 2b,d).

Both the bathymetric and acoustic datasets show clear differences in the form and surface morphology of the western edge of the ATB along its length, with a large protruding fan in the north, smaller overlapping fans characterising the southern edge (Fig. 2a), and a lack of fan shaped accumulations in between. The large fan in the north of the area has a smooth seafloor surface (Fig. 2b), and is situated in the deepest water depths (up to 400 m) along the ATB margin. Shallow acoustic profiles reveal an undulating reflector beneath the fan, which can be traced for approximately 9 km beneath the ATB (Fig. 2b). On 2D seismic data a high amplitude reflector marks the base of the ATB in the north (Fig. 3b), and from SW to NE this surface deepens towards the middle, before shallowing steeply towards the eastern margin of the ATB. Below the eastern end of the high amplitude reflector is a repeating pattern of phase reversed reflections that become increasingly steeper with depth, labelled ‘multiple’ on Figure 3b. To the east, the basal reflector contains three large ridges 30 to 75 m high (white arrows: Fig. 3b), the highest of which coincides with the approximate eastern extent of the ATB. The western margin of the southern sector of the ATB comprises four coalescing smaller fans (average widths of 3.3 km) spaced approximately 3 km apart, that are otherwise similar in planform to the large fan in the north (Fig. 2a). The ATB long profile here contains a small step (Fig. 3c) and the buried reflector is relatively smooth (Figs. 2e, 3c).

4.1.2 Interpretation

The trough-transverse ATB with wedge-shaped cross section (Figs. 2b-e, 3b,c) is consistent with descriptions of grounding-zone deposits (GZD), formed through accumulation of sediments at the grounding-zones of marine-terminating ice streams (Powell 1990; Powell and Alley, 1997; Ottesen and Dowdeswell, 2006; Koch and Isbell, 2013). We suggest that the observed ATB is an intermediate feature on a continuum of described grounding-zone features

formed depending on the relative abundance of subglacial meltwater, between end-member features 'Morainal Banks' characterised by ice-proximal fans on their ice-distal edge, and 'Grounding-Zone Wedges' characterised by asymmetric geometry and homogenous, fine-grained sediments (Powell and Alley, 1997: Batchelor and Dowdeswell, 2015). The GZD described in this study exhibits characteristics of both 'end-member' landforms. We suggest a build-up of material via line-sourced deposition of subglacial and englacial debris over the grounding-line, accounting for the trough-transverse, asymmetric nature of deposited sediments. At the same time, point sourced meltwater plumes and sediment gravity flows at the palaeo-ice margin resulted in grounding-line proximal fans (e.g. Powell and Molnia, 1989; Powell and Domack, 2002). The bulk of deposits in outer-Storfjordrenna are acoustically transparent, reflecting the unsorted depositional processes at the former grounding-line, and the limited number of faint dipping reflections in the northern parts of the GZD (Fig. 3b) indicate sediment progradation associated with continuous delivery of sediments over the grounding-line. The fanned morphology at the western flank of the GZD (Fig. 3a) is similar to grounding-zone deposits described in Kveithola, to the south of Storfjordrenna (Rebesco et al., 2011; Bjarnadóttir et al., 2013).

Based on the large fan in the north and overlapping fans in the south, we suggest that a major contributor to sediment accumulation was suspension settling from meltwater plumes discharged from ice-margin subglacial meltwater outlets. Marginal outlet channels with high discharge and velocity deliver considerable amounts of sediment over and beyond the grounding-line to form fan-shaped accumulations (Powell, 1990; Powell and Alley, 1997), with longer suspended sediment plumes associated to higher meltwater velocities and channel discharge (Syvitski, 1989). The single-fan morphology of the northern parts of the GZD (Fig. 2a) suggests formation by a large meltwater conduit and its associated meltwater plume. Steps in the long profile (Fig. 3a,b) might reflect periods of meltwater conduit inactivity and associated reductions in sediment deposition, which in conjunction with continued ice margin retreat eastwards would result in steps, following the eventual reactivation of the conduit, and resumed sediment deposition.

The coalescing fans that comprise the western edge of the southern sector of the ATB are interpreted to have been shaped by sedimentation from multiple or shifting point sources (i.e. subglacial conduits), and associated changes in suspended sediment output from the margin. In a similar manner to the deposits in the north, the seafloor morphology in the south is interpreted to have formed through the deposition of suspended sediment as meltwater enters the ocean and forms a plume upon exiting the subglacial environment. Basal water conduits are prone to shifting location, and seasonal differences in meltwater input, shifting ice dynamics and changing ice thickness affect glacier hydrology (e.g. Clark and Walder, 1994), all factors which are prominent during deglaciation. Iceberg calving may have also played a role in conduit switching on/off or shifting location, by exposing new faces of the ice front and altering ice margin geometry (Syvitski, 1989). The fans may be smaller here than in the north due to lower

water velocities in the channels and therefore a reduced plume length, limiting the capacity to carry suspended sediment far beyond the ice margin.

4.2 Curvilinear grooves: single-keeled iceberg ploughmarks

4.2.1 Observations

Large curvilinear grooves are observed in the northern parts of the trough, clustered immediately west and south of the large sedimentary fan (Fig. 4a). East-west trending grooves in the north (Fig. 4b) are no more than 2 m deep (Fig. 4c) with lengths reaching at least 7.6 km (most extend beyond the available bathymetric data). Cross cutting is common, making it difficult to assess the full extent of some landforms, and the majority of grooves are flanked on either side by small berms (Fig. 4b-g). Correlation between grooves observed in bathymetric data and grooves observed in subsurface data (Fig. 4b,d), suggests that the grooves visible on the seafloor extend beneath the GZD. A deeper and wider population of northeast-southwest oriented curvilinear grooves are clustered immediately beyond the southern flank of the large ice-proximal fan (Fig. 4e-g), and mostly terminate where the seafloor shallows to the west (Fig. 4e). The grooves are 1 to 12 m in height from trough to peak and up to 9 km in length, though many are overprinted by an east-west trending set of two parallel grooves, can result in underestimation of groove lengths (Fig. 4e). Subsurface data shows that at least one of the grooves has been partially buried by the GZD (Fig. 4g), indicating that this, and potentially others, initiate beneath the deposits.

To the far north of the bathymetric data some linear features with similar orientations to the curvilinear grooves are observed, but they resemble streamlined ridges rather than grooves. The ridges are found in the deepest water depths of the available bathymetric data (up to 400 m), in a small area absent of seafloor grooves. The ridges are several metres high and over 8 km long, extending beyond the available bathymetry dataset (Fig. 4b). Two circular mounds (Fig. 4a) overprint the ridges, which have previously interpreted as Gas-Hydrate Pingos (GHP) (Serov et al., 2017). Additionally, curvilinear grooves with smaller widths and depths than those described above are common throughout the survey area (Fig. 4a), typically <1 m wide and <2 m deep. The smaller grooves change direction often and by up to 180 degrees, regularly cross-cutting each other and other geomorphic features, and generally have small berms on either side. The small grooves are the only resolvable features that overlie the GZD.

4.2.2 Interpretation

Based on their curvilinear planform, flanking berms, and frequent cross-cutting, both the shallower and the deeper/wider curvilinear grooves on the seafloor (Fig. 4a-g) are interpreted as iceberg ploughmarks, formed through scouring of the seabed by the keel of large icebergs. Similar features have been observed elsewhere in the Barents Sea (e.g. Andreassen et al., 2014), in the Canadian Arctic (e.g. Maclean et al., 2010) and Antarctic (e.g. Graham et al., 2016) and are interpreted as evidence of iceberg keel scour. The difference in depth between iceberg ploughmarks to the west and to the south of the large fan (Fig. 4a) can be explained by the 15-20 m difference in water depth (Fig. 3a), limiting iceberg keel scouring in the deeper waters.

Furthermore, relatively high sediment infilling of seafloor features is expected in the north, associated with the high rate of sediment delivery beyond the ice margin from the inferred large subglacial meltwater outlets and their associated plumes.

Based on their high length to width ratio, the streamlined ridges to the far north of the bathymetric dataset (Fig. 4b) are interpreted as mega-scale glacial lineations (MSGL), formed subglacially at an earlier stage to other features discussed here, when the ice stream was grounded at or close to the continental shelf break. MSGL occurrence in the deepest water along the former margin suggests that lineations must be preserved because they are located below the depth of iceberg grounding, limiting scouring of the seafloor and overprinting of the surface, as observed in shallower areas of the dataset.

Smaller grooves with highly variable orientations are interpreted to have been formed through iceberg keel scour from icebergs of a smaller scale to that previously described. Such features are ubiquitous at the marine margins of both palaeo and contemporary ice streams and outlet glaciers (e.g. Lien et al., 1989; Dowdeswell and Ottesen, 2013; Livingstone et al., 2013; Esteves et al., 2017), and their highly variable orientations and sudden changes in direction are attributed to changes in ocean currents and surface winds (Smith and Banke, 1983). The termination of these features usually arises where a sudden increase in depth occurs and the keel is no longer deep enough to be grounded, or when the iceberg has melted sufficiently enough to cause the keel to become ungrounded (Dowdeswell and Bamber, 2007). As the only grooved feature present on top of the GZD in the study area, smaller grooves indicate continued calving of single-keeled icebergs subsequent to the deposition of grounding-zone sediments.

4.3 Sets of parallel curvilinear grooves: multi-keeled iceberg ploughmarks

4.3.1 Observations

Sets of parallel grooves are observed on the seafloor in the southern sectors of the bathymetric dataset (Fig. 4a), clearly marking the seafloor beyond, and beneath the southern parts of the GZD (Figs. 5 and 6). The sets have a wide range of widths, from 300 m to 4.6 km, and the number of grooves per set is variable and not necessarily correlated to width. The GZD covers the full eastern extent and origin of most groove sets, and some extend downstream beyond the available bathymetric data (Fig. 4a). Lengths range from several km to a minimum of 22.3 km, and the number of grooves in each set generally diminishes with increasing water depth. Kinks within otherwise straight sets of grooves occur in the thinner sets (Fig. 5a) and some have large berms on either one or both edges (Figs. 5a and 6a).

The largest of the groove sets (Set 1; Fig. 4a) has a consistent width of 4.6 km and is at least 21 km long, spanning water depths between 350 to 380 m (Fig. 6a,b), although the upstream extent is covered by the GZD, and the downstream extent lies beyond the bathymetry data. Subsurface data indicates that the grooves extend beneath the GZD a minimum of 3.6 km (Fig. 6c,d). Ridges and grooves vary in height throughout set 1, between 0.5 m and 5 m from trough to peak (Fig. 6b). The north-western flank is bordered by a berm up to 5 m high and 600 m

wide (Fig. 6a). Cutting across the largest groove set at 90° is a narrower set (Set 2; Fig. 4a) up to 2 km in width (Fig. 6e), with an origin mostly not covered by the GZD, and most grooves initiating away from the western edge. Set 2 has a berm only on its northern flank (Fig. 6a), and originates with two parallel grooves 1.8 km in length extending from beneath the GZD, before the initiation of 8 more grooves extending west-northwest for 11 km. Groove sets 1 and 2 overprint an array of older sets of predominantly east-west trending parallel grooves (Fig. 4a). Additionally, one set of grooves contains regularly spaced transverse ridges 1 to 2 m high, with consistent spacing of approximately 500 m (Fig. 5a).

4.3.2 Interpretation

Sets of parallel, curvilinear grooves are interpreted to have formed through seabed scouring by multi-keeled icebergs, based on their curvilinearity, kinks in their long profile, flanking berms, and diminishing number of grooves per set with increasing depth. Large, tabular icebergs calving off the ice stream terminus are interpreted to have a number of extruding keels at their base, which scoured the seafloor as icebergs advanced westwards. Burial of ploughmarks by material comprising the GZD suggests that scouring of the seafloor by the multi-keeled icebergs occurred before the deposition of the GZD. The close spacing and organisation of grooves into discrete sets indicates that they have been ploughed by large multi-keeled icebergs rather than by many smaller, single-keeled icebergs trapped in multi-year sea ice. Such features have been described in Antarctica (Lien et al., 1989; Dowdeswell and Bamber, 2007, Wise et al., 2017), the Central Barents Sea (Andreassen et al., 2014; Bjarnadóttir et al., 2014), the northern Svalbard margin (Hogan et al., 2010) and the Canadian Arctic (MacLean et al., 2010). Transverse ridges spanning several grooves (Fig. 5a) are interpreted as corrugation ridges, formed by diurnal tidal forcing on grounded icebergs (Jakobsson et al., 2011; 2012). Corrugation ridges with comparable widths, heights and spacings are described in Pine Island Bay, West Antarctica (Jakobsson et al., 2011; Graham et al.,2013), and on the northern Svalbard shelf (Bjarnadóttir et al., 2014; Dowdeswell and Hogan, 2014).

5.0 Discussion

The grounding-line landform assemblage described and interpreted here from outer-Storfjordrenna demonstrates clear differences in morphology between its north and south sectors (Summarized in Table 2). The following sections discuss the significance of the documented variations in the context of ice stream characteristics and margin retreat (Section 5.1), grounding-zone deposition and subglacial hydrology (Section 5.2), and iceberg calving and seabed scouring (Section 5.3).

	Northern sector	Southern sector
Catchment area (Setting)	Svalbard (Terrestrial)	Barents Sea (Marine)
Bedslope	East-dipping (retrograde slope)	West-dipping (positive slope)
GZD western margin morphology	Large, single sedimentary fan	Small, coalescing sedimentary fans
GZD max. thickness	120 m	25 m
Iceberg calving	Majority deep, single-keeled icebergs	Majority large, multi-keeled icebergs
Topographic pinning	Lateral (Spitsbergen) and basal (bedrock ridges)	Limited lateral (Spitsbergenbanken)
Water depth at ice margin	Deeper (370 - 400 m)	Shallower (364 - 370 m)

Table 2: Summary of the differences in geomorphological and environmental characteristics between the northern and southern sectors of outer-Storfjordrenna.

5.1 Ice stream characteristics and margin retreat

The Storfjordrenna Ice Stream had a large and varied catchment, with the northern parts of the trough fed by ice draining from terrestrial Svalbard through Storfjorden, and the southern parts fed by ice draining the interior of the marine-based Barents Sea Ice Sheet and Spitsbergenbanken (Fig. 1). Ice is therefore sourced from three different ice sheet settings: from areas at relatively high bed altitude and stable ice sources over Svalbard; from the interior of the ice sheet with low-lying bed and fluctuating ice domes; and from the relatively shallow and topographically featureless Spitsbergenbanken closer to the ice sheet periphery. Ice source areas dictate ice thicknesses and temperature regimes, and are influenced by different topographic constraints, thereby contributing to the distinct crevasse spacing and distributions across the former ice margin after the ice converged, and producing spatially clustered iceberg keel scours. Previous studies propose that the Storfjordrenna Ice Stream was comprised of three distinct ice stream lobes while grounded at the shelf break (Pedrosa et al., 2011; Lucchi et al., 2013; Llopart et al., 2015), and our findings show that the ice stream also maintained distinct lateral variations, at least in terms of iceberg production, during the initial stages of deglaciation. We also interpret the differences in GZD morphology and iceberg scouring between the north and south parts of outer Storfjordrenna to reflect variations in ice stream characteristics across the trough (see sections 5.2 and 5.3).

The initiation of deglaciation in Storfjordrenna is estimated at around 20 to 19 cal ka BP based on the onset of hemipelagic sediment and ice rafted debris (IRD) concentration peaks in sediment cores from the TMF and outer shelf (Rasmussen et al., 2007; Jessen et al., 2010). Break-up of the ice margin from the shelf break via large calving events is evidenced by overlapping sets of ploughmarks created by large, tabular icebergs. The subsequent burial of ploughmark sets by the accumulation of grounding-zone sediments, and thin sediment drapes over many of the seafloor features (Figs. 2b-e, 4d,g) indicate grounding-line stabilisation for some time in outer-Storfjordrenna. Grounding-lines are commonly stabilized on pinning points, such as increasingly narrow trough/fjord mouths and topographic highs under basal ice (Thomas, 1979; Benn et al., 2007a; Jamieson et al., 2012). We propose that this was also the case for outer Storfjordrenna where 3 ridges 30 to 75 m high are observed in seismic data at the eastern edge of the GZD (Fig. 3b), providing basal pinning points. Furthermore, the protruding southern tip of Spitsbergen provides a lateral pinning point for the ice stream while it was grounded in outer-Storfjordrenna.

The relatively non-scoured upper surface of the GZD informs us that either calving was minimal subsequent to margin stabilisation and GZD deposition, or that the ice margin was floating, with ice already in buoyant equilibrium with the ocean water prior to calving, resulting in no significant drop in height or seafloor scouring. A floating ice shelf would also extend the calving margin well away from the grounding-line, preserving the surface of the GZD from iceberg scouring. It is difficult to ascertain whether the former margin had a substantial floating ice shelf, although GZW build-up at other ice margins is associated with a sub-shelf cavity beneath floating ice (Batchelor and Dowdeswell, 2015). We tentatively suggest that the Storfjordrenna Ice Stream margin was floating while the grounding-line was stabilised in outer-Storfjordrenna, based on the non-scoured surface of the GZD and the asymmetric shape of deposited sediments which suggest deposition within a sub-shelf cavity.

The break-up of the ice margin during initial retreat from the shelf break, and subsequent margin stabilisation in outer-Storfjordrenna is documented by the intensive seafloor scouring and accumulation of grounding-zone sediments. Retreat of the Storfjordrenna Ice Stream was episodic in nature, at least from the continental shelf edge. This is supported by observations of coarse-massive-IRD subfacies during deglaciation in cores from the TMF (Lucchi et al., 2013), which suggests intermittent periods of intense calving activity and margin break-up. Episodic ice retreat is also documented by a series of GZW in upstream Storfjorden, deposited during the later stages of deglaciation between 15 to 10 cal ka B.P. (Nielsen and Rasmussen, 2018). Minimum deglacial dates in Storfjordrenna to the west and east of the GZD demonstrate 200 km ice margin retreat over approximately 7900 years, indicating relatively slow averaged margin retreat rate of 0.025 km a-1 (Figure 1, Table 1; Rasmussen et al., 2007; Rasmussen and Thomsen, 2014; Patton et al., 2015). Timescales of GZD sedimentation are largely unknown, but given the large volume of sediments accumulated in outer Storfjordrenna, it is reasonable to assume that the ice margin remained stable here for some time. This, together with the

evidence for high magnitude and high frequency iceberg calving, is consistent with a significant ice margin standstill following rapid ice margin break-up.

In addition to the proximal ice sources suggested by Pedrosa et al. (2011), we suggest a topographic influence on earlier ice stream retreat in the north of the area. Long profiles along the former ice stream bed (Fig. 7) show that retrograde bed slopes underlay the northern sectors over much of its profile (Fig. 7b), whereas the bed of the southern lobe has a gentle upward-sloping inland gradient (Fig. 7d). Cores from the outer-shelf indicate that sediment accumulations since the deposition of glacial till are an order of magnitude lower than the 40 m elevation difference between the outer and outer-shelf (Rasmussen et al., 2007), ruling out a post-ice retreat origin for the retrograde bedslope. Ice margins become more unstable with increasing water depth, and margin retreat into deeper waters results in positive feedback, whereby retreat is perpetuated until a seaward-dipping bed slope or pinning point is encountered (Schoof, 2007; Jamieson et al., 2012). Retrograde bed-slopes beneath the northern sectors of the Storfjordrenna Ice Stream and runaway margin retreat through outer-Storfjordrenna may therefore have facilitated earlier retreat in the north. A relatively deeper ice bed in the northern part of the outer trough (Fig. 1b) could result from a more dynamically active and erosive ice stream here. Increased sediment fluxes and earlier ice margin stabilisation in outer-Storfjordrenna for the northern sectors of the ice stream also fits well with our observations, since the northern parts of the GZD are thicker than those farther south (Fig. 3b,c). The overdeepening in the north would promote early retreat from the shelf break, and potentially to more frequent calving of deep-keeled icebergs compared to the tabular icebergs calved from the southern sectors.

The occurrence of iceberg ploughmarks declines in water depths below 380 m (Fig. 4a), indicating a depth limit of keel scouring, and therefore revealing an upper limit to potential iceberg thicknesses. Assuming a eustatic sea level adjustment of 120 m lower than present day and isostatic depression of approximately 80 m following the LGM (Auriac et al., 2016; Patton et al., 2017), we estimate that icebergs calved from the ice stream margin when it was grounded in outer-Storfjordrenna had keels approximately 340 m deep. Given that icebergs are generally 90% submerged below the sea surface, a rough estimate of iceberg and ice margin thicknesses is 380 m. Multi-keeled iceberg ploughmarks continue beneath the GZD in several places (Fig. 6a,c,d), indicating that keel scouring occurred before the deposition of the GZD. We therefore suggest that these ploughmarks formed during initial ice margin break-up and retreat from the shelf edge, before the grounding-line stabilised in outer Storfjordrenna. The size of iceberg ploughmark sets and intensity of scouring suggests that ice retreat from the shelf break was characterised by rapid break-up of the ice margin and calving of large, tabular icebergs.

The geomorphology discussed herein is a record of two main phases of ice stream activity: ice margin retreat from the shelf break, and grounding-zone stabilisation in outer-Storfjordrenna. Ice margin retreat from the continental shelf break is documented in the large, multi-keeled iceberg ploughmarks created by tabular icebergs calved as the ice margin underwent rapid

break-up during early deglaciation. During this phase, we suggest that the bathymetric differences between the northern and southern sectors of the former ice stream bed influenced the asynchronous retreat. Subsequent to this initial retreat, the grounding-line stabilised and the ice margin remained grounded in outer-Storfjordrenna for some time, with sediments continuously being delivered and deposited at the grounding-zone, building up the GZD. During this phase, we suggest that lateral and bed pinning from southern Spitsbergen and underlying bedrock ridges were important factors determining the location of margin stabilisation.

5.2 Grounding-zone deposition and subglacial hydrology

The large accumulation of grounding-zone deposited sediments described here is evidence of the first major standstill in grounding-line retreat during the deglaciation of the Storfjordrenna Ice Stream. The build-up of the majority of sediments via progradational, line-source deposition of subglacial and englacial debris over the grounding-line leads to the overall wedge-shaped cross section of deposited material (Figs. 2b-e, 3b,c). However, the fanned morphology of the northern and southern parts of the grounding-zone deposit (Fig. 2a) indicates additional point-sourced sedimentation from ice marginal meltwater conduits and their associated meltwater plume. On a continuum of described grounding-zone landforms (Powell and Alley, 1997) from the meltwater dominated deposition of 'Morainal Banks' to the relative absence of meltwater-related deposition in 'Grounding-Zone Wedges' (Batchelor and Dowdeswell, 2015), the GZD in outer-Storfjordrenna is an intermediate form with both meltwater and non-meltwater related depositional signatures. In Kveithola, the neighbouring trough to Storfjordrenna (Fig. 1a), a similar intermediate form of grounding-zone landform is described (Bjarnadóttir et al., 2013), where the sediments display characteristics of a GZW (i.e. asymmetric, trough-transverse ridge of homogenous sediments) but include ice-proximal fans on the western flank. In Kveithola this morphology is similarly interpreted to reflect combined deposition from ice marginal meltwater plumes and line-sourced glacigenic deposition over the grounding-line, indicating that similar grounding-zone processes were operating here to those described in Storfjordrenna. Significant subglacial meltwater activity at the ice margin is further supported by sedimentary data from the slope, where gullies and laminated sediment sequences on the Storfjordrenna TMF are attributed to rapid sediment deposition from subglacial meltwater plumes (Lucchi et al., 2012).

Subglacial drainage routing is primarily controlled by the geometry and thickness of overlying ice, which directs subglacial water from areas of high pressure under thicker ice to areas of lower pressure under thinner ice (Shreve, 1972). The occurrence of ice-proximal fans in the north and south of Storfjordrenna and lack of evidence for meltwater-related deposition in between (Fig. 2a) may therefore indicate thicker ice flowing in the centre of the trough. Modelled subglacial drainage routing predicts margin outlets for large drainage basins in the northern sector of Storfjordrenna consistently throughout deglaciation (cf. Figure 8 in Shackleton et al., 2018), therefore supporting the focused drainage routing and large ice marginal meltwater outlet and plume that we propose in the north. This also explains the

difference in thickness of glacigenic diamicton in cores from the TMF, which varies from over 45 m in the northern sectors to 20 m in the southern sectors, despite longer ice margin residence time at the shelf break in the south during the LGM (Lucchi et al., 2013). Several drainage outlets in the south are also predicted by hydraulic potential modelling (Shackleton et al., 2018), but only when the ice margin was stabilised in outer-Storfjordrenna. Predicted outlets are also draining much smaller catchments, thereby supporting our reconstructions of lower-velocity meltwater plumes here, with fluctuating levels of activity. Stable drainage outlets in the north may be a consequence of a catchment comprised of more stable ice over Svalbard, in contrast to the fluctuating catchments feeding the southern sector, especially as the Barents Sea Ice Sheet underwent rapid deglaciation with associated fluctuations in ice flux, geometry and thickness.

At the southern sector of the former ice margin, average spacings of 3 km between the four overlapping fans (Fig. 3a) suggests that a singular, shifting meltwater outlet or several outlets with plumes of 3 km spacing may have been active at the former ice margin. Comparably, marginal meltwater outlets and suspended sediment plumes with the same average spacings of 3 km are observed at the margin of the Austfonna ice cap, northeast Svalbard, and have remained stable for several decades (Dowdeswell et al., 2015). Subglacial outflow across the former margin and the formation of meltwater plumes informs us that the pressure of subglacial water must have been substantial, with potential implications for the stability of the grounding-line. Lower effective pressures as a result of high-pressure basal water can facilitate increased ice velocities (Alley, 1989), leading to increased flux of ice over the grounding-line, therefore potentially increasing mass loss at the northern and southern sectors of the former margin in Storfjordrenna. Additionally, large meltwater outlets at the margin can lead to localized retreat of the ice front (Slater et al., 2015), forming embayments with laterally protruding ice either side. This may have left more of the margin open for calving and ocean driven melting, especially in the north where we infer a stable, high-discharge meltwater conduit.

5.3 Iceberg calving and seabed scouring

The extensive iceberg keel scouring in outer-Storfjordrenna (Fig. 4a) documents significant calving activity during the initial stages of deglaciation, and furthermore records local variations in calving characteristics between the northern (single-keeled icebergs) and southern (multi-keeled icebergs) sectors of the ice stream. Although it is clear that the multi-keeled ploughmarks were created before the deposition of the GZD, based on the burial of the ploughmarks in the south, the relative timing of the calving of deep, single-keeled icebergs in the north is uncertain and may not have occurred contemporaneously. An increased frequency of iceberg calving is observed with increasing water depth, due to greater ice marginal buoyancy (Benn et al., 2007b), and variations in calving characteristics between the north and south might therefore be a consequence of the difference in water depth at the former ice margin. This could promote a higher frequency of calving events, producing large, single-keeled icebergs in the north where water was deeper, and a lower frequency of multi-keeled, tabular icebergs calved in the south.

Iceberg geometry is primarily determined by crevasses within glacial ice, which can be advected passively to the terminus (Motyka et al., 2011) or develop in-situ due to stresses exerted at the margin (Benn et al., 2007a). Tabular icebergs are associated to crevasse/rift opening by glaciologically derived stresses rather than oceanic or atmospherically derived forcing (Joughin and Macayeal, 2005). Hence, the calving of large tabular icebergs in the southern sector of outer Storfjordrenna, might be linked to glaciologically controlled crevasse formation and crevasse spacings set upstream of the grounding-zone. Higher strain rates lead to deeper crevasses, and spatial disparities in ice velocity determine the strain rate, with greater stress gradients leading to increased crevassing (Benn et al., 2007a), therefore controlling both the rate and characteristics of iceberg calving. In Storfjordrenna, several hypothesised ice stream lobes converge in central Storfjordrenna to flow towards the shelf break (Fig. 1), and longitudinal stress gradients inherent in these separate ice stream lobes before they converged would become even greater once converged, leading to large numbers of deep crevasses which are advected to the margin. In addition, lateral pinning from the southern tip of Svalbard and Spitsbergenbanken provides resistance through lateral drag, which would generate strong velocity gradients, leading to higher strain rates and consequently more crevasses and calving events. Similarly, basal pinning by bedrock ridges observed upstream of the inferred grounding-line on subsurface datasets (Fig. 3b) might further spatial disparities in ice flow velocity and facilitate increased crevassing. The clustering of large, single-keeled iceberg ploughmarks in the north and multi-keeled, tabular icebergs in the south (Fig. 4a) might also therefore reflect continued production of distinct strain-induced crevasses as the ice stream lobes interacted upstream.

Subglacial meltwater drainage at the margin may also influence iceberg calving characteristics, as undercutting and selective erosion of the ice margin is associated with marginal meltwater outlets (Syvitski, 1989; Slater et al., 2015). The development of ice caves and undercut ice protrusions in the Storfjordrenna Ice Stream margin associated with continued marginal meltwater activity would have led to increased iceberg calving and embayments forming especially in the north, potentially leaving a protruding ice face in the centre of the trough. Additionally, channelised meltwater and freshwater plumes can influence local ocean circulation, leading to convective cells upwelling cold, buoyant glacial meltwater at the surface, and drawing in warmer seawater to the margin at depth, resulting in increased melting near the grounding-line (Jenkins, 2011; Motyka et al., 2011; Chauché et al., 2014; Kimura et al., 2014). The convective cells may also have influenced the movement of icebergs and keel scour orientation, which is generally the same direction as inferred palaeo-ice stream flow (Fig. 4a). Furthermore, plume-driven submarine melting can undercut the submerged portion of the calving front which may lead to submarine iceberg calving (Rignot et al., 2010) and/or more rapid rates of calving (Motyka et al., 2003).

Sea ice and/or ice melange acts as a buffer to iceberg calving, providing longitudinal backstress, whilst also preventing existing icebergs from floating away from the calving margin (Amundson et al., 2010). Further, an ice melange may strengthen sufficiently to inhibit the

overturning of large, unstable icebergs, providing a mechanism by which tabular and even non-tabular icebergs may resist overturning. The influence of ice melange on calving and subsequent seabed scour is well-evidenced at two localities in the neighbouring Bjørnøyrenna palaeo-ice stream bed (Andreassen et al., 2014; Bjarnadóttir et al., 2014). Icebergs stuck fast within an ice melange or multi-year sea ice are plausible in Storfjordrenna, given reconstructed winter surface water temperatures 1˚C above freezing for the south-eastern Svalbard margin between 20 and 15 ka BP (Rasmussen et al., 2007). Compatibly, Lucchi et al. (2013) propose that multi-year sea ice could explain occasional reductions in IRD on the Storfjordrenna TMF during deglaciation. We suggest that break-up of an ice melange containing stuck-fast tabular icebergs is a potential cause of the sudden initiation of multi-keeled iceberg ploughmark set 2 (Fig. 4a), and that melange-led drift of trapped icebergs might further explain the consistent west-southwest direction of keel scour in this region.

6.0 Conclusions

Seabed and subsurface investigations of the former grounding-zone of the Storfjordrenna Ice Stream reveal a trough-transverse wedge of sediments, with fans protruding from its western edge. This is interpreted as a GZD, comprised of both line-sourced, glacigenic sediments and point-sourced glacifluvial sediments deposited out of marginal meltwater plumes. Additionally, curvilinear grooves in the seafloor indicate intensive scouring by the keels of large icebergs. The geomorphology of outer-Storfjordrenna documents two main phases of ice stream activity: ice margin retreat from the shelf break, and the subsequent stabilisation of the retreating grounding-line. Partial burial of iceberg ploughmarks indicates that the scouring of large sets of parallel grooves occurred during initial retreat of the ice margin through outer-Storfjordrenna via rapid ice margin break-up. Earlier ice margin retreat in the north was facilitated by retrograde bedslopes on the outer shelf and proximal ice sources over Spitsbergen. We suggest that lateral and bed pinning points promoted ice margin stabilisation at the southern tip of Spitsbergen.

The GZD we describe is evidence of the first ice margin standstill during overall deglaciation of the Storfjordrenna Ice Stream. The fanned surface morphology of the GZD suggests that subglacial meltwater outlets and plumes contributed to the build-up of grounding-zone sediments here, indicating that subglacial conduits were active during retreat. Subglacial drainage at the ice margin may have influenced the stability of the grounding-line through regulating basal hydraulic pressure and the nature of iceberg calving by undercutting and shaping the ice margin. Spatial clustering of single-keeled iceberg ploughmarks in the north and multi-keeled iceberg ploughmarks at the southern sector of the former ice margin suggest that iceberg calving at the northern sector was characterised by deep-drafted, single-keeled icebergs, and the southern sectors by large, tabular icebergs. Greater water depths at the northern sector of the ice margin likely contributed to differences in the character of calved icebergs, the scouring of the seafloor by iceberg keels, and the preservation of older landforms. Local environmental differences along the length of the former ice margin therefore had strong

impacts on ice margin stability and grounding-zone deposition, and may be relevant for reconstructions of recently deglaciated ice margins and predicting changes to modern ice margins.

7.0 Acknowledgements

This research is part of the Centre for Arctic Gas Hydrate, Environment and Climate and was supported by the Research Council of Norway through its Centres of Excellence funding scheme, grant No. 223259. We thank the captain and crew of the R/V 'Helmer Hanssen' and engineers Steinar Iversen and Anoop Nair for their role in the collection and processing of geophysical data.

8.0 Figures

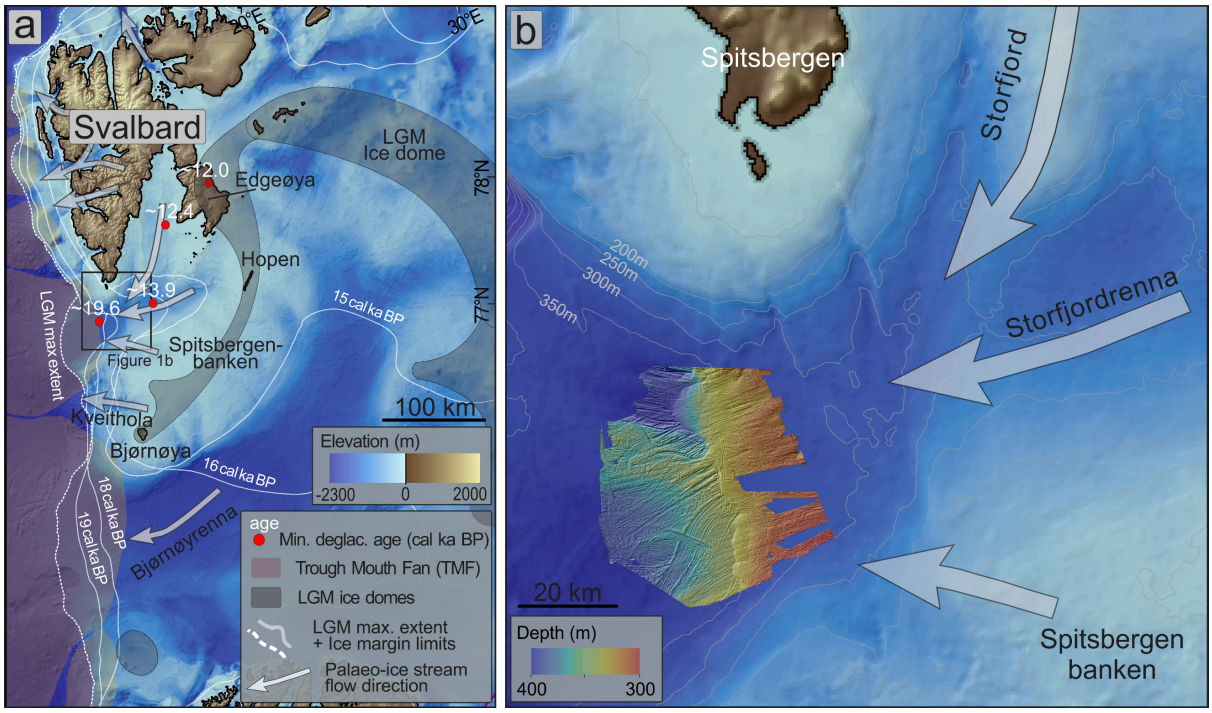

Figure 1: (a) Western Barents Sea with positions of reconstructed and modelled ice domes (Andreassen et al., 2008; Patton et al., 2017) and palaeo-ice stream flow directions (Ottesen et al., 2005; Dowdeswell et al., 2010a; Pedrosa et al., 2011; Bjarnadóttir et al., 2013; Ingólfsson and Landvik, 2013; Andreassen et al., 2014; Patton et al., 2015). Core locations (red dots) show minimum deglaciation age as median probability ages (cal ka BP) within ±2σ. Full calibrated age ranges and sources are given in table 1. The Last Glacial Maximum (LGM) ice extent maxima and most probable margin limits during retreat at 19, 18 and 15 cal ka BP are also drawn, from the ice sheet margin estimates presented by Hughes et al. (2015). Trough mouth Fan (TMF) deposits are also drawn. **(b)** The bathymetry of outer-Storfjordrenna, with the bathymetric dataset presented in this study overlain and palaeo-ice stream flow directions drawn.

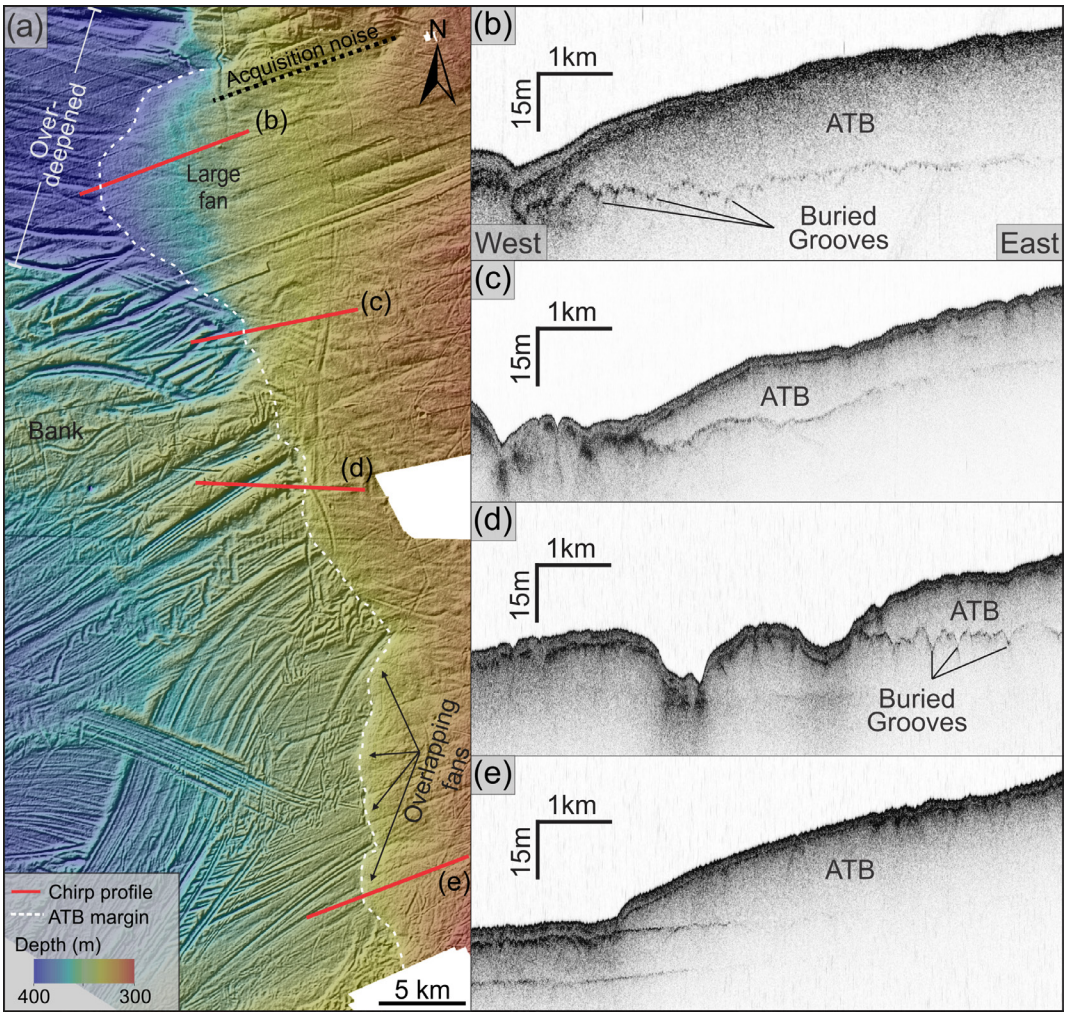

Figure 2: (a) Seafloor bathymetry at the western edge of an acoustically transparent body (ATB), mapped using Chirp sub-bottom sediment profiles. **(b-e)** Chirp sub-bottom profiles along the ATB.

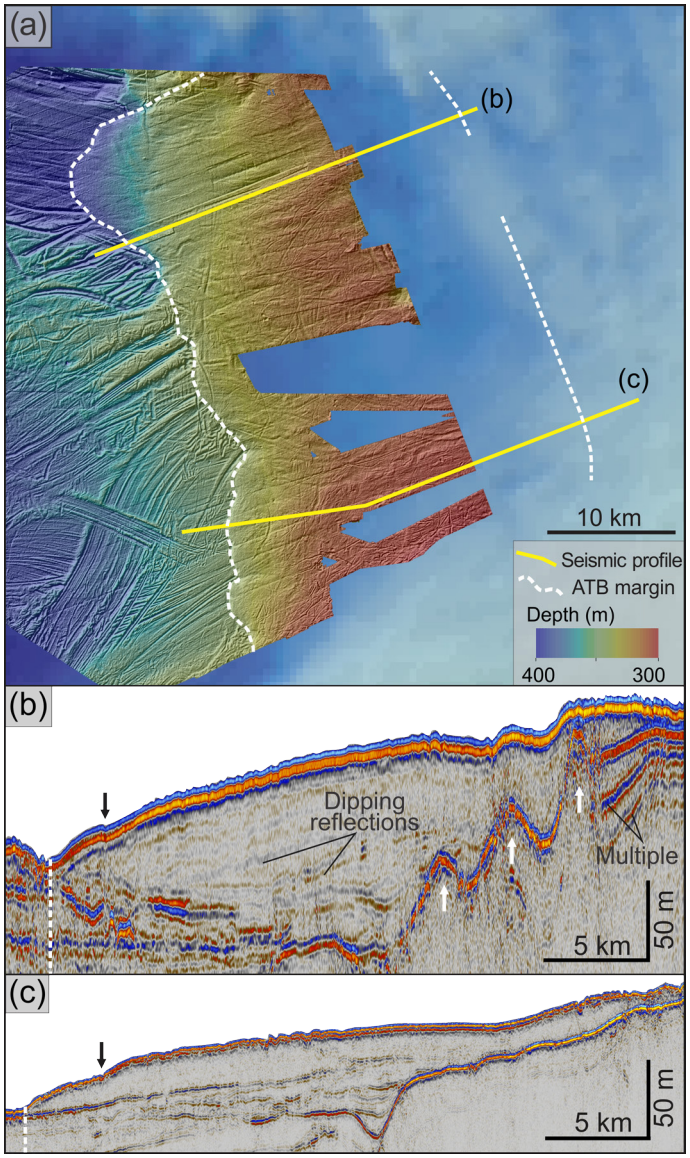

Figure 3: (a) Seafloor bathymetry across the full extent of the acoustically transparent body (ATB), with eastern extent and thickness mapped using 2D seismic profiles **(b)** in the north and **(c)** in the south. Dotted white line shows the extent of the ATB, black arrows point to steps in the long profile, and white arrows point to basal ridges.

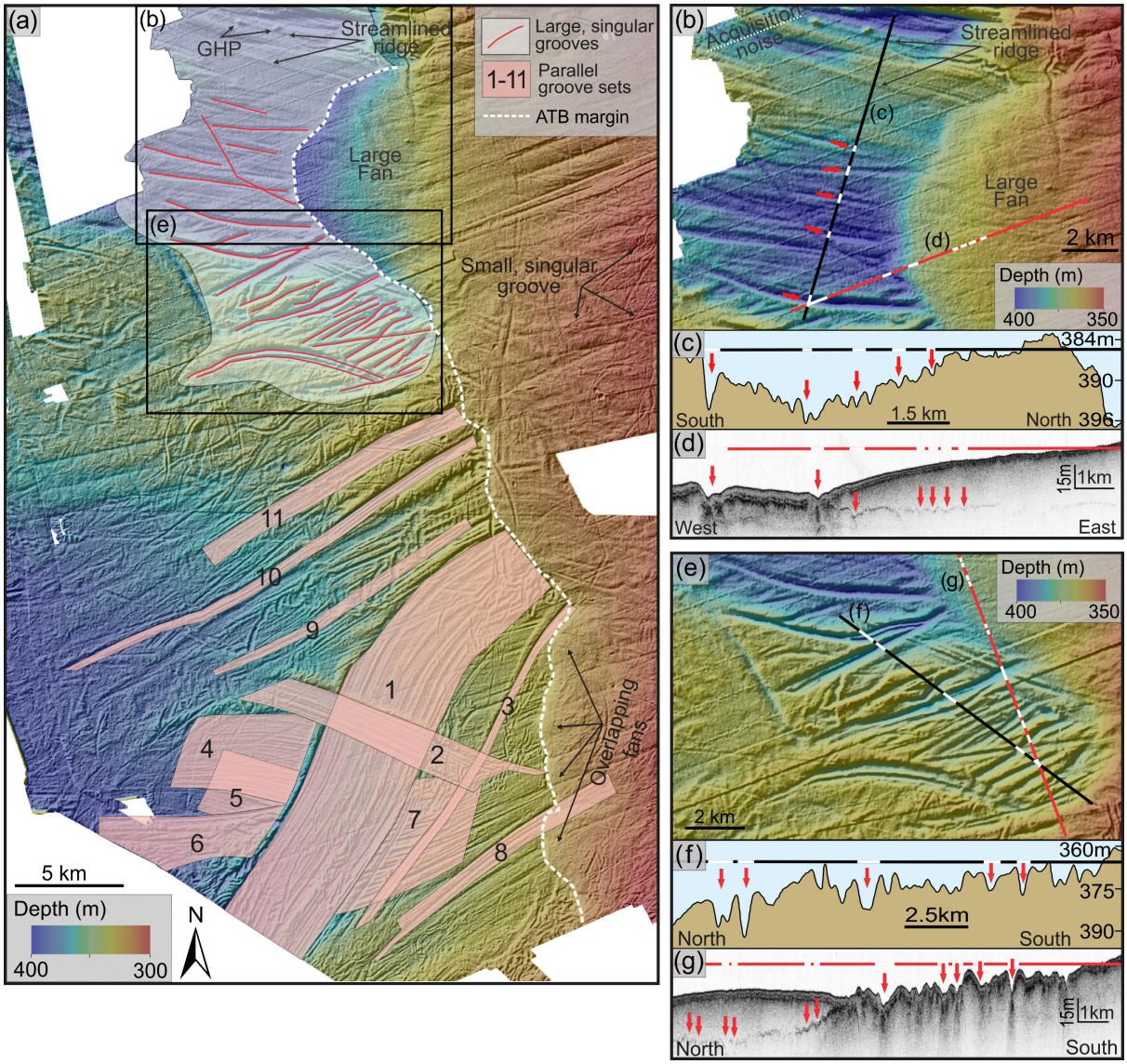

Figure 4: (a) Distribution of seafloor ridges and grooves, highlighting the locations of deep, single-grooves and with numbered sets of parallel grooves. **(b)** Singular, east-west oriented grooves to the north of the region, with **(c)** cross profile showing water depth and groove dimensions, and **(d)** sub-surface profile indicating buried grooves beneath the large fan. **(e)** Deep singular grooves to the south of the large fan, with **(f)** cross profile showing water depth and groove dimensions, and **(g)** subsurface profiles showing grooves buried by the large fan.

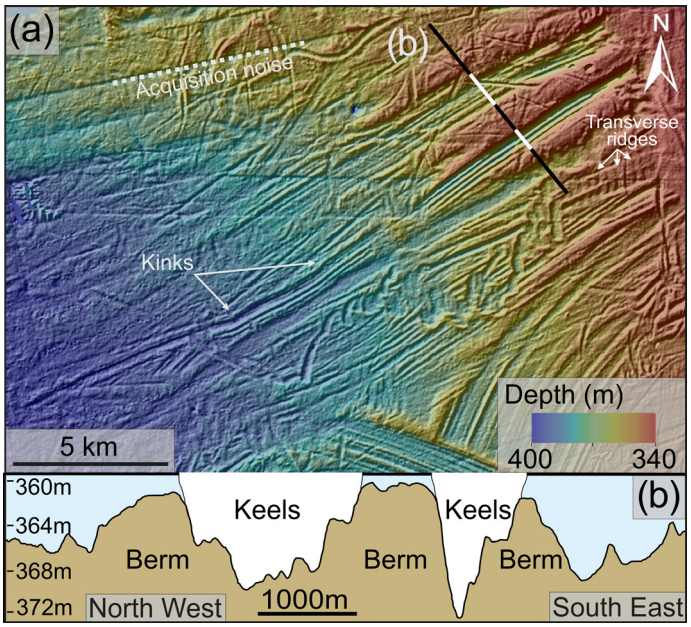

Figure 5: (a) Sets of parallel seafloor grooves with **(b)** cross profile of two of the larger sets, highlighting berms in between and at the edges of each set.

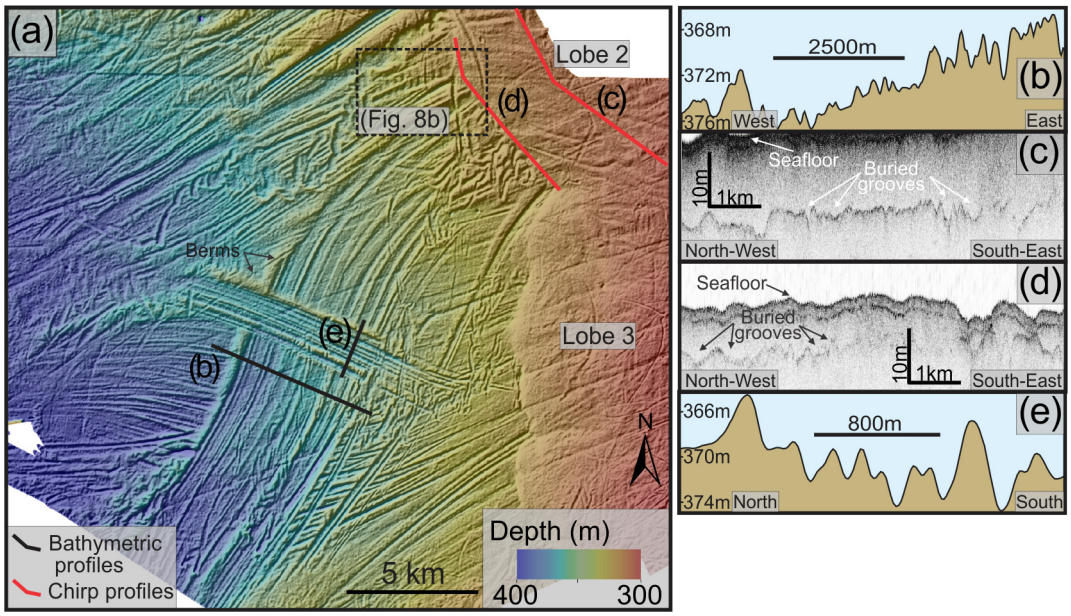

Figure 6: (a) Large, cross cutting sets of parallel grooves with **(b)** cross profile of the largest set and **(c-d)** sub-surface profiles showing that this set is buried by the grounding-zone deposits. **(e)** Cross profile of a cross-cutting groove set.

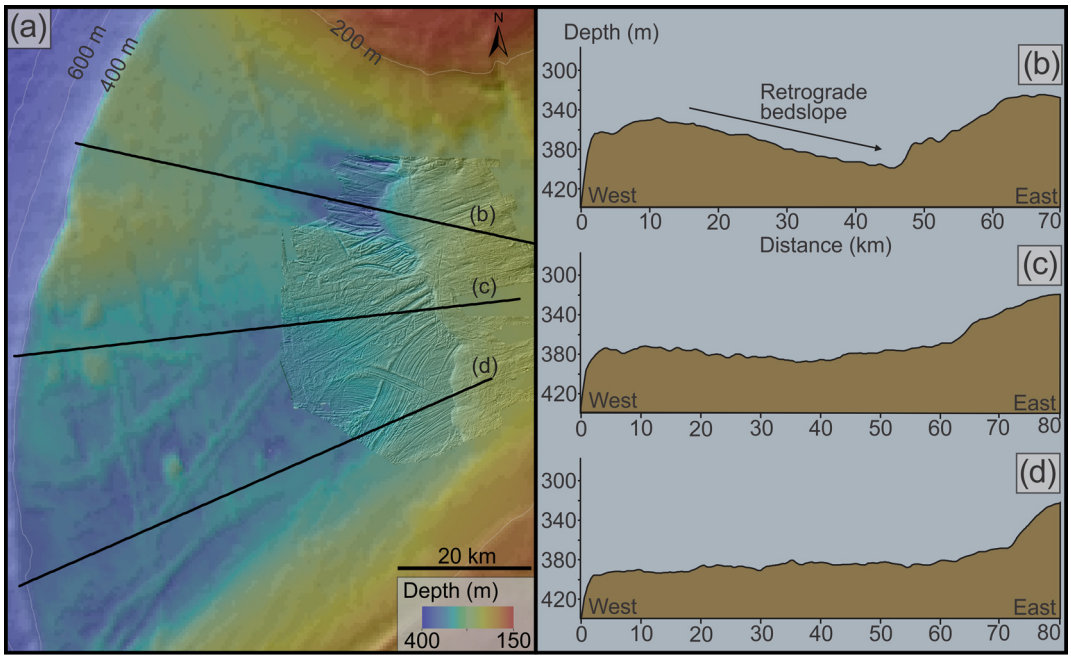

Figure 7: (a) Bathymetry of the outer-shelf from the International Bathymetric Chart of the Arctic Ocean (IBCAO; Jakobsson et al., 2008) and the bathymetric dataset presented in this study. **(b-d)** Long profiles from the continental shelf through outer-Storfjordrenna, showing retrograde bed slopes in the north.

9.0 References

Alley, R.B., 1989. Water-pressure coupling of sliding and bed deformation: 1. Water system. *J. Glaciol.* 35, 108–118.

Amundson, J.M., Fahnestock, M., Truffer, M., Brown, J., Lüthi, M.P., Motyka, R.J., 2010. Ice melange dynamics and implications for terminus stability, Jakobshavn Isbræ, Greenland. *J. Geophys. Res. Earth Surf.* 115, 1–12.

Andreassen, K., Laberg, J.S., Vorren, T.O., 2008. Seafloor geomorphology of the SW Barents Sea and its glaci-dynamic implications. *Geomorphology* 97, 157–177. doi:10.1016/j.geomorph.2007.02.050

Andreassen, K., Winsborrow, M., Bjarnadóttir, L.R., Rüther, D.C., 2014. Ice stream retreat dynamics inferred from an assemblage of landforms in the northern Barents Sea. *Quat. Sci. Rev*. 92, 246–257.

Auriac, A., Whitehouse, P.L., Bentley, M.J., Patton, H., Lloyd, J.M., Hubbard, A., 2016. Glacial isostatic adjustment associated with the Barents Sea ice sheet: A modelling inter-comparison. *Quat. Sci. Rev.* 147, 122–135. doi:10.1016/j.quascirev.2016.02.011

Bassis, J.N., Jacobs, S., 2013. Diverse calving patterns linked to glacier geometry. Nat. Geosci. 6, 833–836.

Batchelor, C.L., Dowdeswell, J.A., 2014. The physiography of High Arctic cross-shelf troughs. *Quat. Sci. Rev*. 92, 68–96.

Batchelor, C.L., Dowdeswell, J.A., 2015. Ice-sheet grounding-zone wedges (GZWs) on high-latitude continental margins. *Mar. Geol.* 363, 65–92.

Benn, D.I., Hulton, N.R.J., Mottram, R.H., 2007a. " Calving laws ", " sliding laws " and the stability of tidewater glaciers. *Ann. Glaciol.* 46, 123–130.

Benn, D.I., Warren, C.R., Mottram, R.H., 2007b. Calving processes and the dynamics of calving glaciers. *Earth-Science Rev.* 82, 143–179.

Bjarnadóttir, L.R., Rüther, D.C., Winsborrow, M.C.M., Andreassen, K., 2013. Grounding-line dynamics during the last deglaciation of Kveithola, W Barents Sea, as revealed by seabed geomorphology and shallow seismic stratigraphy. *Boreas* 42, 84–107.

Bjarnadóttir, L.R., Winsborrow, M.C.M., Andreassen, K., 2014. Deglaciation of the central Barents Sea. *Quat. Sci. Rev.* 92, 208–226.

Chauché, N., Hubbard, A., Gascard, J.-C., Box, J.E., Bates, R., Koppes, M., Sole, A., Christoffersen, P., Patton, H., 2014. Ice–ocean interaction and calving front morphology at two west Greenland tidewater outlet glaciers. *Cryosph*. 8, 1457–1468. doi:10.5194/tc-8-1457-2014

Clark, P.U., Walder, J.S., 1994. Subglacial drainage, eskers, and deforming beds beneath the Laurentide and Eurasian ice sheets. *Geol. Soc. Am. Bull.* 106, 304–314.

Dowdeswell, J.A., Villinger, H., Whittington, R.J., Marienfeld, P., 1993. Iceberg scouring in Scoresby Sund and on the East Greenland continental shelf. *Mar. Geol.* 111, 37–53.

Dowdeswell, J. A., Bamber, J.L., 2007. Keel depths of modern Antarctic icebergs and implications for sea-floor scouring in the geological record. *Mar. Geol.* 243, 120–131.

Dowdeswell, J.A., Hogan, K.A., Evans, J., Noormets, R., Ó Cofaigh, C., Ottesen, D., 2010a. Past ice-sheet flow east of Svalbard inferred from streamlined subglacial landforms. *Geology* 38, 163–166.

Dowdeswell, J. A., Jakobsson, M., Hogan, K. A., O'Regan, M., Backman, J., Evans, J., Hell, B., Löwemark, L., Marcussen, C., Noormets, R., Ó Cofaigh, C., Sellén, E., Sölvsten, M., 2010b. High-resolution geophysical observations of the Yermak Plateau and northern Svalbard margin: Implications for ice-sheet grounding and deep-keeled icebergs. *Quat. Sci. Rev.* 29, 3518–3531.

Dowdeswell, J.A., Ottesen, D., 2013. Buried iceberg ploughmarks in the early Quaternary sediments of the central North Sea: A two-million year record of glacial influence from 3D seismic data. *Mar. Geol*. 344, 1–9. doi:10.1016/j.margeo.2013.06.019

Dowdeswell, J.A., Hogan, K.A., 2014. Huge iceberg ploughmarks and associated corrugation ridges on the northern Svalbard shelf. In: Dowdeswell, J.A., Canals M., Jakobsson, M., Todd, B.J., Dowdeswell, E.K., Hogan, K.A. (Eds.), Atlas of Submarine Glacial Landforms: Modern, Quaternary and Ancient. *Geol. Soc. London, Memoirs,* 46: 269-270.

Dowdeswell, J.A., Hogan, K.A., Arnold, N.S., Mugford, R.I., Wells, M., Hirst, J.P.P., Decalf, C., 2015. Sediment-rich meltwater plumes and ice-proximal fans at the margins of modern and ancient tidewater glaciers: Observations and modelling. *Sedimentology* 62, 1665–1692.

Esteves, M., Bjarnadóttir, L.R., Winsborrow, M.C.M., Shackleton, C.S., Andreassen, K., 2017. Retreat patterns and dynamics of the Sentralbankrenna glacial system, Central Barents Sea. *Quat. Sci. Rev.* 169, 131–147. doi:10.1016/j.quascirev.2017.06.004

Graham, A.G.C., Dutrieux, P., Vaughan, D.G., Nitsche, F.O., Gyllencreutz, R., Greenwood, S.L., Larter, R.D., Jenkins, A., 2013. Seabed corrugations beneath an Antarctic ice shelf revealed by autonomous underwater vehicle survey: Origin and implications for the history of Pine Island Glacier. *J. Geophys. Res. Earth Surf.* 118, 1356–1366.

Graham, A.G.C., Jakobsson, M., Nitsche, F.O., Larter, R.D., Anderson, J.B., Hillenbrand, C.-D., Gohl, K., Klages, J.P., Smith, J.A., Jenkins, A., 2016. Submarine glacial-landform distribution across the West Antarctic margin, from grounding line to slope: the Pine Island–Thwaites ice-stream system. *Geol. Soc. London, Mem.* 46, 493–500. doi:10.1144/M46.173

Hogan, K.A., Dowdeswell, J.A., Noormets, R., Evans, J., Ó Cofaigh, C., 2010. Evidence for full-glacial flow and retreat of the Late Weichselian Ice Sheet from the waters around Kong Karls Land, eastern Svalbard. *Quat. Sci. Rev.* 29, 3563–3582.

Horgan, H.J., Christianson, K., Jacobel, R.W., Anandakrishnan, S., Alley, R.B., 2013. Sediment deposition at the modern grounding zone of Whillans Ice Stream, West Antarctica. *Geophys. Res. Lett.* doi:10.1002/grl.50712

Howat, I.M., Joughin, I., Scambos, T.A., 2007. Rapid changes in ice discharge from Greenland outlet glaciers. *Science* 315, 1559–61.

Howat, I.M., Box, J.E., Ahn, Y., Herrington, A. and McFadden, E.M. 2010. Seaonal variability in the dynamics of marine-terminating outlet glaciers in Greenland. *Journal of Glaciology* 56, 601-613.

Hughes, A.L.C., Gyllencreutz, R., Lohne, Ø.S., Mangerud, J., Svendsen, J.I., 2015. The last Eurasian ice sheets - a chronological database and time-slice reconstruction, DATED-1. *Boreas* 45, 1–45. doi:10.1111/bor.12142

Ingólfsson, Ó., Landvik, J.Y., 2013. The Svalbard-Barents Sea ice-sheet-Historical, current and future perspectives. *Quat. Sci. Rev.* 64, 33–60.

Jakobsson, M., Macnab, R., Mayer, L., Anderson, R., Edwards, M., Hatzky, J., Schenke, H.W., Johnson, P., 2008. An improved bathymetric portrayal of the Arctic Ocean: Implications for ocean modeling and geological, geophysical and oceanographic analyses. *Geophys. Res. Lett.* 35. doi:10.1029/2008GL033520

Jakobsson, M., Anderson, J.B., Nitsche, F.O., Dowdeswell, J.A., Gyllencreutz, R., Kirchner, N., Mohammad, R., O'Regan, M., Alley, R.B., Anandakrishnan, S., Eriksson, B., Kirshner, A., Fernandez, R., Stolldorf, T., Minzoni, R., Majewski, W., 2011. Geological record of ice shelf break-up and grounding line retreat, Pine Island Bay, West Antarctica. *Geology* 39, 691–694.

Jakobsson, M., Anderson, J.B., Nitsche, F.O., Gyllencreutz, R., Kirshner, A.E., Kirchner, N., O'Regan, M., Mohammad, R., Eriksson, B., 2012. Ice sheet retreat dynamics inferred from glacial morphology of the

central Pine Island Bay Trough, West Antarctica. *Quat. Sci. Rev.* 38, 1–10.
Jamieson, S.S.R., Vieli, A., Livingstone, S.J., Ó Cofaigh, C., Stokes, C., Hillenbrand, C.-D., Dowdeswell, J. A., 2012. Ice-stream stability on a reverse bed slope. *Nat. Geosci.* 5, 799–802.
Jenkins, A., 2011. Convection-Driven Melting near the Grounding Lines of Ice Shelves and Tidewater Glaciers. J. Phys. *Oceanogr*. 41, 2279–2294.
Jessen, S.P., Rasmussen, T.L., Nielsen, T., Solheim, A., 2010. A new Late Weichselian and Holocene marine chronology for the western Svalbard slope 30,000-0 cal years BP. *Quat. Sci. Rev.* 29, 1301–1312.
Joughin, I., Macayeal, D.R., 2005. Calving of large tabular icebergs from ice shelf rift systems. *Geophys. Res. Lett.* 32, L02501.
Katz, R.F., Worster, M.G., 2010. Stability of ice-sheet grounding lines. *Proc. R. Soc. A Math. Phys. Eng. Sci.* 466, 1597–1620.
Kimura, S., Holland, P.R., Jenkins, A., Piggott, M., 2014. The effect of meltwater plumes on the melting of a vertical glacier face. *J. Phys. Oceanogr.* 44, 3099–3117.
Koch, Z.J., Isbell, J.L., 2013. Processes and products of grounding-line fans from the Permian Pagoda Formation, Antarctica: Insight into glacigenic conditions in polar Gondwana. *Gondwana Res.* 24, 161–172.
Laberg, J.S., Vorren, T.O., 1996. The glacier-fed fan at the mouth of Storfjorden trough, western Barents Sea: a comparative study. *Geol. Rundschau* 85, 338–349.
Łącka, M., Zajączkowski, M., Forwick, M., Szczuciński, W., 2015. Late Weichselian and Holocene palaeoceanography of Storfjordrenna, southern Svalbard. *Clim. Past* 11, 587–603. doi:10.5194/cp-11-587-
Landvik, J. H., Bolstad, M., Lycke, A. K., Mangerud, J. and Sejrup, H. P., 1992. Weichselian stratigraphy and palaeoenvironments at Bellsund, western Svalbard, *Boreas*, 21: 335–358.
Landvik, J.Y., Bondevik, S., Elverhøi, A., Fjeldskaar, W., Mangerud, J., Salvigsen, O., Siegert, M.J., Svendsen, J.-I., Vorren, T.O., 1998. The last glacial maximum of Svalbard and the Barents Sea area: Ice sheet extent and configuration. *Quat. Sci. Rev*. 17, 43–75.
Lien, R., Solheim, A., Elverhøi, A., Rokoengen, K., 1989. Iceberg scouring and sea bed morphology on the eastern Weddell Sea shelf , Antarctica. *Polar Res*. 7, 43–57.
Livingstone, S.J., Cofaigh, C.Ó., Stokes, C.R., Hillenbrand, C.-D., Vieli, A., Jamieson, S.S.R., 2013. Glacial geomorphology of Marguerite Bay Palaeo-Ice stream, western Antarctic Peninsula. *J. Maps* 9, 558–572.
Llopart, J., Urgeles, R., Camerlenghi, A., Lucchi, R.G., Rebesco, M., De Mol, B., 2015. Late Quaternary development of the Storfjorden and Kveithola Trough Mouth Fans, northwestern Barents Sea. *Quat. Sci. Rev.* 129, 68–84.
Lucchi, R.G., Pedrosa, M.T., Camerlenghi, A., Urgeles, R., De Mol, B., Rebesco, M., 2012. Recent Submarine Landslides on the Continental Slope of Storfjorden and Kveithola Trough-Mouth Fans (North West Barents Sea). In: Yamada, Y., Kawamura, K., Ikehara, K., Ogawa, Y., Urgeles, R.,Mosher, D., Chaytor, J., Strasser, M. (Eds.), Submarine Mass Movements and Their Consequences. Advances in Natural and Technological Hazards Research, Springer Science book series, 31, pp. 735–745.
Lucchi, R.G., Camerlenghi, A., Rebesco, M., Colmenero-hidalgo, E., Sierro, F.J., Sagnotti, L., Urgeles, R., Melis, R., Morigi, C., Barcena, M.A., Giorgetti, G., Villa, G., Persico, D., Flores, J.A., Rigual-Hernandez, A.S., Pedrosa, M.T., Macri, P., Caburlotto, A., 2013. Postglacial sedimentary processes on the Storfjorden and Kveithola trough mouth fans: Significance of extreme glacimarine sedimentation. *Glob. Planet. Change* 111, 309–326.
MacLean, B., Blasco, S., Bennett, R., England, J., Rainey, W., Hughes-Clarke, J., Beaudoin, J., 2010. Ice keel seabed features in marine channels of the central Canadian Arctic Archipelago: Evidence for former ice streams and iceberg scouring. *Quat. Sci. Rev.* 29, 2280–2301.
Mangerud, J., Bondevik, S., Gulliksen, S., Karin Hufthammer, A., Høistæter, T., 2006. Marine 14C reservoir ages for 19th century whales and molluscs from the north Atlantic. Quat. Sci. Rev. 25(23-24), 3228-3245.
Moon, T., Joughin, I., 2008. Changes in ice front position on Greenland's outlet glaciers from 1992 to 2007. *J. Geophys. Res*. 113, F02022.
Motyka, R.J., Hunter, L., Echelmeyer, K.A., Connor, C., 2003. Submarine melting at the terminus of a temperate tidewater glacier, LeConte Glacier, Alaska, U.S.A. *Ann. Glaciol.* 36, 57–65.
Motyka, R.J., Truffer, M., Fahnestock, M., Mortensen, J., Rysgaard, S., Howat, I., 2011. Submarine melting of the 1985 Jakobshavn Isbræ floating tongue and the triggering of the current retreat. *J. Geophys. Res. Earth Surf.* 116, 1–17.
Nick, F.M., Vieli, A., Howat, I.M., Joughin, I., 2009. Large-scale changes in Greenland outlet glacier dynamics triggered at the terminus. *Nat. Geosci.* 2, 110–114.
Nielsen, T., Rasmussen, T.L., 2018. Reconstruction of ice sheet retreat after the Last Glacial maximum in Storfjorden, southern Svalbard. *Mar. Geol*. 402, 228–243. doi:10.1016/j.margeo.2017.12.003
Ottesen, D., Dowdeswell, J.A., Rise, L., 2005. Submarine landforms and the reconstruction of fast-flowing ice streams within a large Quaternary ice sheet: The 2500-km-long Norwegian-Svalbard margin (57-80N).

Bull. Geol. Soc. Am. 117, 1033–1050.
Ottesen, D., Dowdeswell, J. A., 2006. Assemblages of submarine landforms produced by tidewater glaciers in Svalbard. *J. Geophys. Res. Earth Surf.* 111, F01016.
Ottesen, D., Stokes, C.R., Rise, L., Olsen, L., 2008. Ice-sheet dynamics and ice streaming along the coastal parts of northern Norway. *Quat. Sci. Rev.* 27, 922–940.
Patton, H., Andreassen, K., Bjarnadóttir, L.R., Dowdeswell, J.A., Winsborrow, M.C.M., Noormets, R., Polyak, L., Auriac, A., Hubbard, A., 2015. Geophysical constraints on the dynamics and retreat of the Barents Sea Ice Sheet as a palaeo-benchmark for models of marine ice-sheet deglaciation. *Rev. Geophys*. 53, 1–31. doi:10.1002/2014RG000468
Patton, H., Hubbard, A., Andreassen, K., Auriac, A., Whitehouse, P.L., Stroeven, A.P., Shackleton, C., Winsborrow, M.C.M., Heyman, J., Hall, A.M., 2017. Deglaciation of the Eurasian ice sheet complex. *Quat. Sci. Rev.* 169, 148–172.
Pattyn, F., Huyghe, A., De Brabander, S., De Smedt, B., 2006. Role of transition zones in marine ice sheet dynamics. *J. Geophys. Res. Earth Surf.* 111, 1–10.
Pedrosa, M.T., Camerlenghi, A., De Mol, B., Urgeles, R., Rebesco, M., Lucchi, R.G., 2011. Seabed morphology and shallow sedimentary structure of the Storfjorden and Kveithola trough-mouth fans (North West Barents Sea). *Mar. Geol.* 286, 65–81.
Powell, R.D., 1990. Glacimarine processes at grounding-line fans and their growth to ice-contact deltas. *Geol. Soc. London, Spec. Publ.* 53, 53–73.
Powell, R.D., Molnia, B. 1989. Glacimarine sedimentary processes, facies and morphology of the south-southeast Alaska shelf and fjords. *Marine Geology* 85, 359-390.
Powell, R.D., Alley, R.B., 1997. Grounding-line systems: processes, glaciological inferences and the stratigraphic record. Geology and Seismic Stratigraphy of the Antarctic Margin, Part 2. *Antarctic Research Series,* 71, 169–187.
Powell, R.D., Dawber, M., McInnes, J.N., Pyne, A.R., 1996. Observations of the grounding-line area at a floating glacier terminus. *Ann. Glaciol.* 22, 217–223.
Powell, R.D., Domack, E., 2002. Modern glaciomarine environments, in: Modern and Past Glacial Environments. Butterworth-Heinmann, Oxford, pp. 361–389.
Pritchard, H.D., Arthern, R.J., Vaughan, D.G., Edwards, L. A, 2009. Extensive dynamic thinning on the margins of the Greenland and Antarctic ice sheets. *Nature* 461, 971–5.
Rasmussen, T.L., Thomsen, E., Ślubowska, M.A., Jessen, S., Solheim, A., Koç, N., 2007. Paleoceanographic evolution of the SW Svalbard margin (76°N) since 20,000 14C yr BP. *Quat. Res.* 67, 100–114.
Rasmussen, T. L. and Thomsen, E., 2014. Brine formation in relation to climate changes and ice retreat during the last 15,000 years in Storfjorden, Svalbard, 76-78°N. *Paleoceanography*, 29.(10). doi:10.1002/2014PA002643.
Rebesco, M., Liu, Y., Camerlenghi, A., Winsborrow, M.C.M., Sverre, J., Caburlotto, A., Diviacco, P., Accettella, D., Sauli, C., Wardell, N., Tomini, I., 2011. Deglaciation of the western margin of the Barents Sea Ice Sheet — A swath bathymetric and sub-bottom seismic study from the Kveithola Trough. *Mar. Geol*. 279, 141–147. doi:10.1016/j.margeo.2010.10.018
Reimer, P.J., Bard, E., Bayliss, A., Beck, J.W., Blackwell, P.G., Bronk Ramsey, C., Buck, C.E., Cheng, H., Edwards, R.L., Friedrich, M, Grootes, P.M., 2013. IntCal13 and Marine 13 radiocarbon age calibration curves 0-50,000 years cal BP. *Radiocarbon* 55(4), 1869-1887.
Rignot, E., Koppes, M., Velicogna, I., 2010. Rapid submarine melting of the calving faces of West Greenland glaciers. *Nat. Geosci.* 3, 187–191.
Rignot, E., Mouginot, J., Scheuchl, B., 2011. Ice flow of the Antarctic ice sheet. Science 333, 1427-1430.
Schoof, C., 2007. Ice sheet grounding line dynamics: Steady states, stability, and hysteresis. *J. Geophys. Res. Earth Surf.* 112, 1–19.
Serov, P., Vadakkepuliyambatta, S., Mienert, J., Patton, H., Portnov, A., Silyakova, A., Panieri, G., Carroll, M.L., Carroll, J., Andreassen, K., Hubbard, A., 2017. Postglacial response of Arctic Ocean gas hydrates to climatic amelioration. *Proc. Natl. Acad. Sci.* 114, 6215–6220. doi:10.1073/pnas.1619288114
Shackleton, C., Patton, H., Hubbard, A., Winsborrow, M., Kingslake, J., Esteves, M., Andreassen, K., Greenwood, S.L., 2018. Subglacial water storage and drainage beneath the Fennoscandian and Barents Sea ice sheets. *Quat. Sci. Rev.* 201, 13–28. doi:10.1016/J.QUASCIREV.2018.10.007
Shreve, R.L., 1972. The movement of water in glaciers. *J. Glaciol.* 11, 205–214.
Slater, D.A., Nienow, P.W., Cowton, T.R., Goldberg, D.N., Sole, A.J., 2015. Effect of near-terminus subglacial hydrology on tidewater glacier submarine melt rates. *Geophys. Res. Lett.* 42, 2861–2868.
Smith, S.D., Banke, E.G., 1983. The influence of winds, currents and towing forces on the drift of icebergs. *Cold Reg. Sci. Technol.* 6, 241–255.
Sole, A., Payne, T., Bamber, J., Nienow, P., Krabill, W., 2008. Testing hypotheses of the cause of peripheral thinning of the Greenland Ice Sheet: Is land-terminating ice thinning at anomalously high rates? *Cryosph*.

2, 205–218.
Stokes, C. and Clark, C., 2001. Palaeo-ice streams. *Qua. Sci. Rev.* 20, 1437-1457.
Stuiver, M., Reimer, P.J., 1993. Extended ^{14}C database and revised CALIB 3.0 ^{14}C age calibration program. *Radiocarbon* 35, 215–230.
Syvitski, J.P.M., 1989. On the deposition of sediment within glacier-influenced fjords: Oceanographic controls. *Mar. Geol.* 85, 301–329.
Thomas, R.H., 1979. The dynamics of marine ice sheets. *J. Glaciol.* 24, 167-177.
Vorren, T.O., Laberg, J.S., 1997. Trough mouth fans — palaeoclimate and ice-sheet monitors. *Quat. Sci. Rev.* 16, 865–881.
Wise, M.G., Dowdeswell, J.A., Jakobsson, M. and Larter, R.D. 2017. Evidence of marine ice-cliff instability in Pine Island Bay from iceberg-keel plough marks. *Nature* 550, 506-510.

Paper 3

Transitions in subglacial drainage and influences on glacial dynamics in the central Barents Sea, reconstructed from meltwater landforms.

Calvin Shackleton, Monica Winsborrow, Henry Patton, Mariana Esteves, Lilja Bjarnadóttir, Karin Andreassen. 2019.

Manuscript in preparation